RESEARCH REPORT

Fire Performance of Houses. Phase I.
Study of Unprotected Floor Assemblies in
Basement Fire Scenarios
Part 6

CMHC—HOME TO CANADIANS

Canada Mortgage and Housing Corporation (CMHC) has been Canada's national housing agency for more than 60 years.

Together with other housing stakeholders, we help ensure that Canada maintains one of the best housing systems in the world. We are committed to helping Canadians access a wide choice of quality, affordable homes, while making vibrant, healthy communities and cities a reality across the country.

For more information, visit our website at **www.cmhc.ca**

You can also reach us by phone at 1-800-668-2642 or by fax at 1-800-245-9274.

National Research Council Canada

Conseil national de recherches Canada

NRC · CNRC

Fire Performance of Houses

Phase I

Study of Unprotected Floor Assemblies in Basement Fire Scenarios

Part 6 – Results of Tests UF-07 and UF-08 (Metal-Web-Connected Wood Trusses)

Research Report: IRC-RR-251

Date: March 31, 2009

Authors: J.Z. Su, N. Bénichou, A.C. Bwalya, G.D. Lougheed, B.C. Taber, P. Leroux, J.R. Thomas

INSTITUTE FOR RESEARCH IN CONSTRUCTION
Fire Research Program

TABLE OF CONTENTS

NRC·CNRC

NRC·CNRC

LIST OF FIGURES

NRC·CNRC

LIST OF TABLES

NRC·CNRC

ABSTRACT

This report documents part of the research project involving a series of full-scale fire experiments in a test facility that simulated a two-storey single-family house with a severe, fast growing fire originating in an unfinished basement to study the fire performance of the floor/ceiling assembly constructed over the basement. The report presents the results and analysis of Test UF-07 and Test UF-08 carried out in the test house with an unprotected metal-web wood truss floor/ceiling assembly above the basement. The two tests were identical except for the state of the door in the doorway leading from the first storey to the basement, which was absent in Test UF-07 (i.e., completely open basement doorway) and completely closed in Test UF-08 (i.e., closed basement doorway). A number of measurements were taken at various locations during the tests such as temperatures, smoke alarm activation times, smoke optical density, floor deflection and concentrations of CO, CO_2 and O_2. For Test UF-07, untenable conditions on the upper storeys were reached before structural failure of the test floor assembly. While for Test UF-08, untenable conditions for occupants of average susceptibility on the upper storeys were reached after structural failure of the test floor assembly. The results showed that closing the door to the basement delayed the structural failure of the unprotected floor assembly as well as the onset of untenable conditions on the upper storeys.

NRC·CNRC

FIRE PERFORMANCE OF HOUSES

PHASE I

STUDY OF UNPROTECTED FLOOR ASSEMBLIES IN BASEMENT FIRE SCENARIOS

Part 6 – Results of Tests UF-07 and UF-08 (Metal-Web-Connected Wood Trusses)

J.Z. Su, N. Bénichou, A.C. Bwalya, G.D. Lougheed, B.C. Taber, P. Leroux and J.R. Thomas

1   INTRODUCTION

1.1   Background

Risk of fires in buildings and concerns about their potential consequences are always present. Canada's fire death rate has continuously declined for the last three decades; much of this decline is attributed to the introduction of residential smoke alarms (this is also the case in the United States). With the advent of new materials and innovative products for use in construction of single-family houses, there is a need to understand what impacts these materials and products will have on occupant life safety under fire conditions and a need to develop a technical basis for the evaluation of their fire performance.

The National Building Code of Canada (NBCC) [1] generally intends that major structural load-bearing elements (floors, walls and roofs) have sufficient fire resistance to limit the probability of premature failure or collapse during the time required for occupants to evacuate safely [2]. Historically, the NBCC has not specified a minimum level of fire performance (fire resistance) of these structural elements in single-family houses.

In Canada, the Canadian Construction Materials Centre (CCMC) is called upon to evaluate the use of new materials and innovative construction products for compliance with the NBCC. Some of the more recent innovative structural products, seeking recognition for use in housing, are made of new composite and non-traditional materials that may have unknown fire behaviour. When evaluating new structural products, part of the CCMC challenge is related to the fact that no guidance or criteria are provided in the NBCC regarding the fire performance of structural systems used in single-family houses.

The Canadian Commission on Construction Materials Evaluation (CCCME) guides the operation of CCMC. Through the CCCME, CCMC sought the views of the Canadian Commission on Building and Fire Codes (CCBFC), which guides the development of the NBCC. After review and discussion, both the CCBFC and CCCME agreed that a study on the factors that affect the life safety of occupants of single-family houses should be conducted.

1.2 Goals of the Research

The National Research Council of Canada Institute for Research in Construction (NRC-IRC) undertook research into fires in single-family houses to understand the impact of residential construction products and systems on occupant life safety.

This research project sought to achieve the following goals:
1. To determine the significance of the fire performance of structural materials used in houses to the life safety of occupants.
2. To identify methods of measuring the fire performance of unprotected structural elements used in houses.
3. To measure and establish the fire performance of traditional house construction to facilitate the evaluation of the fire performance of innovative construction products and systems.

1.3 General Research Approach

Figure 1 shows a possible chronological sequence of relevant critical events that might occur in a fire scenario. It is acknowledged that the chronology of the occurrence of events may differ, and in some cases can shift in ordering.
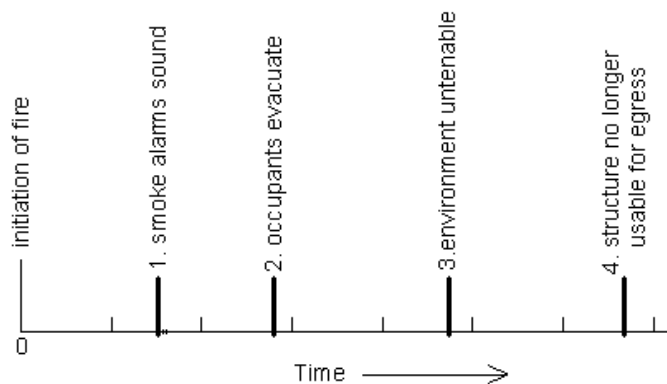
Figure 1. Possible chronological sequence of events affecting the life safety of occupants in a fire situation

The research sought to establish, through experimental studies and using specific fire test scenarios, the typical sequence of the following events (measured from initiation of a fire), using a test facility intended to represent a typical code-compliant single-family house:
1. Sounding of smoke alarms (Event 1 as shown in Figure 1).
2. Loss of tenability within the environment of the first, second or subsequent storey(s) (Event 3).
3. Loss of integrity of the floor assembly and/or loss of its function as a viable egress route on the first or second storey(s)[1] (Event 4).

---

[1] The state of the egress route(s) on the first storey is relevant to the evaluation of the performance of the basement foundation walls and floor structure constructed over the basement;

NRC·CNRC

The research also sought to establish a basis for prediction or estimation of the required safe egress times expected for ambulatory occupants assuming a tenable indoor environment and a structurally sound evacuation route. A review of the literature on the waking effectiveness of occupants to smoke alarms, the delay time to start evacuation and the timing of escape in single-family houses was conducted. The objective of the review was to identify a range of estimated times families would take to awake, prepare and move out of their home after perceiving the sound of a smoke alarm during the night in winter conditions (Event 2 shown in Figure 1). This literature review was a separate but parallel study to the experimental studies. The results of the literature review are provided in Reference [3].

1.4   Scope of the Research Projects

The overall research consisted of a number of phases of experimental studies with each phase investigating a specified structural element based on specified fire scenarios.

Phase 1 (2004 to 2007) of the experimental study focused on basement fires and their impacts on the structural integrity of unprotected floor assemblies above a basement and the tenability conditions in a full-scale test facility. It is acknowledged that, a basement is not the most frequent site of household fires but it is the fire location that is most likely to create the greatest challenge to the structural integrity of the 1st storey structure, which typically provides the main egress routes. The study of fires originating in basements also provides a good model for the migration of combustion products throughout the house and its egress paths. The data collected during this phase of the project provided important indicators for identifying and evaluating the sequence for the occurrence of critical events shown in Figure 1.

This research focused on the life safety of occupants in single-family houses. The safety of emergency responders in a fire originating in single-family houses was not within the scope of this research project. Technical data collected during this research could aid in clarifying the potential risks associated with firefighting activities.

1.5   Content of this Document

This report documents the results of the initial phase of work involving an experimental study of the structural fire performance of the floor/ceiling assembly (1st floor) constructed over the basement level of a test house. Specifically, this report contains the data and analysis of Tests UF-07 and UF-08 of the Phase I study carried out in the test house with an unprotected metal-web wood truss floor/ceiling assembly. This includes results on the fire scenarios, tenability, structural integrity, and the sequence of Events 1, 3 and 4, as illustrated in Figure 1.

---

the state of the egress route on the second storey is relevant to the evaluation of the performance of the above-grade wall structures and floor structure over the first storey.

NRC·CNRC

2   EXPERIMENTAL STUDY

To undertake this research, NRC-IRC constructed a three-level experimental facility, representing a typical two-storey detached single-family house with a basement. The facility allows the study of structural fire performance, as well as smoke movement and tenability under fire conditions for single-family houses. The facility has a total floor area of approximately 95 m^2 per storey and is shown in Figure 2.

Figure 2. Three-storey facility

2.1   Geometry - Compartments in the Facility

2.1.1   Fire Compartment in Basement

The layout of the basement is shown in Figure 3. The basement was partitioned to create a fire room representing a 27.6 m2 basement living area, or about 1/4 of the total basement area. This compartment size was chosen based on a survey carried out by NRC [4]. The area of the basement that was not used for the fire compartment was blocked off during the fire tests. The height of the basement was 2.44 m. The ceiling clear height depended on the depth of the floor assembly being tested. A rectangular exterior opening measuring 2.0 m wide by 0.5 m high and located 1.8 m above the floor was provided in the south wall of the fire room. The size of the opening was chosen based on the results of the survey carried out by NRC [4]. A 0.91 m wide by 2.05 m high doorway opening located on the north wall of the fire room led into an empty stairwell enclosure (without a staircase). At the top of this stairwell, a 0.81 m wide by 2.05 m high doorway led into the first storey, as shown in Figure 4. This doorway either had no door (open basement doorway) or had a door in the closed position (closed basement doorway), depending on the scenario being studied. There is no requirement for a basement door in the NBCC. Section on "Openings and their States" provides more details.
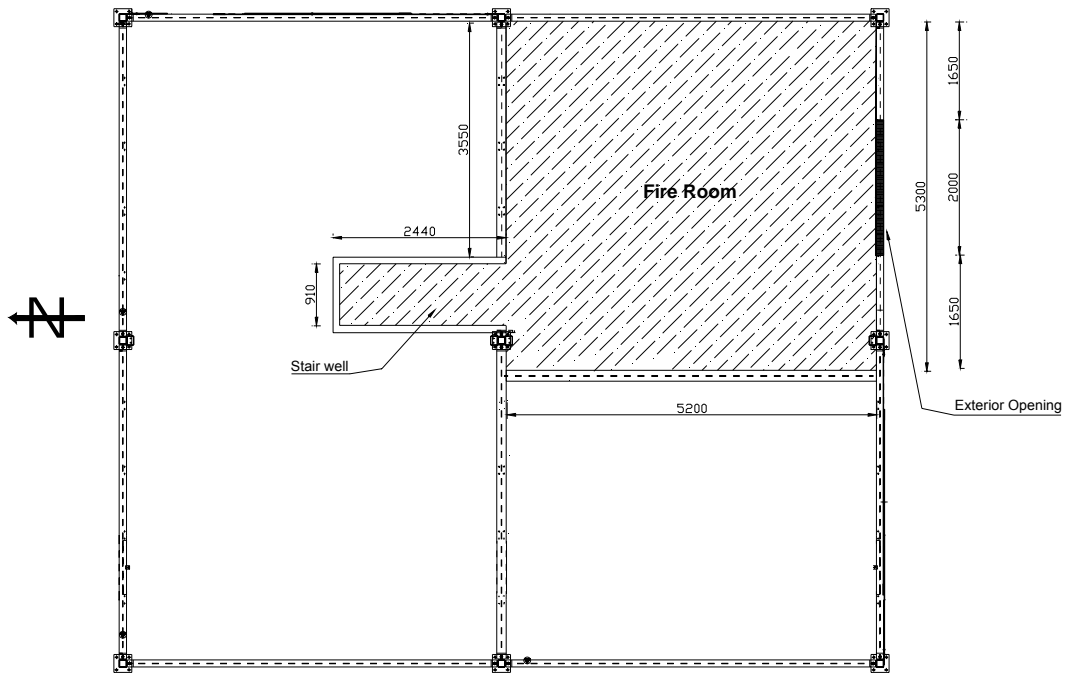
Figure 3. Basement level layout (dimensions in mm)

2.1.2 First Storey

The first storey had an open-plan layout with no partitions, as shown in Figure 4. A test floor assembly was constructed on the first storey directly above the fire room for each experiment. The remainder of the floor on the first storey was constructed out of non-combustible materials. The height of the storey was about 2.44 m. As shown in Figure 4, this storey had 2 door openings: a door opening to the outside (dimensions of 0.89 m by 2.07 m) and a door opening that connected the basement to the first storey (dimensions of 0.81 m by 2.05 m). This storey also connected to the 2nd storey by a staircase in the middle of the storey area. This staircase to the second storey was not enclosed. The floor being tested was positioned in the southeast quarter of the first storey, on top of the fire compartment.

2.1.3 Second Storey

The layout of the second storey is shown in Figure 5. This storey was partitioned to contain two identical bedrooms with dimensions of 3.75 m by 4.47 m connected by a corridor with dimensions of 1.1 m x 4.45 m. The height of the storey was 2.44 m. In all tests, the door of the southeast bedroom remained closed whereas the door on the southwest bedroom was kept open. The size of the door openings was 0.81 m by 2.05 m. The remaining area of the second storey that was not used was blocked off during the fire tests.

NRC·CNRC
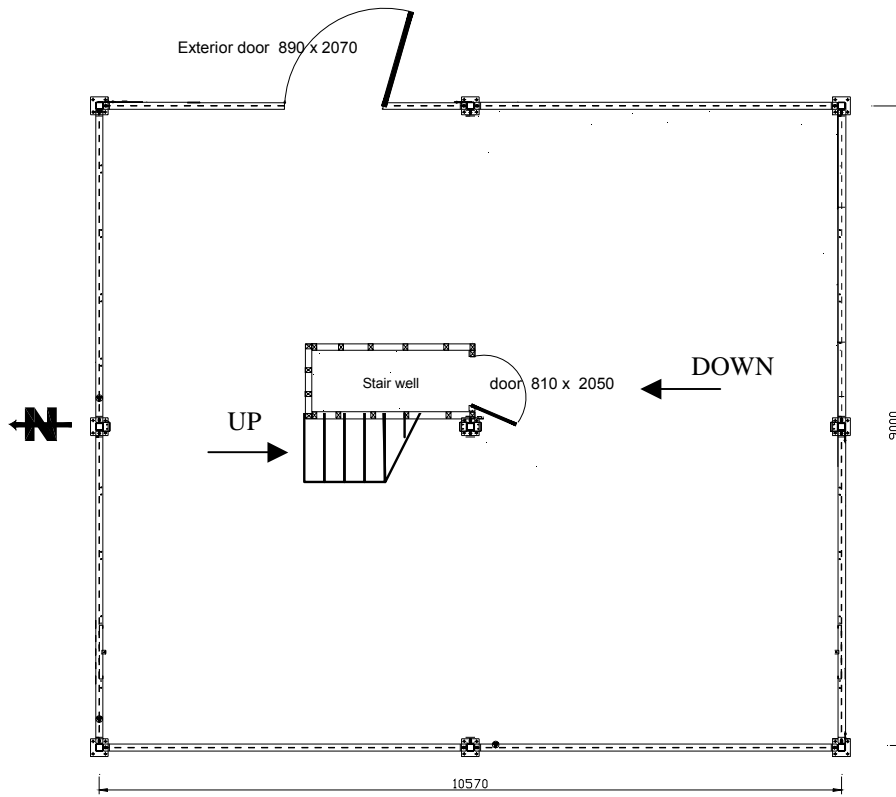
Figure 4. First storey layout (dimensions in mm)
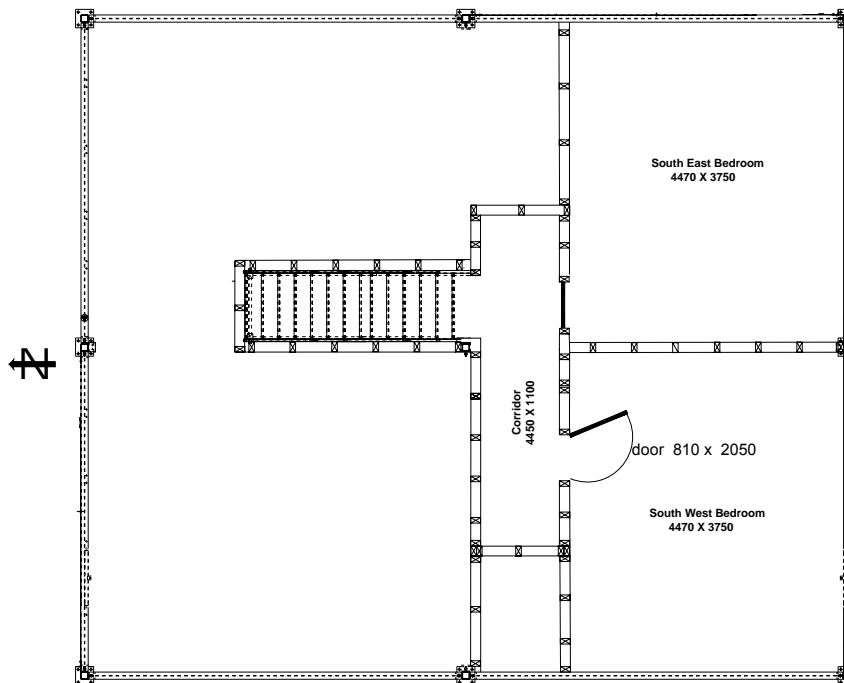
Figure 5. Second storey layout (dimensions in mm)

6

NRC·CNRC

2.2 Lining Materials in Compartments

The compartments were lined with different materials. For the basement level, the walls of the fire compartment were lined with 12.7 mm thick regular gypsum board. There was no ceiling finish in the fire compartment, so the floor assembly, including both the framing supports (trusses) and the underside of the subfloor (oriented strand board, OSB), was unprotected and exposed. For the first and second storeys, cement board covered the walls, and the ceilings were covered with 12.7-mm thick regular gypsum board. There was no finished floor in the 1st storey, so the upper surface of the OSB subfloor used on the floor assembly being tested was exposed. In the remainder of the compartment on the first storey, the floor was noncombustible. The OSB that was used for the subfloor was chosen on the basis of a study on the performance of different OSBs when exposed to fire [5].

2.3 Openings and their States

The openings included: on the basement level, a rough window opening; on the first storey, a door opening to the outside and a door opening at the top of the empty stairwell enclosure (contained no stairs) leading from the basement level; on the second storey, a door opening in the corridor at the top of the stairs leading from the first storey and door openings from the corridor leading to each of the two bedrooms. The size of all the doorways were typical of those used in housing. The single window opening in the basement (2.0 m x 0.5 m) represents an area equal to the size of two typical basement windows.

The doors on the door openings were inexpensive moulded-fibreboard hollow-core interior doors with minimum size styles and rails or solid-core exterior wood doors. The rough window opening in the basement level was covered with a noncombustible panel that could open at the appropriate time in each fire test.

At the start of a test, the rough window opening in the basement and the exterior door on the first storey leading to the outside were closed. Both were opened at critical times during a test (see Section 2.6 Testing Procedure). The doorway on the first storey leading to the basement either had a door in the opening in the closed position (closed basement doorway) or had no door (open basement doorway) depending on the scenario being studied. In Test UF-07, the open basement doorway was used; in Test UF-08, the closed basement doorway was used. On the second storey, during the test, the door to the southwest bedroom was open, and the door to the southeast bedroom was closed.

There was no heating, ventilating and air-conditioning or plumbing system installed in the test house, i.e., no associated mechanical openings in the floor.

2.4 Fuel Load in the Fire Compartment

The selection of the fuel load and its arrangement in the fire compartment was a critical element in this experimental work. A study was conducted to select the fire scenario and fuel package, which was used in this phase of the project [6]. This fuel package

NRC·CNRC

consisted of a mock-up sofa constructed with 9 kg of exposed polyurethane foam (PUF), the dominant combustible constituent of upholstered furniture, and 190 kg of wood cribs beside and underneath the mock-up sofa. A photograph of the fuel package is shown in Figure 6. The mock-up sofa was constructed with 6 blocks of flexible polyurethane foam (with a density of 32.8 kg/m^3) placed on a metal frame. Each block was 610 mm long by 610 mm wide and 100 mm or 150 mm thick. The 150-mm thick foam blocks were used for the backrest and the 100 mm thick foam blocks for the seat cushion. The PUF foam was used without any upholstery fabric that is used in typical upholstered furniture. The wood cribs were made with spruce lumber pieces, each piece measuring 38 mm x 89 mm x 800 mm. For the small cribs located under the mock-up sofa, four layers with six pieces per layer were used. The other two cribs used eight layers.

The placement of the fuel package in the basement fire compartment is illustrated in Figure 7. The mock-up sofa was located at the center of the floor area. The mock-up sofa was ignited in accordance with the ASTM 1537 test protocol [7] and the wood cribs provided the remaining fire load to sustain the fire for the desired period of time.

Figure 6. Fuel package
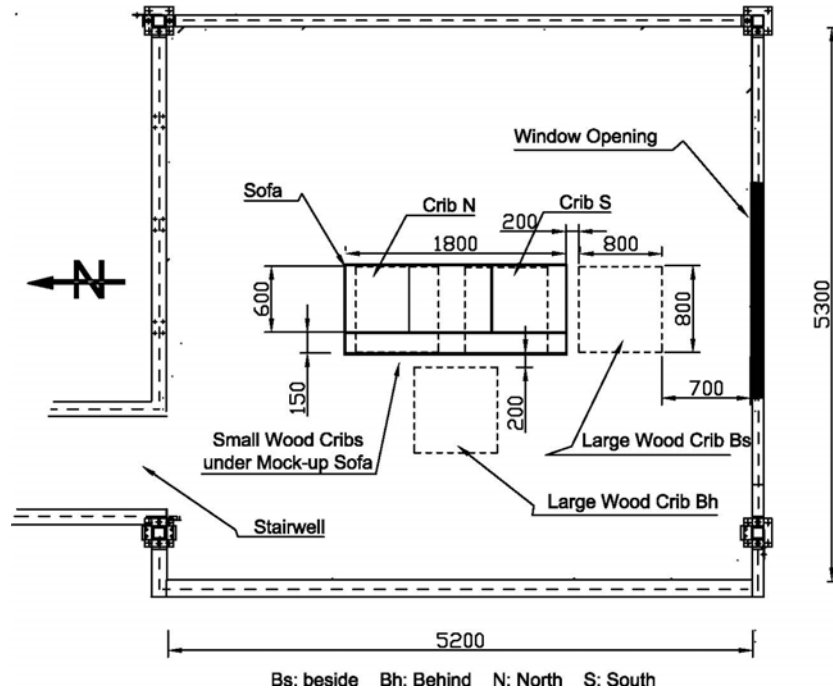
Figure 7. Arrangement of the fuel package in the fire compartment

(dimensions in mm)

2.5 Instrumentation in the Different Compartments and Exterior

The following is a summary of the instrumentation installed inside and around the exterior of the test facility.

2.5.1 Fire Compartment in Basement

The instrumentation in the basement fire room included the following:
- Four vertical arrays of thermocouples located at the quarter points of the fire room to measure temperatures at heights of 0.4, 0.9, 1.4, 1.9 and 2.4 m above the floor level.
- Thermocouples located at the basement exterior opening (window) to measure the temperature at the simulated window and the temperature of the gas plume after the mock-window was opened.
- Thermocouples located on the exposed side of the door to the basement at the centre and at three heights: 0.9, 1.4 and 1.9 m (for UF-08 only).
- Residential photoelectric smoke alarms located near the stairwell.
- Air velocity measurements at the basement exterior opening (window).
- Differential pressure measurement between the fire compartment and the exterior of the test facility, located 2.0 m above the floor.
- Video recording of the burning fuel package.
- Thermocouples measuring temperatures in the wood cribs.

NRC·CNRC

The positioning of the instrumentation in the fire compartment on the basement level is shown in Figure 8.
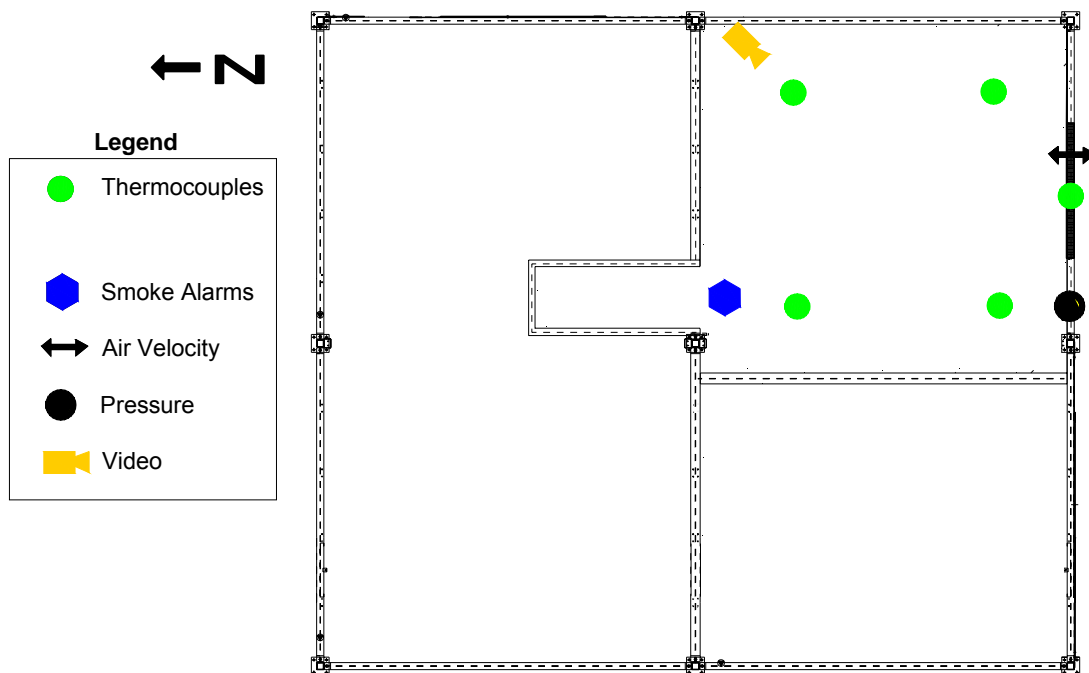
Figure 8. Fire Compartment instrumentation

2.5.2   First Storey

The instrumentation on the first storey included the following:

- Four vertical thermocouple arrays at the quarter points of the whole floor area.
- One vertical thermocouple array located at the door opening of the stairwell from the basement level.
- Gas sampling ports at the southwest quarter point, including:
  - $CO/CO_2/O_2$ at 0.9 m and 1.5 m above the floor.
  - Fourier Transform Infrared Spectroscopy (FTIR) at 1.5 m above the floor.
- Smoke density measurements at the southwest quarter point at 0.9 m and 1.5 m above the floor.
- Residential ionization and photoelectric smoke alarms located on the ceiling near the doorway to the basement.
- Air velocity measurements located at top of the basement stairwell at ceiling height and at 1.5 m above the floor.
- Differential pressure measurement between the fire compartment in the basement level and the first storey.
- Video recording from two locations.

The positioning of the instrumentation on the first storey is shown in Figure 9.

NRC·CNRC
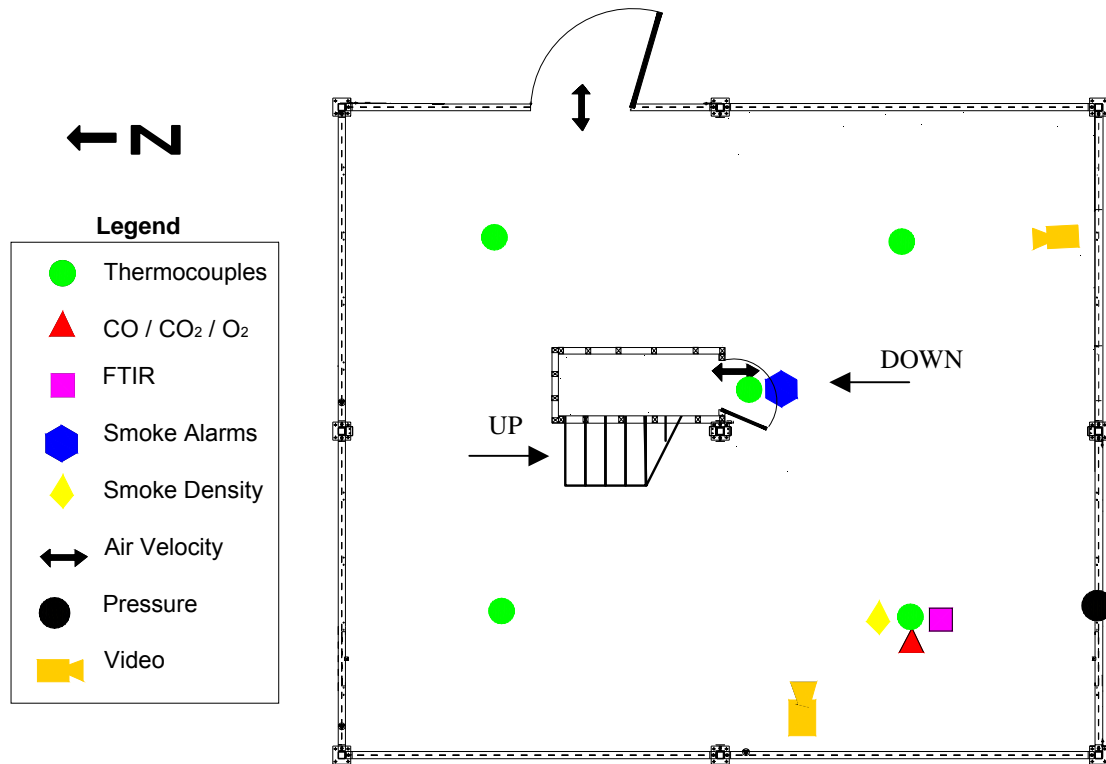
Figure 9. First storey instrumentation

2.5.3   Second Storey

The instrumentation on the second storey included the following:

- One vertical thermocouple array in the corridor at the top of the stairs.
- One vertical thermocouple array in the center of each bedroom.
- Residential ionization and photoelectric smoke alarms located on the ceiling in the corridor at the top of the stairs.
- Residential ionization and photoelectric smoke alarms located on the ceiling at the centre of each bedroom.
- Gas analysis ($CO/CO_2/O_2$) in the corridor at the top of the stairs at 0.9 m and 1.5 m above the floor.
- Smoke density measurements in the corridor at the top of the stairs at 0.9 m and 1.5 m above the floor.
- Air velocity measurements located at the top of the stairs at ceiling height and at 1.5 m above the floor.
- Video recording in the corridor.

The positioning of the instrumentation on the second storey is shown in Figure 10.

NRC·CNRC
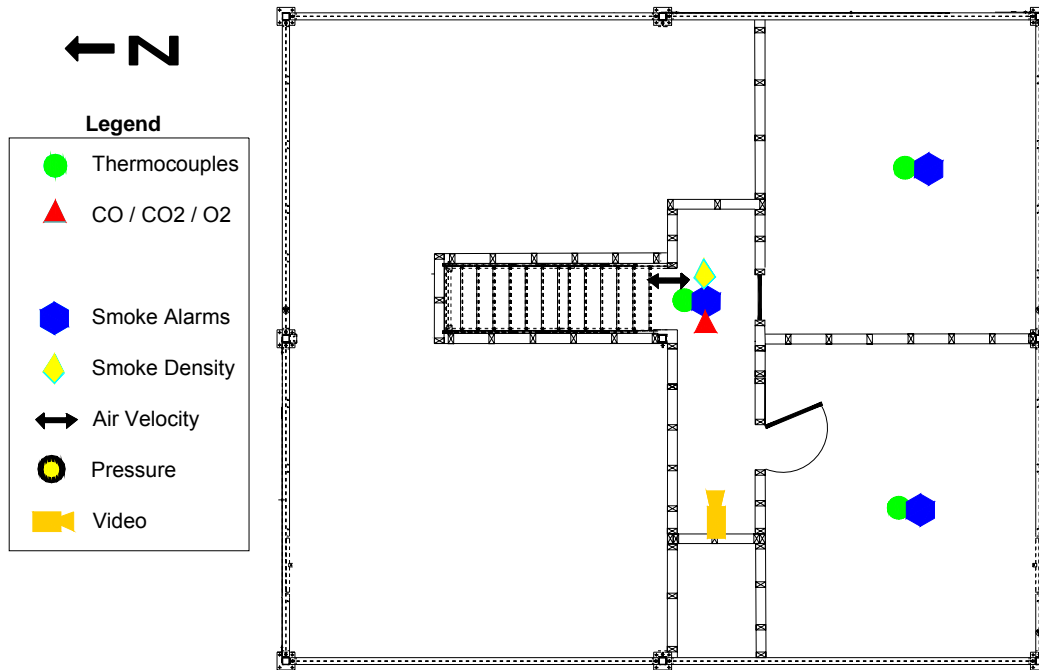
Figure 10. Second storey instrumentation

2.5.4   Exterior

Instrumentation of the facility exterior included the following:

- Air velocity measurements located at the basement window opening.
- Air velocity measurements located at the exterior door opening on the first storey.
- Video recording of the exterior window opening in the fire compartment on the basement level and the exterior door opening on the first storey.

2.6   Testing Procedure

The mock-up sofa was ignited in accordance with the ASTM 1537 test protocol [7] and data was collected at 5 s intervals throughout each test.

The non-combustible panel that covered the fire room's exterior rough window opening during the initial stage of each test was manually removed when the temperature measured at the top-center of the opening reached 300°C. The removal of the panel was to provide ventilation air necessary for combustion.

The exterior door on the first storey was opened at 180 s after ignition and left open, simulating a situation where some occupants, who would have been in the test house, escaped leaving the exterior door open while other occupants may still have been inside the house.

NRC·CNRC

The tests were terminated by extinguishing the fires using a manually operated sprinkler system when one of the following occurred (singly or in combination):
- Excessive flame penetration through the floor assembly;
- Structure failure of any part of the floor assembly;
- Compromise of safety of the test facility.

2.7 Construction Details of the Floor Assemblies

Eleven full-scale floor assemblies were tested in this first phase of the project. In each test, the floor assembly was installed in the three-storey test facility to create the ceiling portion over the fire compartment in the basement level. The floor assemblies had no ceiling sheathing attached on the underside, leaving the framing members and the subfloor exposed and unprotected from exposure to the fire from the burning fuel package.

For each type of floor assembly tested, the floor joist/truss spans were either chosen from the appendices of the NBCC or calculated based on the ultimate and serviceability limit states. Therefore, the floor joists/trusses could either span the entire length of the fire compartment space or require an intermediate beam support for shorter spans. When designing the assemblies, various aspects were considered including what is typically used for framing and subfloor materials in housing today, consideration of serviceability limit states, typical spacing, typical spans, typical depths, etc. As well, the assemblies were loaded at 50% of the specified load in the NBCC (see Section 2.9).

Details on the two tested assemblies (metal-web-connected wood trusses) are provided below.

2.7.1 Floor Assemblies with Metal-Web-Connected Wood Trusses

The two tests, documented in this report, were conducted using wood frame floor assemblies constructed using metal-web wood trusses and an OSB subfloor. The overall dimensions of the metal-web wood truss assemblies were 5079 mm by 5150 mm. Specific dimensions of the various components of the assemblies are provided in Figure 11 to Figure 14.

The metal-web-connected wood trusses were 302 mm deep, with cords of dimensions 38 mm x 64 mm. The metal webs (20 gauge) had teeth 9.5 mm long and 0.0171 teeth per square millimeter. The trusses were spaced at 400 mm on centre (see Figure 11). The bottom cords of the trusses were reinforced with 2 strongbacks 38 mm x 140 mm located toward the centre of the span (see Figure 11). Based on calculations of maximum strength and deflection, the truss span length chosen was 4.813 m (see Figure 11). This span allowed the metal-web wood trusses to extend across the entire length of the fire compartment (with no need for an intermediate support). Figure 12 shows the supporting beams.

13

NRC·CNRC
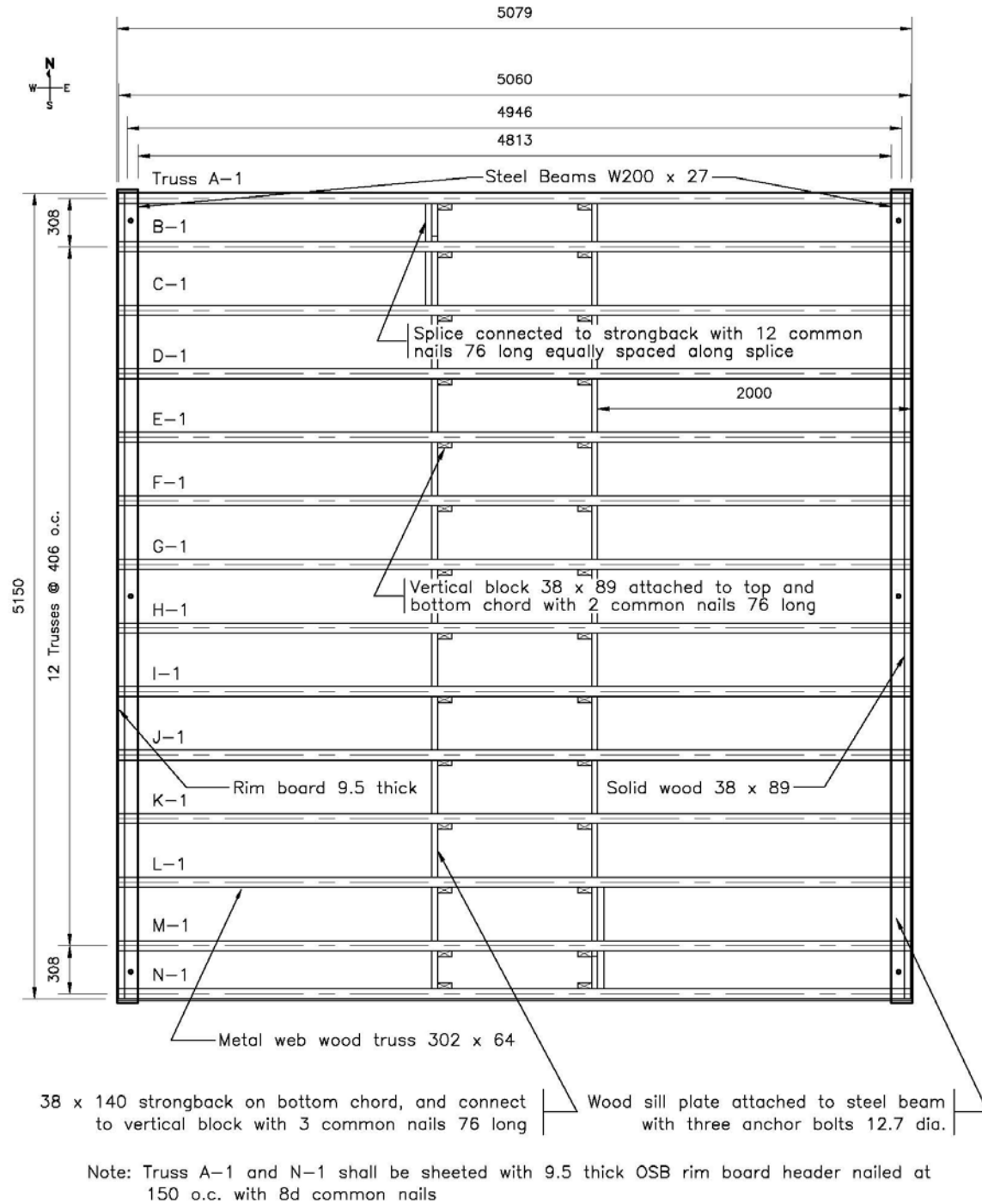
Figure 11. Metal-Web-Connected Wood Truss layout details (all dimensions in mm)
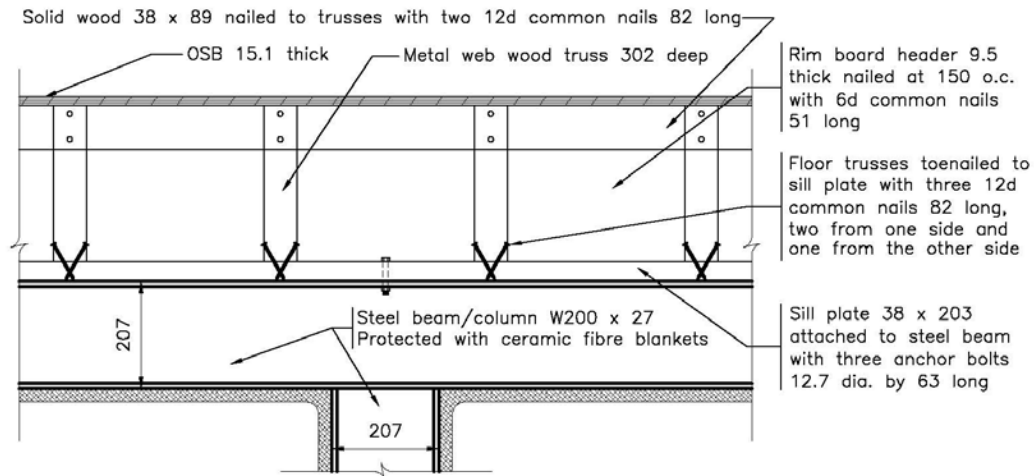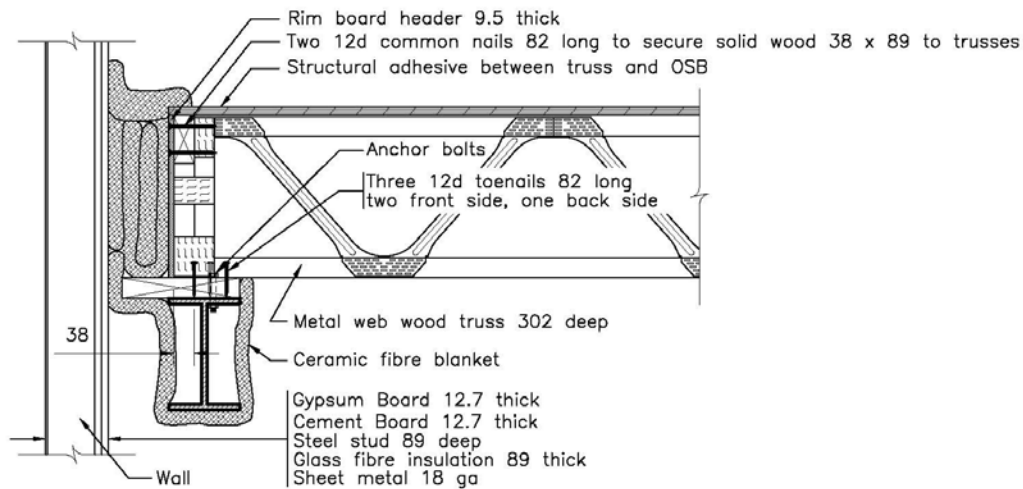
Figure 12. **End connection details and supports** (all dimensions in mm)

Each metal-web wood truss floor assembly was supported by two horizontal beams, each of which was supported by two columns (a total of four columns for each assembly) as illustrated in Figure 12. The beams were bolted to the columns, which were stiffened by bars and rested stably on the floor under the weight of the assembly and beams.

Figure 12 also shows the details of the end connection. Ceramic fibre blankets were used to fill any gaps between the assembly and the end walls. Ceramic fibre blankets were also used to protect the steel beams and columns so that they were not subjected to fire and would not fail during the tests.

In the metal-web wood truss test assemblies, rim boards (headers) 9.5 mm thick x 302 mm deep, were placed around the assemblies as shown in Figure 11. In addition, a

NRC·CNRC

solid wood 38 mm x 89 mm was added at the top ends of the trusses to provide lateral support, see Figure 11 and Figure 12.

OSB was used as the subfloor material in the floor assemblies. The specific OSB material used was selected based on a separate study documented in reference [5]. The subfloor panels were 15.1 mm thick in both assemblies, with a full panel size being 1.2 x 2.4 m. The longer panel edges had a tongue and groove profile while the short panel edges were square-butt ends. Figure 13 shows the layout of the subfloor. The screw pattern and description of screws used to attach the OSB panels to the metal-web wood trusses are shown in Figure 14.
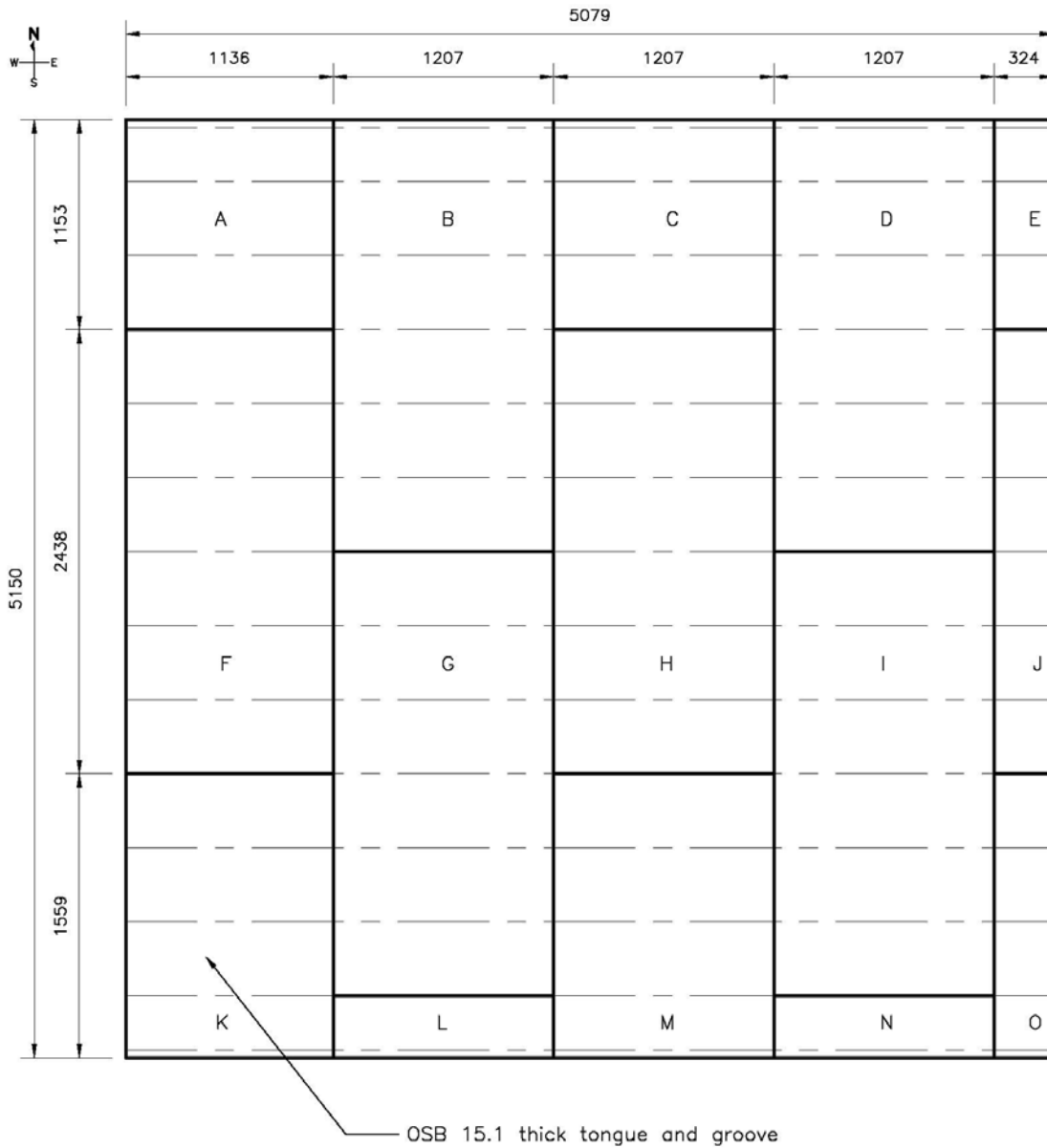
Figure 13. Subfloor layout details (all dimensions in mm)

NRC·CNRC
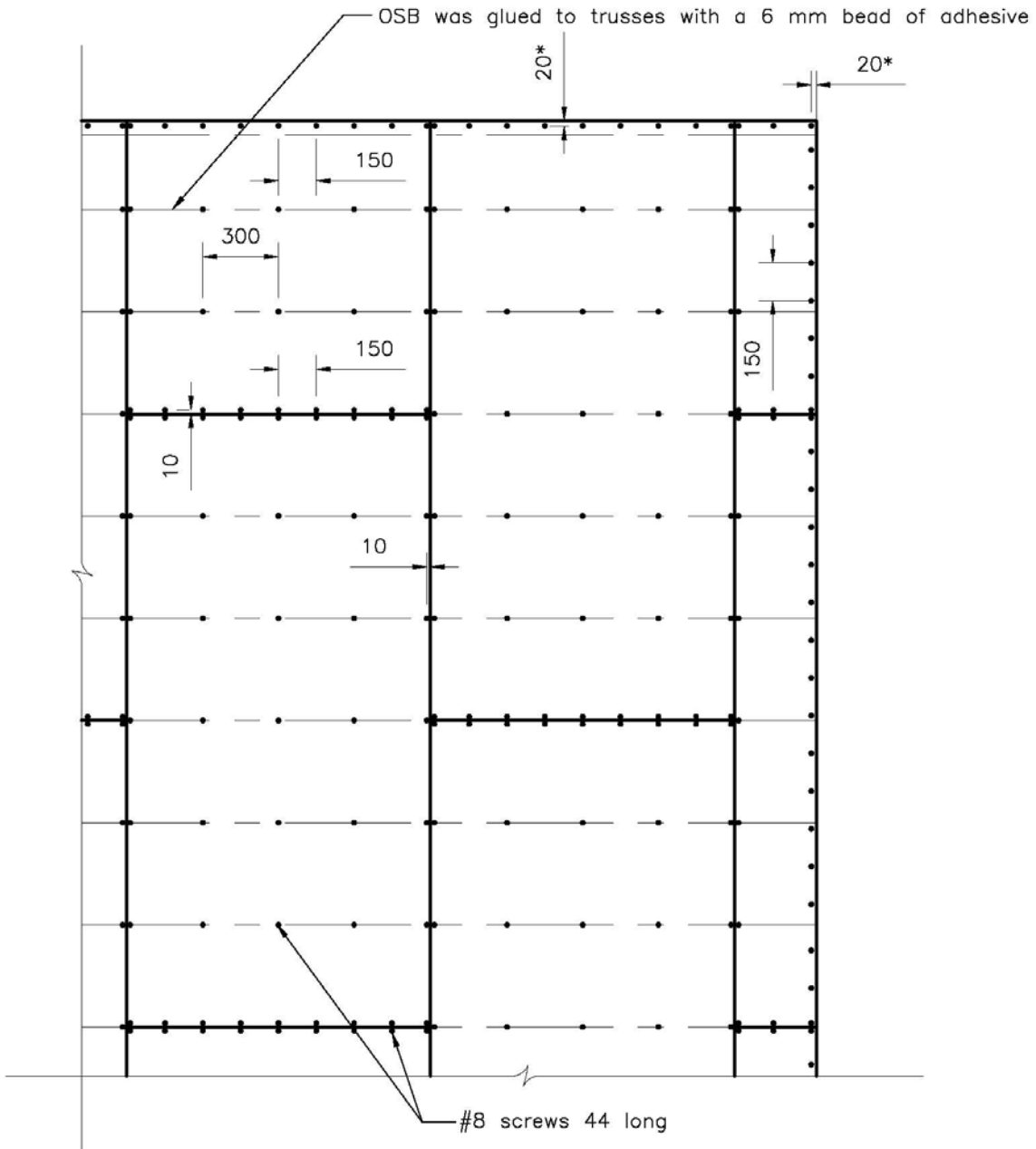
Note: — OSB should be fully secured within 10 minutes of applying adhesive
or sooner, if required by the subfloor adhesive manufacturer.
— Two 6 mm bead of adhesive shall be used at abutting panel edges.
* 20 mm from edges to allow screws to be secured to the trusses due
to the 9.5 mm thick rim board around the perimeter of the assembly.

PARTIAL VIEW

Figure 14. Subfloor screw pattern and screw description (all dimensions in mm)

NRC·CNRC

2.8 Instrumentation of the Floor Assemblies

2.8.1 Temperatures in the Floor Assemblies

One hundred and eight Type K (20 gauge) chromel-alumel thermocouples, with a thickness of 0.91 mm, were used for measuring temperatures at a number of locations throughout each assembly. The thermocouple locations on the unexposed and exposed sides of the assemblies are shown in Figure 15 and Figure 16. These locations were chosen to monitor the conditions of the assembly at critical locations during the fire tests.
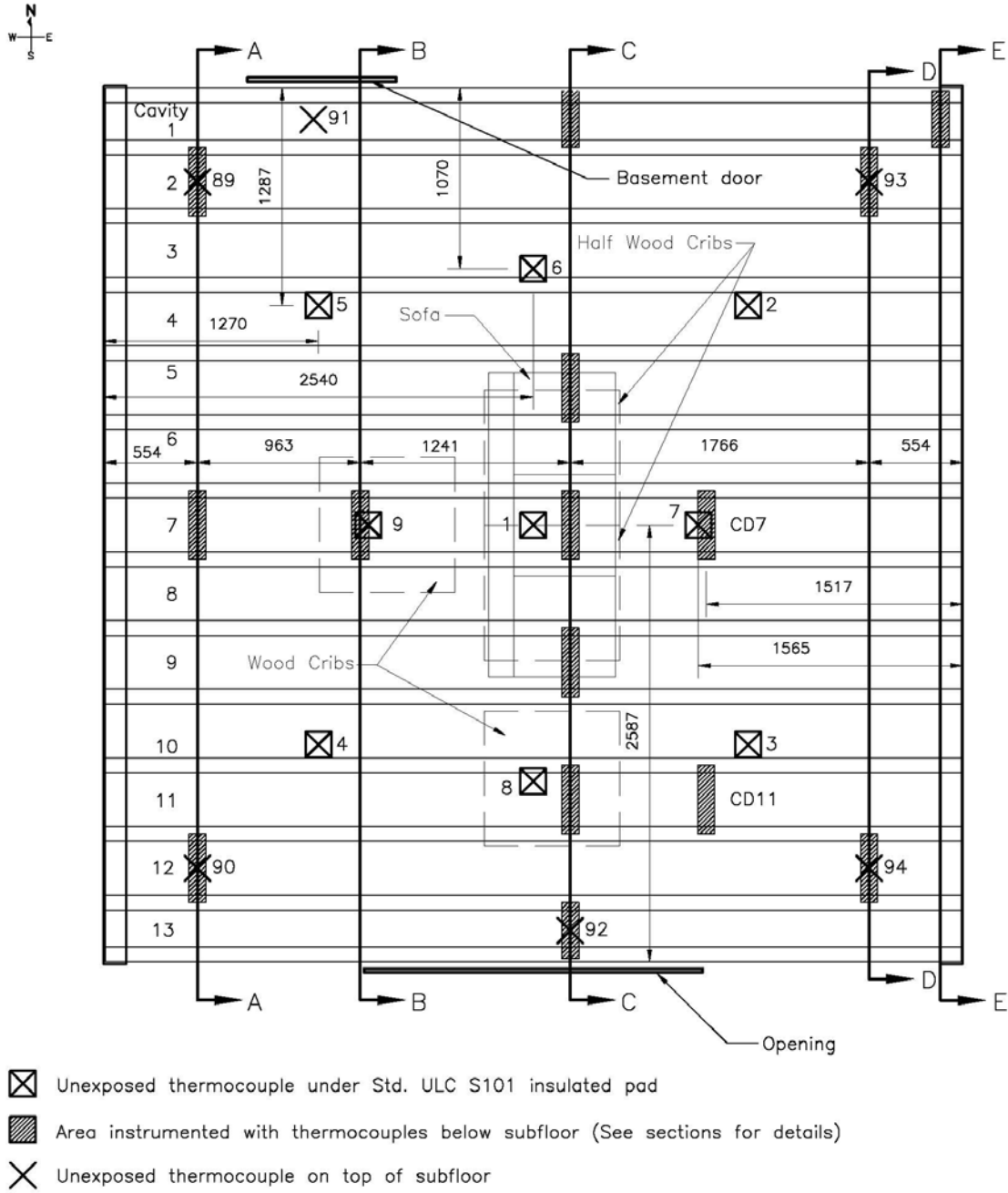
Figure 15. Thermocouples locations (all dimensions in mm)
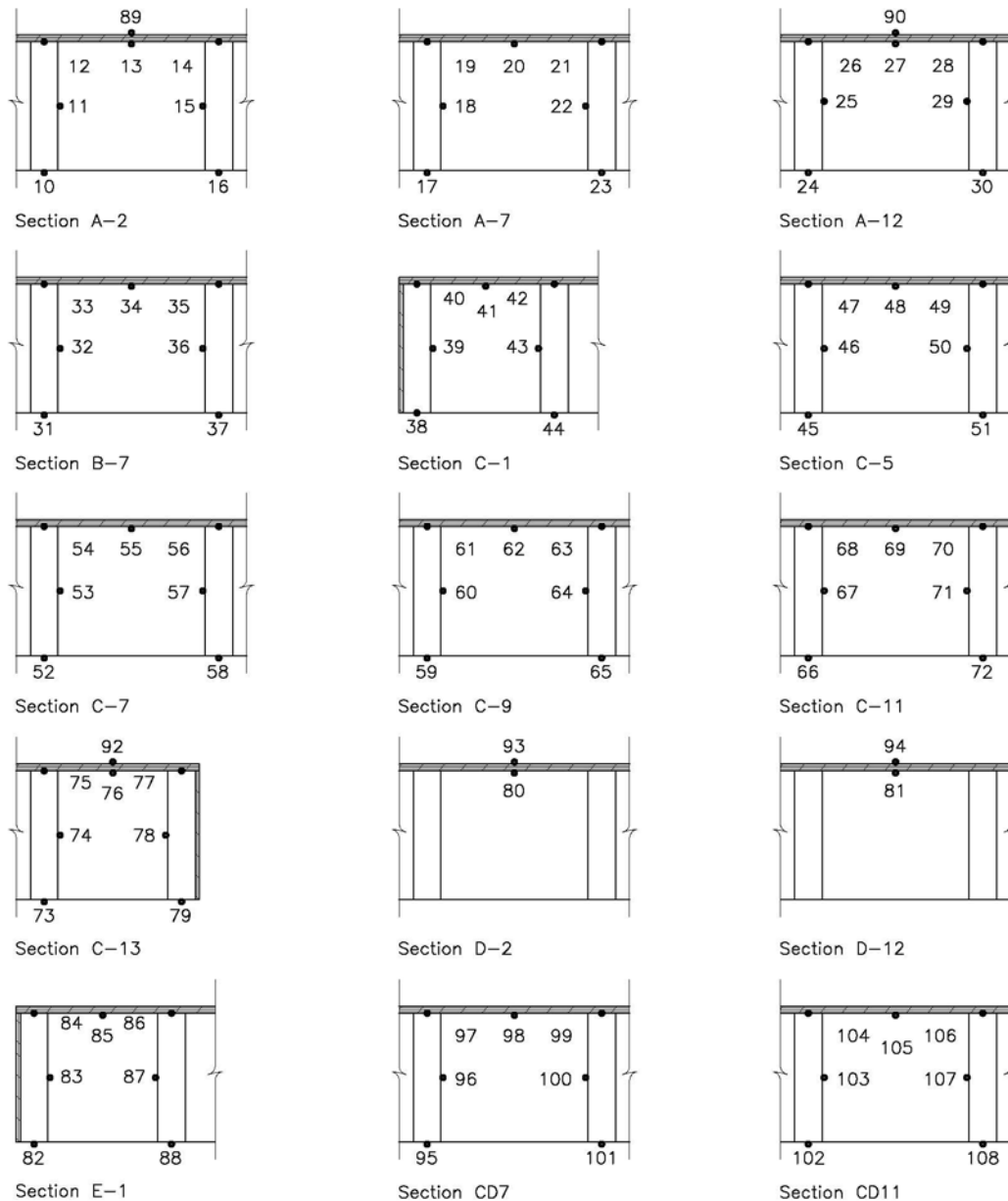
Figure 16. Thermocouples locations reflecting the different sections shown in Figure 15

2.8.2 Flame Penetration of the Floor Assembly

Flame penetration through the floor assembly is considered to be an initial indicator of the impending failure of the assembly. A device was developed and used for the tests to better determine the time for flames to penetrate the floor. The special device consisted of a wire mesh placed at 3 locations on the unexposed surface of the floor assembly, specifically at three of the tongue and groove joints, as shown in Figure 17. A detailed description of the device is provided in reference [8].

19

Flame penetration devices

OSB 15.1 thick tongue and groove

NRC·CNRC
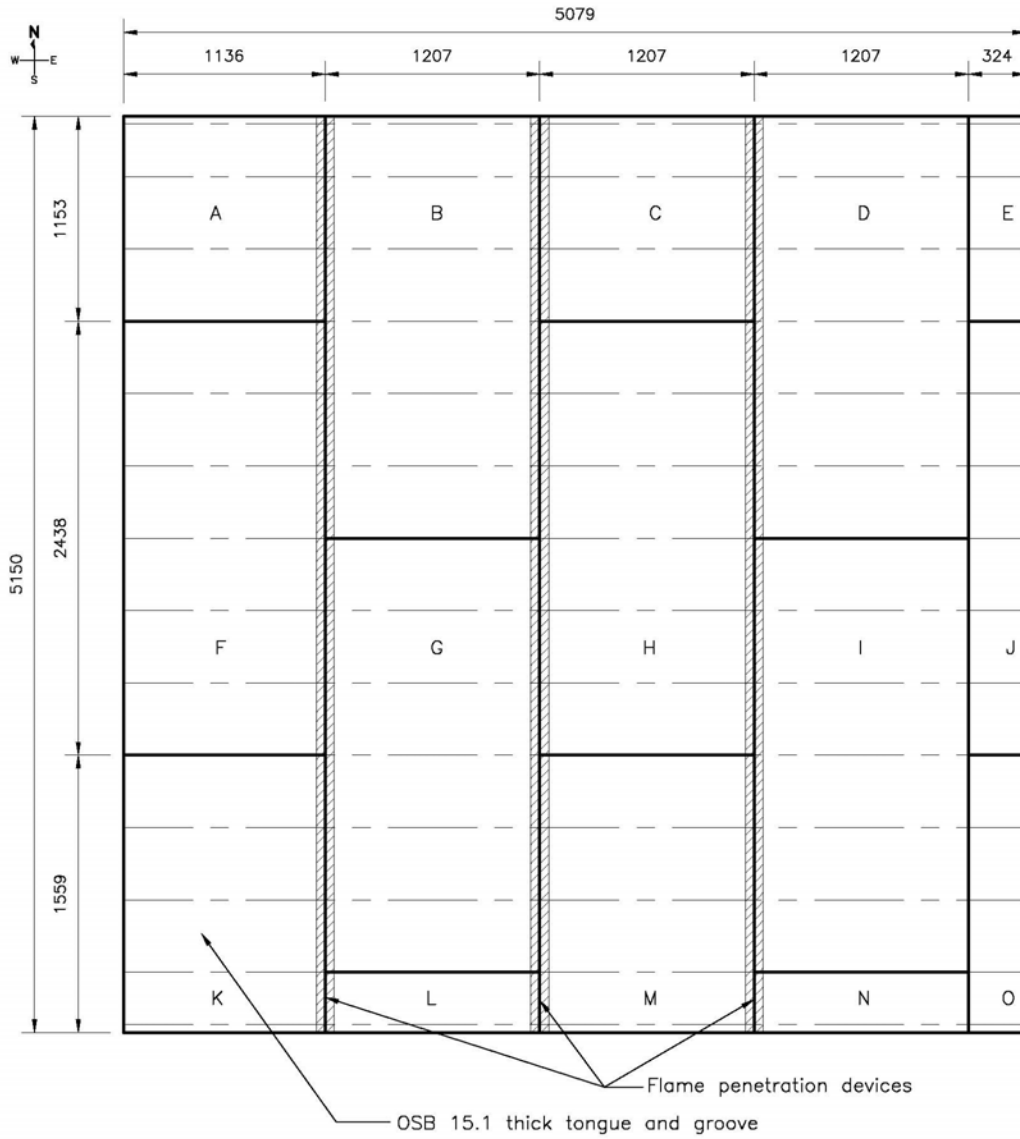
Figure 17. Wire mesh device to detect flame penetration (all dimensions in mm)

2.8.3   Deflection of the Floor Assemblies

The floor deflection was measured at 9 points. The measurement technique utilized 9 rods that were touching the tops of 9 concrete blocks placed on the unexposed surface of the floor assembly at the locations shown in Figure 18.   This ensured that the downward movement of the subfloor was monitored during the fire exposure.   The deflections were recorded using the electro-mechanical method described in reference [9].
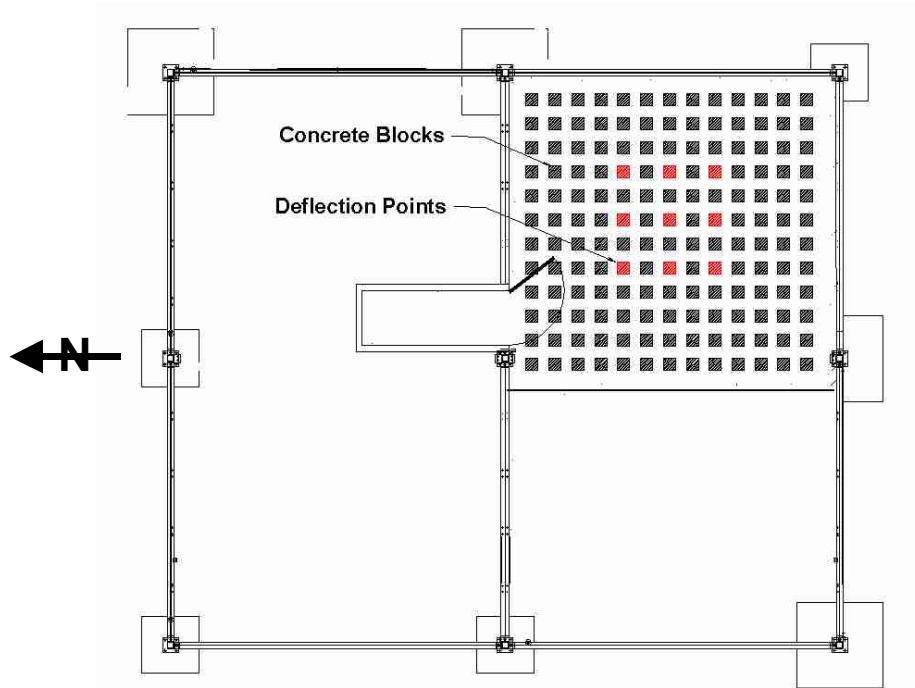
Figure 18. Loading blocks and locations of the deflection measurement points on the unexposed side of the floor

2.9   Loading of the Floor Assembly

The load applied on the floor assemblies was equal to the self-weight (dead load) of the assembly plus an imposed load (live load) of 0.95 kPa (i.e., half of that prescribed by the NBCC [1] for residential occupancies, i.e., half of 1.90 kPa). The rationale to use this combination was based on the fact that in a fire situation, only part of the prescribed load is available. In fact, a number of international standards (Eurocode [10], New Zealand and Australian standards [11 and 12], and ASCE [13]) use a load combination similar to the one used in this study for fire design purposes. The total imposed load applied to the floor was equal to 0.95 kPa multiplied by the floor area; this is equivalent to approximately 25 kN.

The loading method consisted of 144 concrete blocks (totalling 2490 kg) distributed uniformly on the floor as shown in Figure 18. The blocks were 190 x 190 x 390 mm (nominal 8" x 8" x 16") and weighed 17.3 kg each. To prevent the blocks from falling into the basement and causing any damage, a restraining system was designed using a series of pipes attached to beams on both ends, which were secured to the steel frame of the 3-storey house, as shown in Figure 19. The pipes were inserted through the hollow cores of the concrete blocks prior to the fire tests. The weight of the pipes was included in the total imposed load.
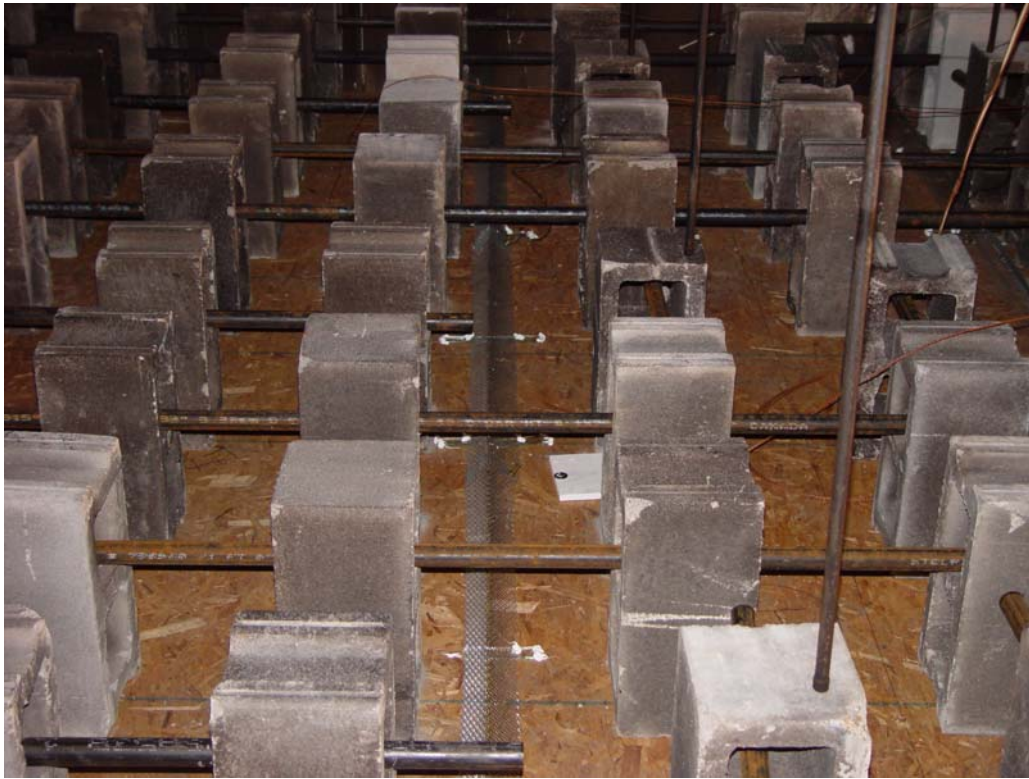
Figure 19. Device to hold the loading blocks

Calculations of the maximum imposed loads (live load) that the floors were capable of supporting (based on the span used and production of maximum allowable bending stress/deflection, whichever applies, calculated in accordance with CAN/ULC-S101 standard [14]) indicate that these floors had a large strength reserve. The calculated reserves in %, based on comparison of the loading requirement with maximum imposed loads, which govern in this case, are shown in Table 1.

Table 1. Reserve Live Load Capacity

Test Number	Imposed load (kPa)	Maximum imposed load (kPa)		Reserve of live load capacity (governed by strength) (%)	Reserve of live load capacity (governed by deflection) (%)
		Strength	Deflection		
UF-07	0.95	2.58	3.45	63%	72%
UF-08	0.95	2.58	3.45	63%	72%

NRC·CNRC

3   RESULTS OF THE TESTS

3.1   Recording of Results

Compartments and floor assemblies were instrumented with smoke alarms, thermocouples, gas analyzers (CO, CO_2 and O_2), smoke density instruments, pressure measurement instruments, and video cameras.   The measurements of temperatures, gas concentrations, smoke density and pressure were recorded at 5-second intervals using a Solotron data acquisition system.

In the following sections, discussions of the different recorded results are provided. Figures showing various quantities have been organized as follows:
- Figure 20 to Figure 34 show the test results for temperatures vs. time in the compartments, and at different openings (basement window opening, door opening to the basement, door opening to the outside), and at the top of the stairs (between the basement and first storey, and between the first and second storeys).
- Figure 35 and Figure 36 show the test results for temperatures vs. time on the unexposed side of the floor assemblies.
- Figure 37 and Figure 38 show the test results for temperatures vs. time on the exposed side of the floor assemblies.
- Figure 40 and Figure 41 show the test results for deflection vs. time on the unexposed side of the floor assemblies.
- Figure 42 and Figure 43 show the results from the flame-sensing devices.
- Figure 44 to Figure 53 show the smoke and gas measurement results (CO, CO_2, O_2 and optical density) and tenability conditions vs. time in the compartments.
- Figure 54 and Figure 55 show the test results for the sequence of fire events in Tests UF-07 and UF-08.

Although velocity measurements were recorded at various openings during the experiments, they are not discussed in this report.   However, these results may be useful for fire modeling purposes in the future.

3.2   Observations and Recordings

Table A 1 and Table A 2 show the test summary for UF-07 and UF-08, respectively. This includes a short description of the tests, the times for various events, and the detection times for all smoke alarms that operated.   The tests were stopped after indications of either the structural or load-bearing failure of the floors.

3.3   Time-temperature Curves at Different Locations

3.3.1   Temperatures in the Compartments

In the following sections, the temperatures in the basement, first storey, and second storey are discussed. All thermocouple trees provided measurements at 0.4, 0.9, 1.4, 1.9 and 2.4 m above the floor level. Figure 20 to Figure 25 show these temperatures.

3.3.1.1 Basement

Figure 20 (a, b, c, and d) and Figure 21 (a, b, c, and d) show the temperatures in the basement fire compartment at the 4 room quarter points, southeast (SE), southwest (SW), northeast (NE) and northwest (NW) in Test UF-07 and Test UF-08, respectively.

In Test UF-07 (open basement doorway, Figure 20), the temperatures rose to a maximum of 700 to 800ºC in the first 100 to 130 s. The initial peak temperature was likely due to the high rate of heat release from the mock-up sofa near its peak burning rate. As shown in the figure, the initial temperature rise was faster at the 2.4 and 1.9 m heights than the other heights because the hot smoke layer formed first at the ceiling and flames also impinged on the ceiling. Just after the maximum temperature was reached, there was a slight decrease in temperatures likely due to the combined effect of opening the basement window at 95 s and the fact that a significant portion of the polyurethane foam component of the fuel package had been consumed. The temperatures decreased further after the exterior door on the first storey was opened, which created a movement of air and smoke between the basement and first storey. The fresh air coming from the basement window increased combustion of the wood cribs and the exposed floor assembly, which caused the temperatures to increase steadily again, reaching a maximum temperature of about 850 to 900ºC in the SE and SW quadrants. It should be noted that the temperatures (due to the mock-up sofa burning) were lower at the location of the NE thermocouple tree. This may be partially attributed to the fact that the NE corner was less impacted by the fire, as it was farthest away from the fire source and that most of the hot gases were moving to the upper storeys through the SE to NW path.

In Test UF-08 (closed basement doorway, Figure 21), the trend was similar to Test UF-07. There was an initial increase in temperatures in the first 120 s followed by an appreciable decrease due to the combined effect of opening the basement window and depletion of the polyurethane foam component of the fuel package. A sustained gradual temperature rise followed as the wood crib fire continued to grow. In this test, compared to the results in Test UF-07, the temperatures at the different heights were more clearly distinguished from each other until very late in the test. Except for the NE thermocouple tree, the peak temperature during the burning of the mock-up sofa was higher than the temperatures reached during the burning of the wood cribs and floor assembly for the first 460 s. Beyond this time, the temperatures reached higher values (about 800ºC). At about 470 s, the temperatures measured at the thermocouple tree locations showed the highest values. This may be due to the flames penetrating through the floor, creating holes, and allowing air to enter the basement and increase the combustion in that region. The temperatures started decreasing after extinguishing the fire using sprinklers.

For both Tests UF-07 and UF-08, combustion was dominated by the mock-up sofa during the first 100 to 140 s, while the wood cribs and floor assembly, including the subfloor, provided the fuel for combustion after this period. The duration of the fire was shorter for Test UF-07 compared to Test UF-08 because the availability of more air in Test UF-07 resulted in faster and more efficient combustion. For Test UF-08, combustion air was limited until late in the test.

NRC·CNRC
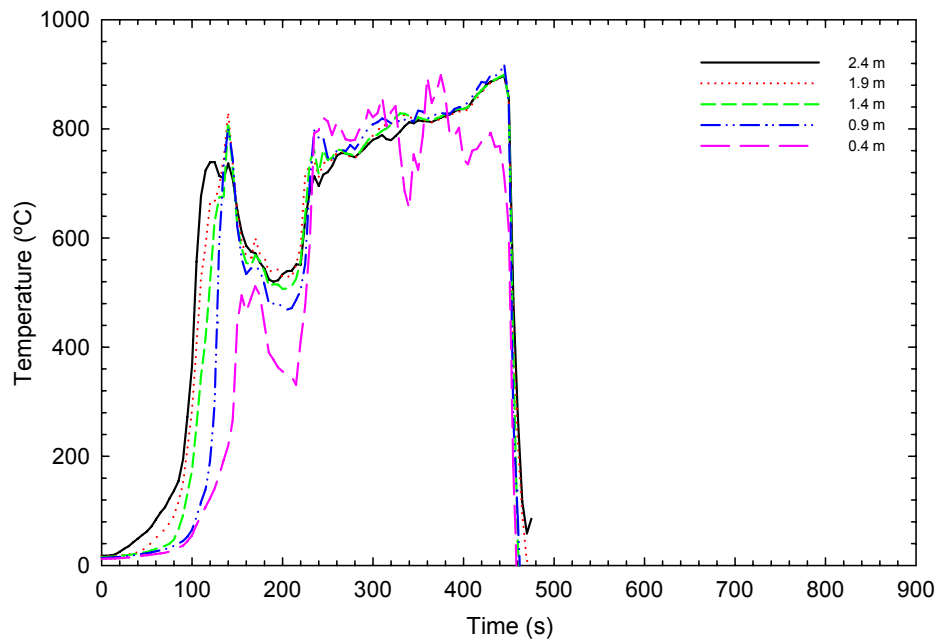
a) Basement SE quadrant
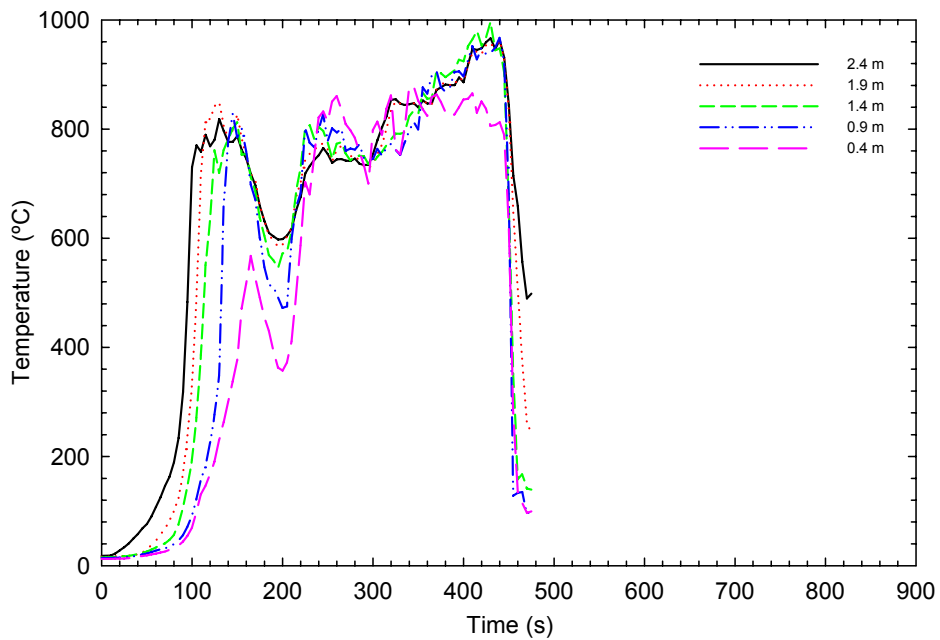
b) Basement SW quadrant

Figure 20 (a and b). TC Trees in the basement for Test UF-07

NRC·CNRC
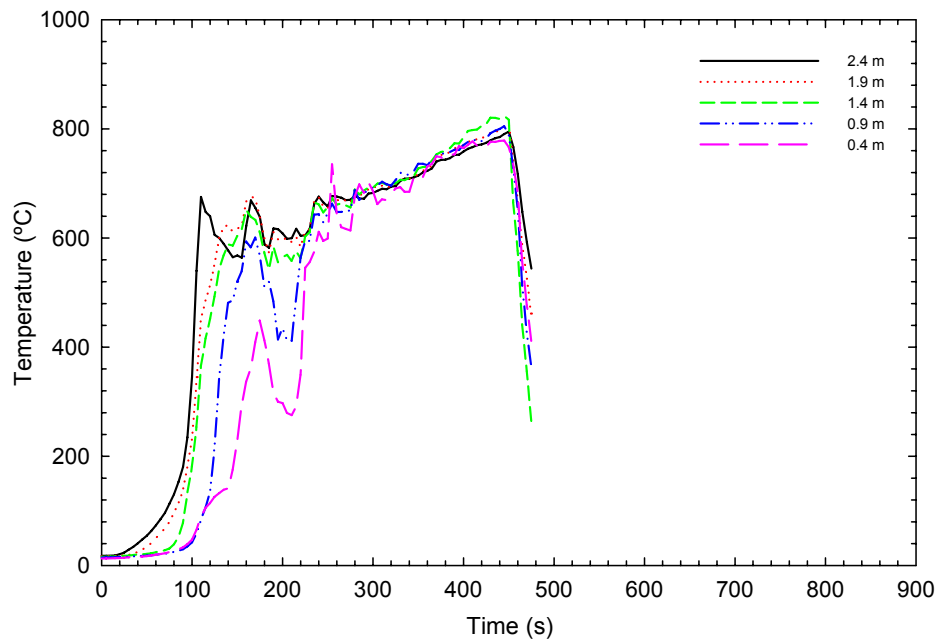
c) Basement NE quadrant
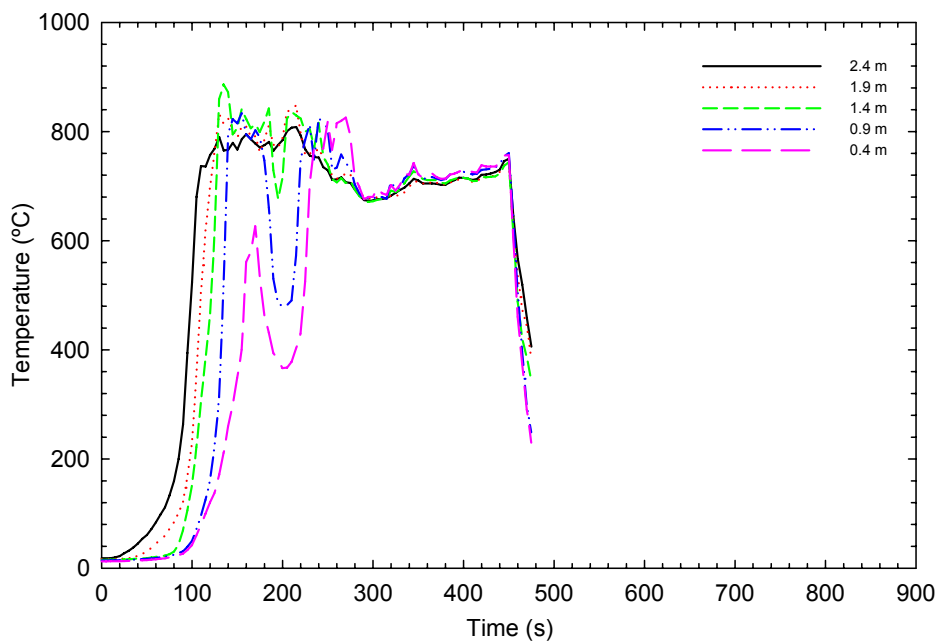
d) Basement NW quadrant

Figure 20 (c and d). TC Trees in the basement for Test UF-07

NRC·CNRC
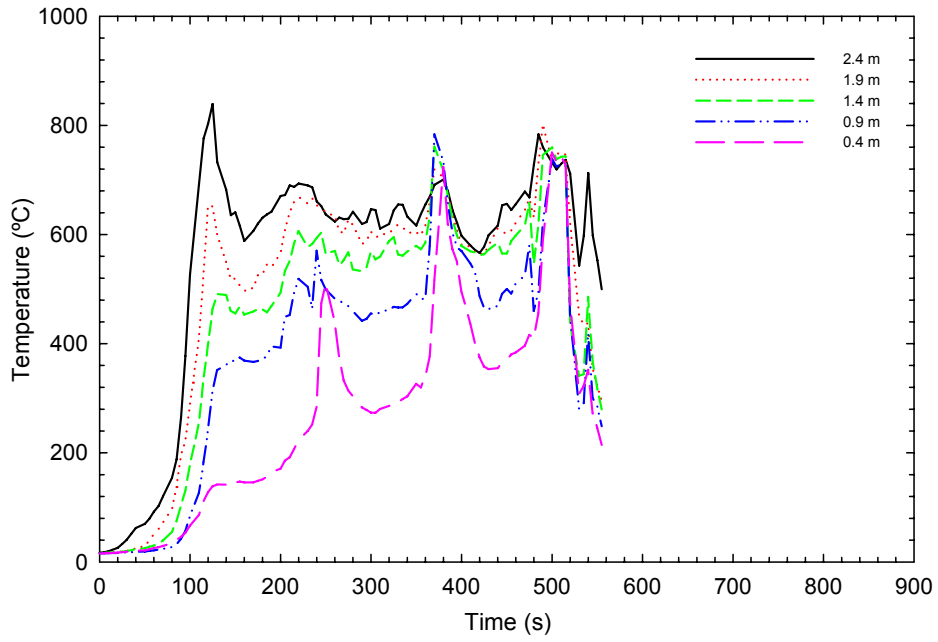
a) Basement SE quadrant
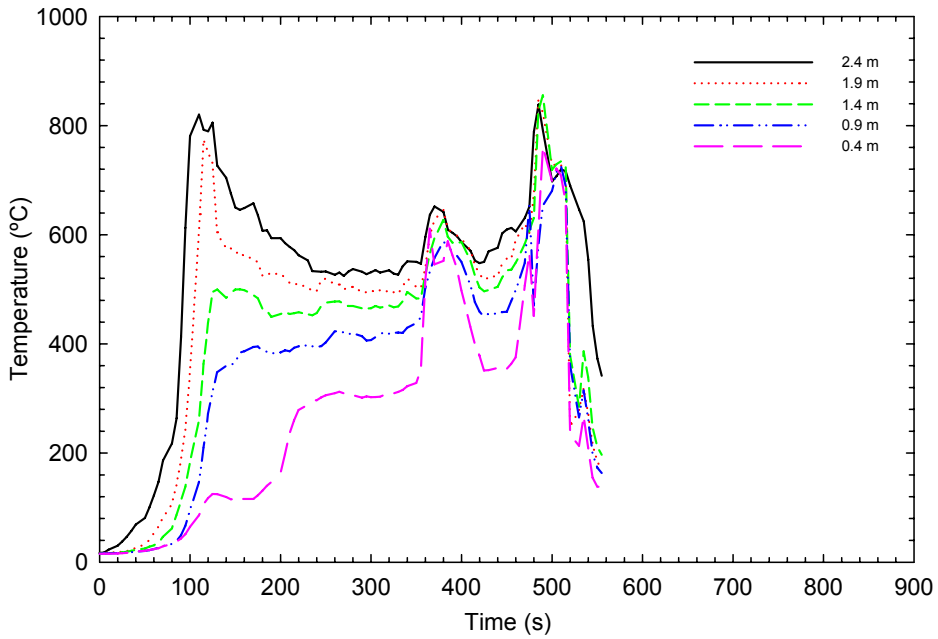
b) Basement SW quadrant

Figure 21 (a and b). TC Trees in the basement for Test UF-08

27
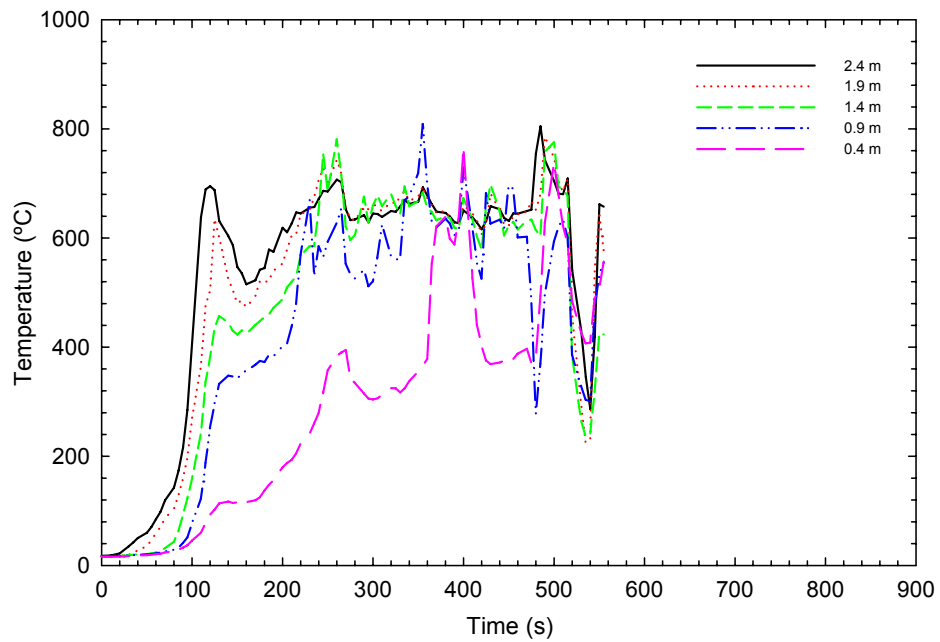
c) Basement NE quadrant
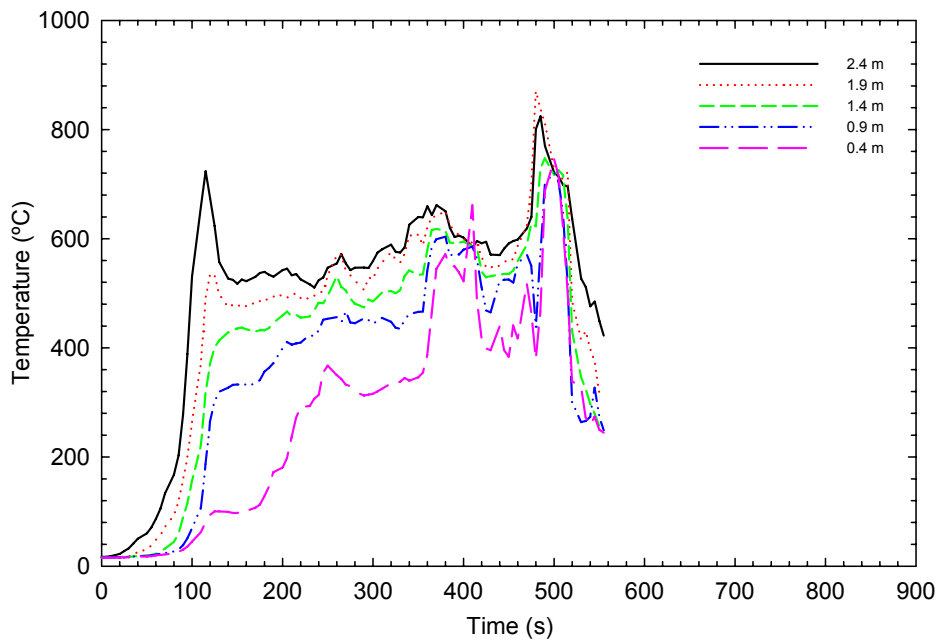
d) Basement NW quadrant

Figure 21 (c and d). TC Trees in the basement for Test UF-08

28

NRC·CNRC

3.3.1.2 First storey

Figure 22 (a, b, c, and d) and Figure 23 (a, b, c, and d) show the temperatures measured at the thermocouple tree locations on the first storey at the 4 quarter points, SE, SW, NE and NW in Tests UF-07 and UF-08, respectively.

In Test UF-07 (open basement doorway, Figure 22), the temperatures increased due to the heating of the floor from the basement fire underneath and due to the hot gases and smoke migrating from the basement. The temperatures peaked at around 220 s and started coming down after this time probably due to the opening of the exterior door allowing fresh air to enter into the first storey. The highest temperatures were recorded at the SE thermocouple tree because the fire in the basement fire compartment was just underneath this thermocouple tree.

In Test UF-08 (closed basement doorway, Figure 23), the temperatures increased very slowly mainly because the doorway to the basement was closed. The migration of the hot gases and smoke to the first storey did not start until late in the test when openings started forming in the floor or the door to the basement started burning. Before 460 s, the temperatures measured at the thermocouple tree locations were low and comparable. Near the end of the test, there was a sharp increase in temperatures at the thermocouple tree locations. The test was terminated after the collapse of the floor assembly at 474 s; consequently the temperatures started decaying.

The temperatures recorded on the first storey for Test UF-08 were much lower before flame penetration occurred than those recorded in Test UF-07. After flame penetration, temperatures in Test UF-08 showed a very sharp increase.
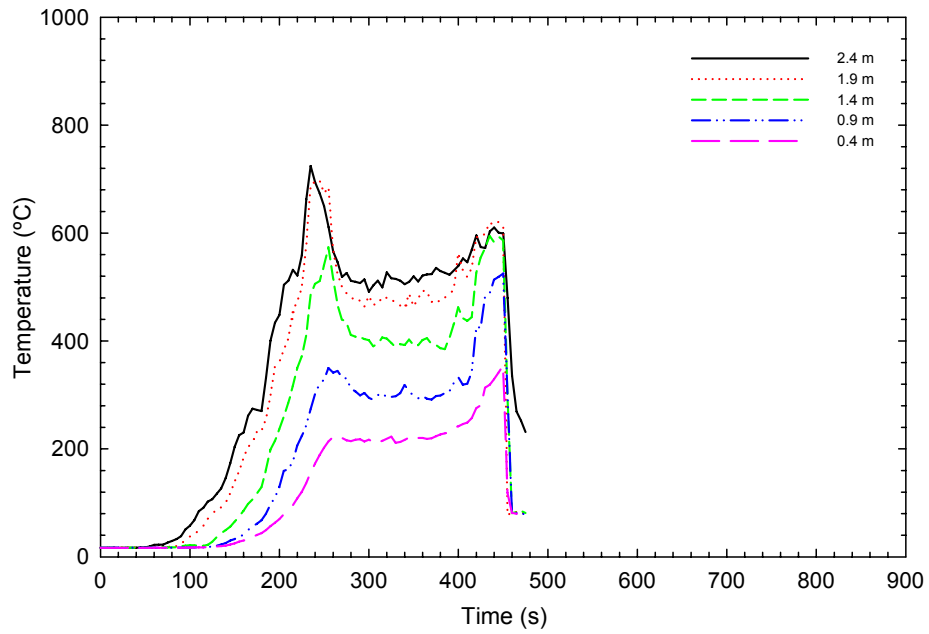
a) 1st Storey SE quadrant
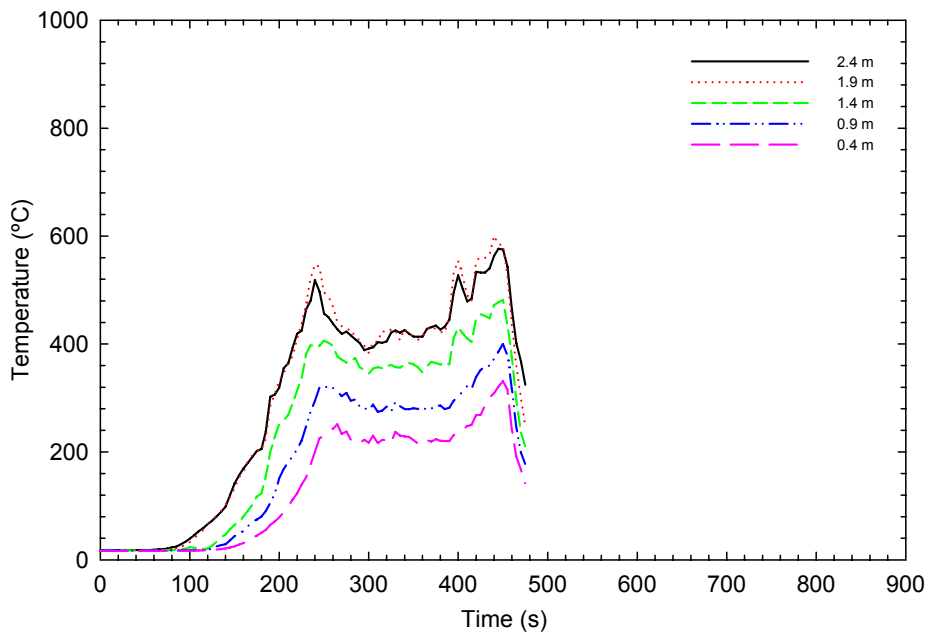
b) 1st Storey SW quadrant

Figure 22 (a and b). TC trees in the first storey for Test UF-07

NRC·CNRC
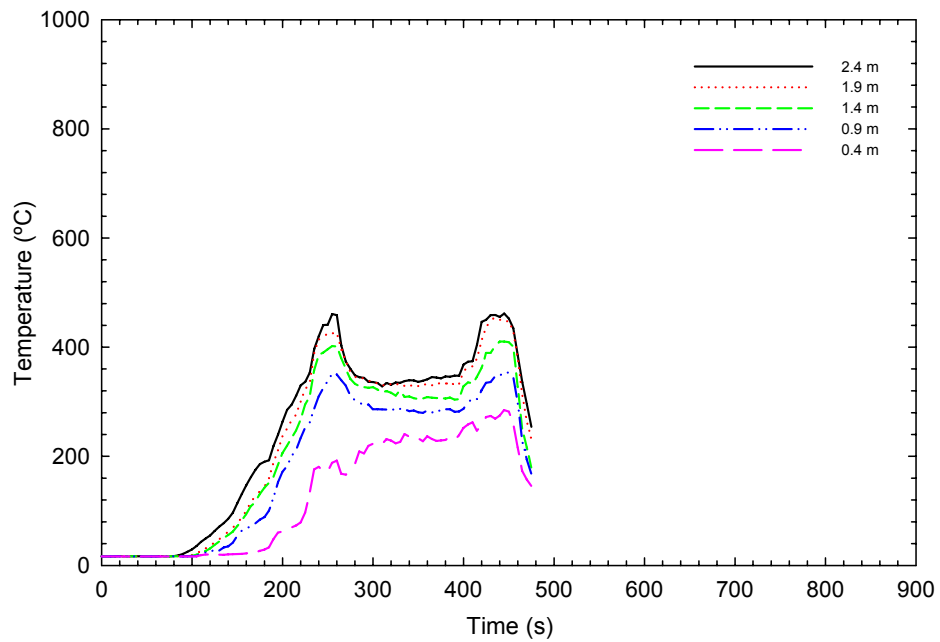
c) 1st Storey NE quadrant
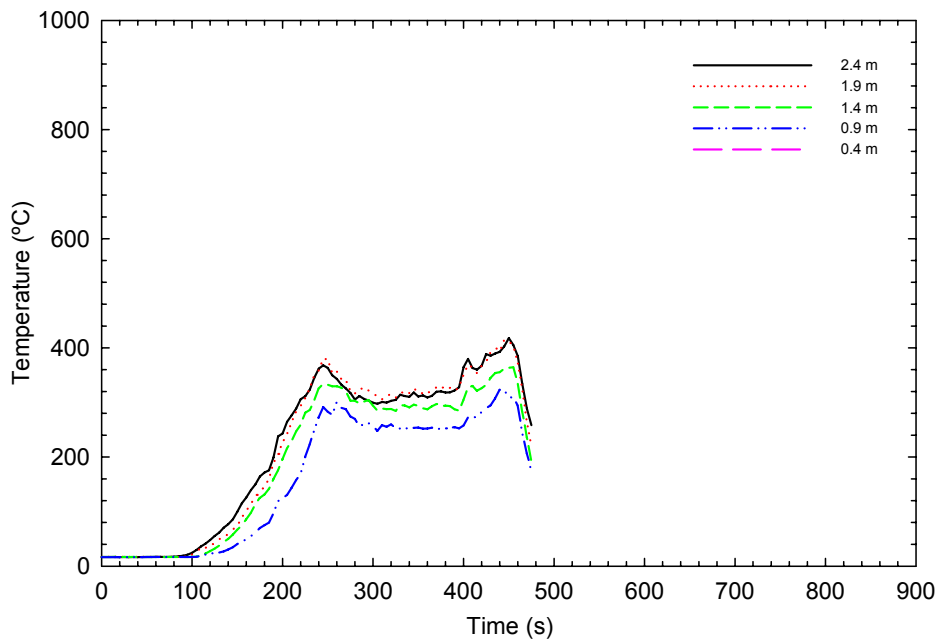
d) 1st Storey NW quadrant

Figure 22 (c and d). TC trees in the first storey for Test UF-07

NRC·CNRC
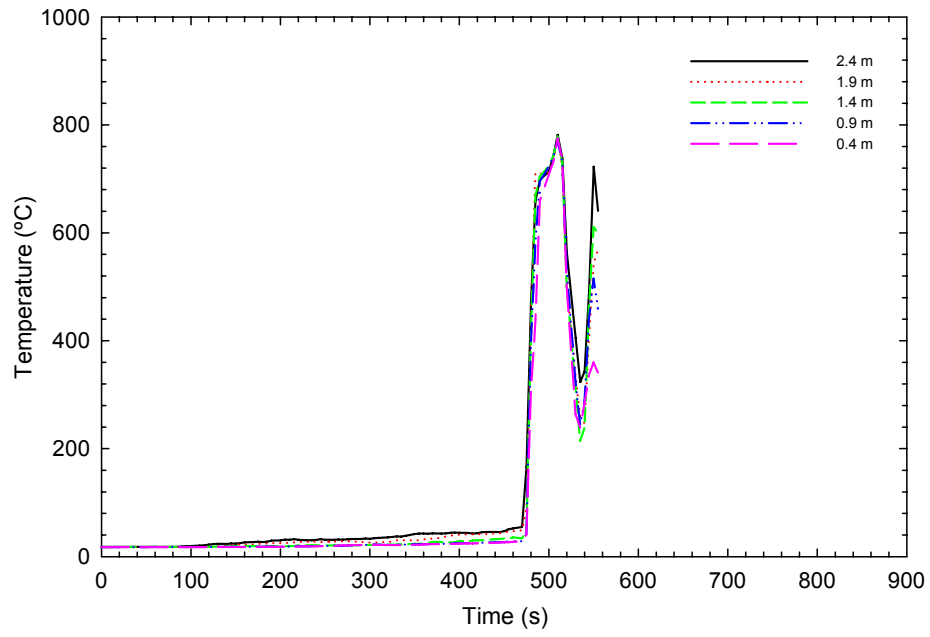
a) 1st Storey SE quadrant
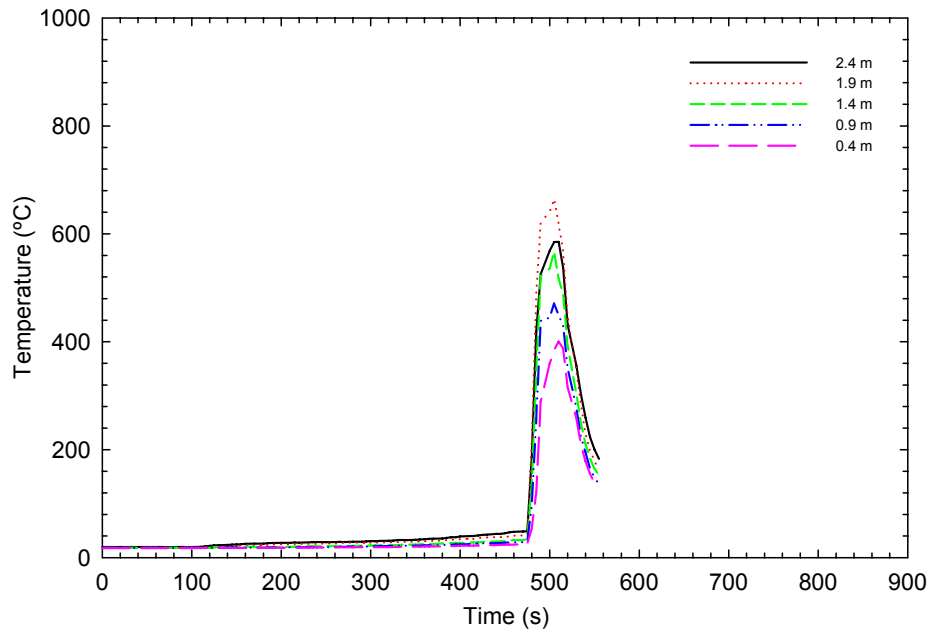
b) 1st Storey SW quadrant

Figure 23 (a and b). TC trees in the first storey for Test UF-08

NRC·CNRC
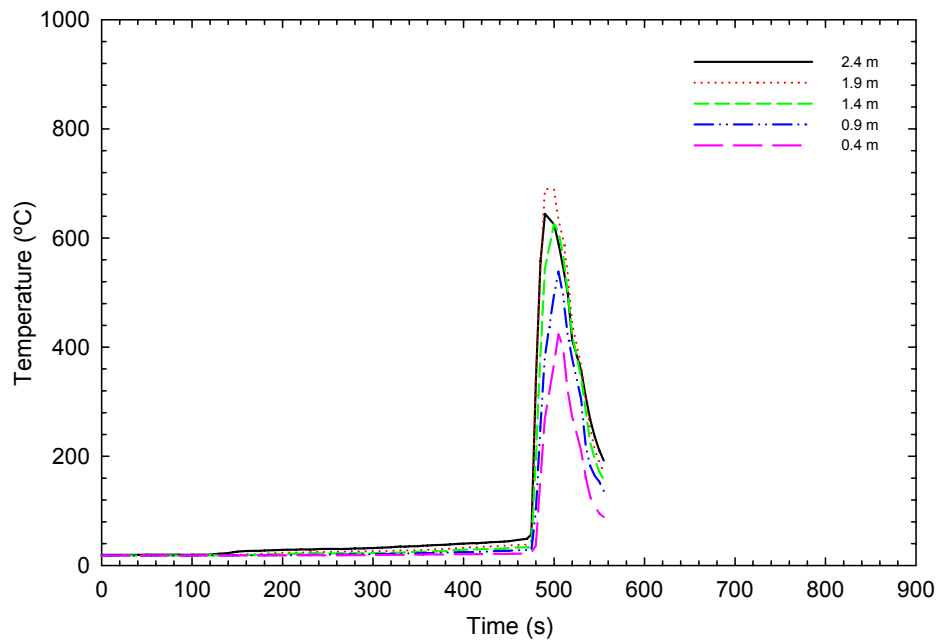
c) 1st Storey NE quadrant
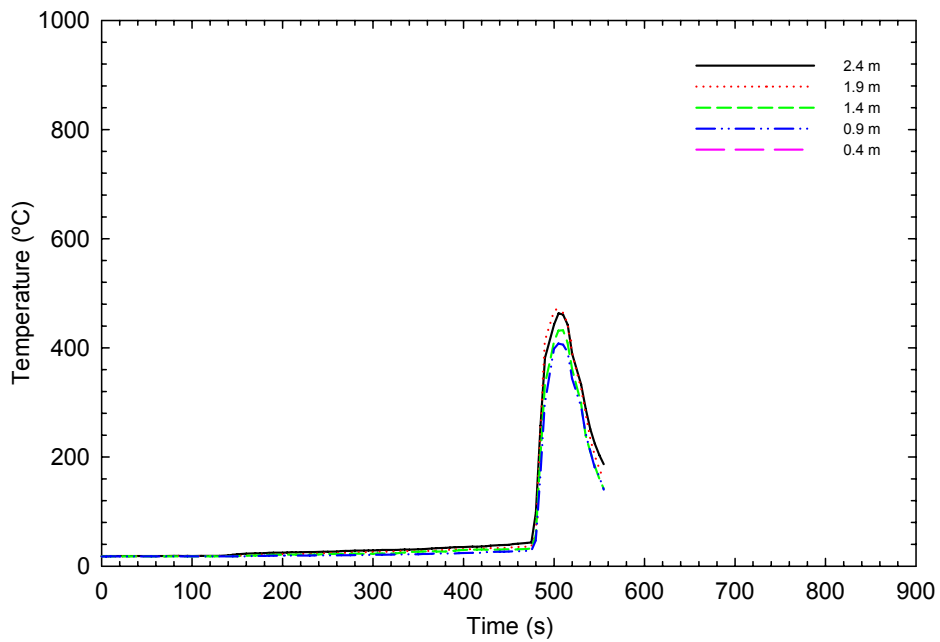
d) 1st Storey NW quadrant

Figure 23 (c and d). TC trees in the first storey for Test UF-08

NRC·CNRC

3.3.1.3   Second storey

Figure 24 (a) and Figure 24 (b) show the temperatures in the SE and SW bedrooms, respectively for Test UF-07. The door to the SE bedroom was closed while the door to the SW bedroom was open. The temperatures remained at ambient temperature for about the first 200 s for the SE bedroom and 120 s for the SW bedroom. After these times, the temperatures, at different heights within the rooms, started increasing. This increase was greater for the SW bedroom than the SE bedroom because the door to the SW bedroom was open. Smoke entered the SE bedroom mainly through gaps around the door. Maximum temperatures of about 25ºC and 160ºC were reached at the 2.4 m height above the floor level in the SE and SW bedrooms, respectively. For the SW bedroom, the temperatures peaked around 250 s and subsequently decreased probably due to fresh air coming from the opening of the exterior door on the first storey.

Figure 25 (a) and Figure 25 (b) show the temperatures in the SE and SW bedrooms, respectively for Test UF-08. The door to the SE bedroom was closed while the door to the SW bedroom was open. Ambient temperature was measured for the duration of the fire test in the SE bedroom and for about the first 200 s in the SW bedroom. After 200 s in the SW bedroom, the temperatures, at different heights, started increasing. The temperatures in the SW bedroom were higher than those in the SE bedroom because the door to the SW bedroom was open. The smoke entered the SE bedroom mainly through gaps around the door. Maximum temperatures of about 160ºC were reached at the 2.4 m height above the floor level in the SW bedroom. For the SW bedroom, the temperatures showed a sudden increase around 480 s with flame penetration into the first storey, and then they started decaying after the extinguishment of the fire was initiated.

NRC·CNRC
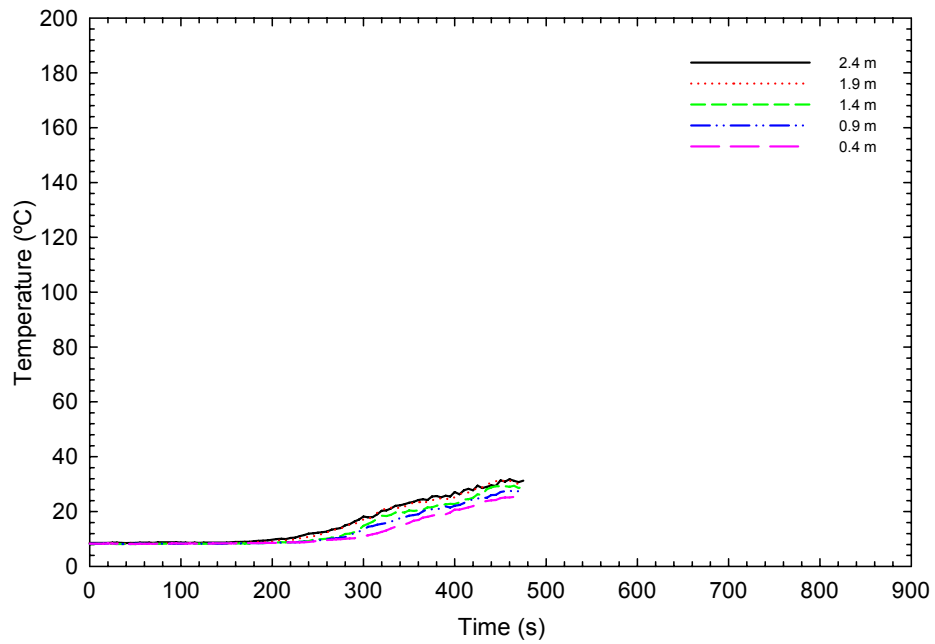
a) 2nd Storey SE bedroom
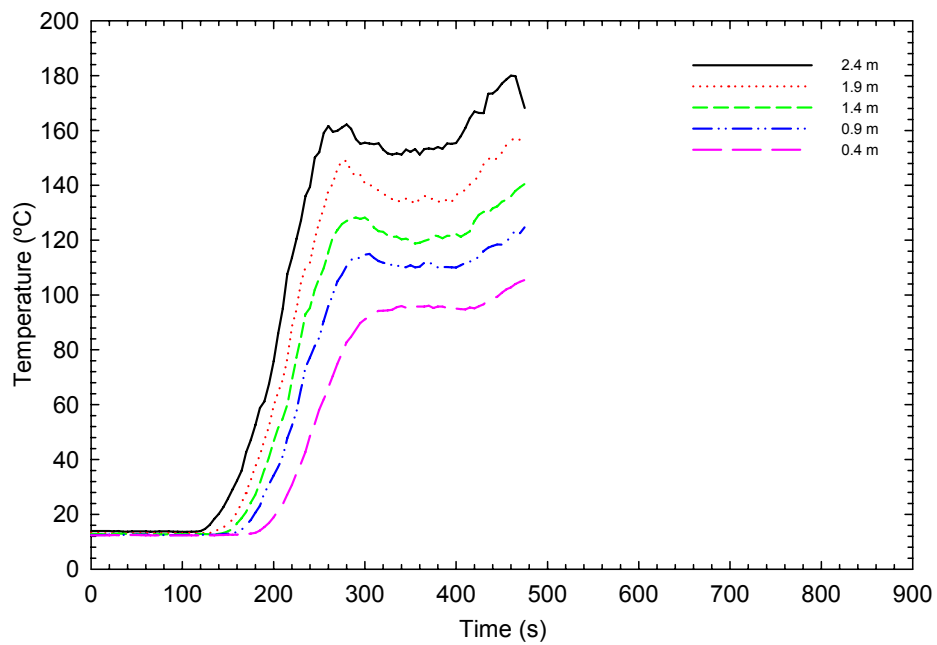
b) 2nd Storey SW bedroom

Figure 24. TC trees in the second storey bedrooms for Test UF-07

(SE bedroom: door closed; SW bedroom: door open)

NRC·CNRC
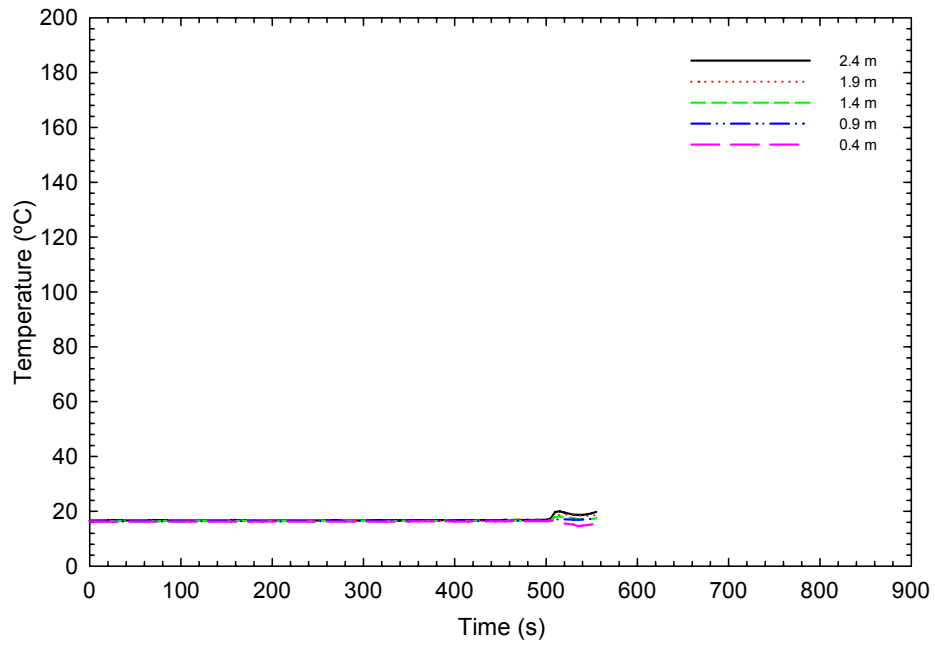
a) 2nd Storey SE bedroom
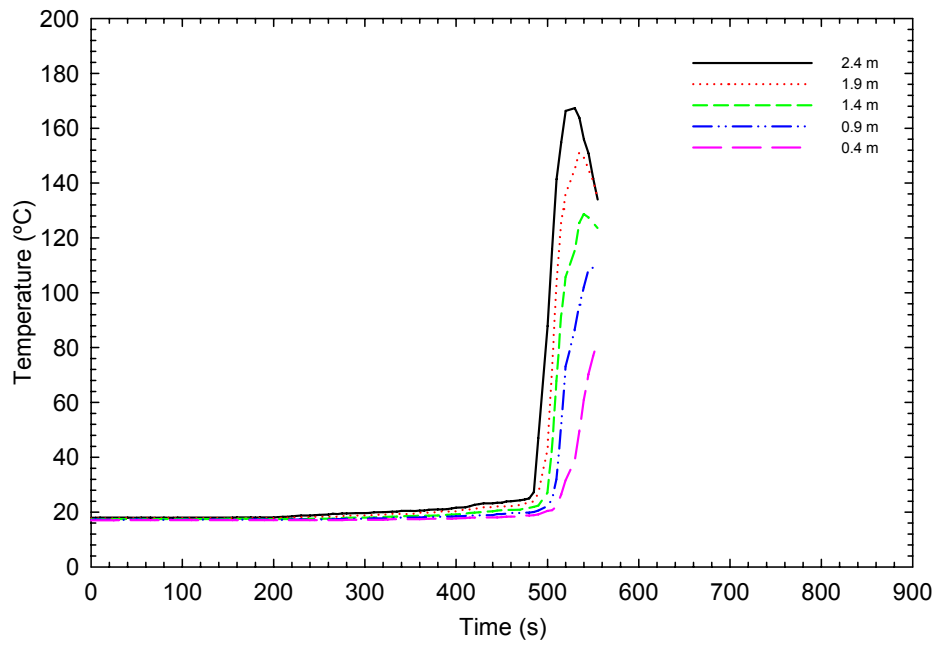
b) 2nd Storey SW bedroom

Figure 25. TC trees in the second storey bedrooms for Test UF-08

NRC·CNRC

3.3.2 Temperatures at the Window in the Basement

Five thermocouples were located in the basement window opening. Three were located along the vertical centreline of the opening, 125 mm from the bottom, 250 mm from the bottom and 375 mm from the bottom, respectively. The remaining two thermocouples were located 375 mm up from the bottom of the opening and 500 mm in from each side of the opening.

Figure 26 and Figure 27 show the temperatures recorded at the basement window for Test UF-07 and Test UF-08, respectively. For both tests, the temperatures increased to 600ºC in the first 100 s. The window was opened 95 s and 90 s after ignition, for UF-07 and UF-08, respectively, when the temperatures reached 300ºC at the window. After 120 s, due to air entering and smoke exiting the basement through the window opening, the temperatures varied depending on whether or not the flames were touching the thermocouples (the bottom TC was probably below the neutral plane).
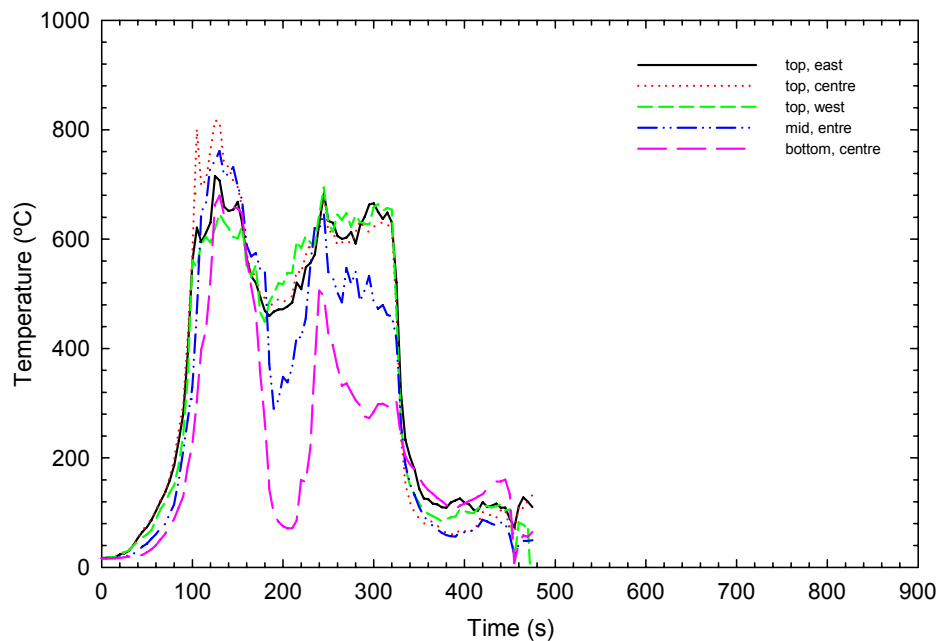
Figure 26. Temperatures at the window in the basement for Test UF-07
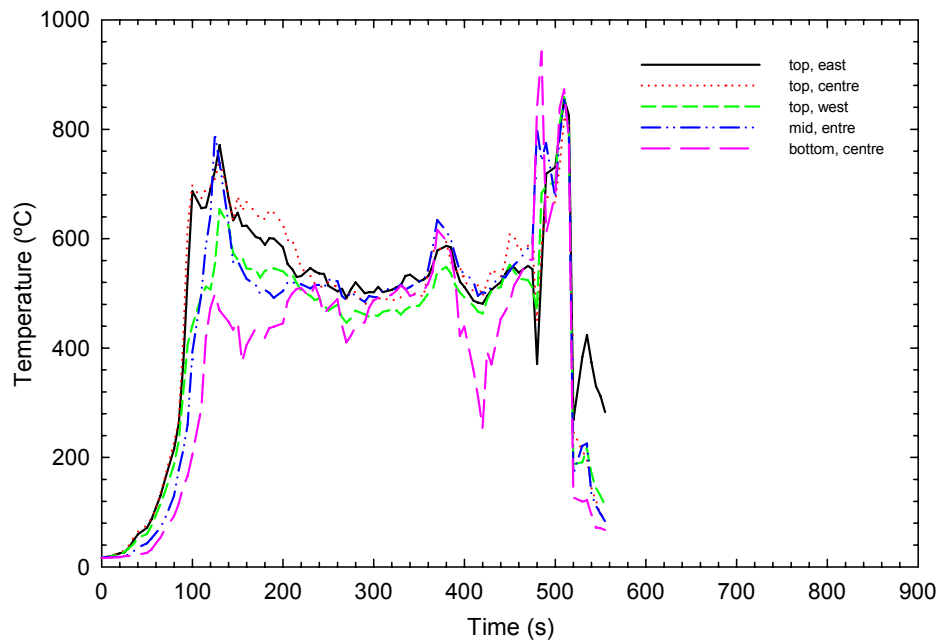
Figure 27. Temperatures at the window in the basement for Test UF-08

3.3.3 Temperatures at the Doorway to the Basement

The temperature at the doorway to the basement was measured for Test UF-08 only, since this test was conducted with a closed door to the basement. Figure 28 shows the temperatures on the exposed side [basement side] of the door at the centre and at three heights: 0.9, 1.4 and 1.9 m. The temperatures initially remained constant and then increased in the first 120 s to a value of about 160ºC (due to rapid hot gas build up in the staircase); then there was a gradual increase to about 360ºC between 120 and 470 s. Just after 470 s, the temperatures increased, at all the heights, to a maximum 720ºC. The last peak is an indication of the burning of the door. The temperature decayed after the extinguishment of the fire.

NRC·CNRC
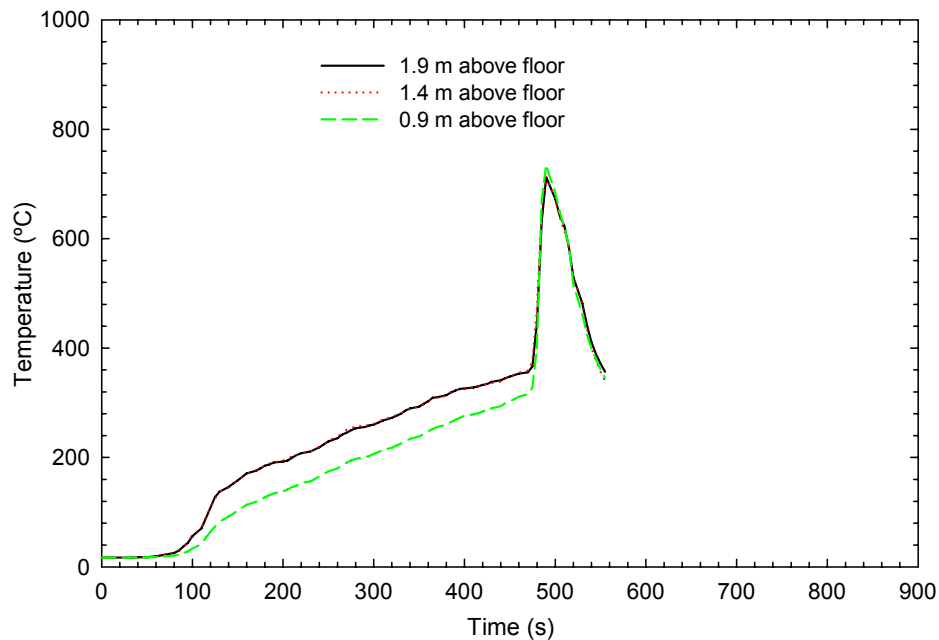
Figure 28. Temperatures at the exposed side [basement side] of the basement door for Test UF-08

3.3.4   Temperatures on the First Storey at the Top of the Stairs from the Basement

Figure 29 shows the temperatures at the top of the stairs on the first storey at different heights for Test UF-07. The conditions remained at ambient temperature for about the first 50 s. After this, temperatures, at different heights, started increasing due to the migration of hot gases and smoke from the basement to the upper storeys. A maximum temperature of about 960ºC was reached and then there was a decline in temperatures after the exterior door on the first storey was opened and fresh air entered the compartment. The temperatures then increased at some locations. The maximum temperature was not at the 2.4 m level but at the 0.9, 1.4 and 1.9 m levels. This is probably an indication that cooler air was entering into the basement at both the upper level and lower level of the doorway.

Figure 30 shows the temperatures at the top of the stairs on the first storey at different heights for Test UF-08. The conditions remained at ambient temperature for about the first 80 s. After this time, the temperatures, at different heights, started increasing very gradually due to the migration of hot gases and smoke through gaps around the floor assembly. The temperatures showed a sudden increase at about 470 s, which may be related to flame penetrating into the first storey through the burning floor or flame breaching the door to the basement. The temperatures started decaying after the extinguishment of the fire was initiated. A maximum temperature of about 760ºC was reached.

NRC·CNRC
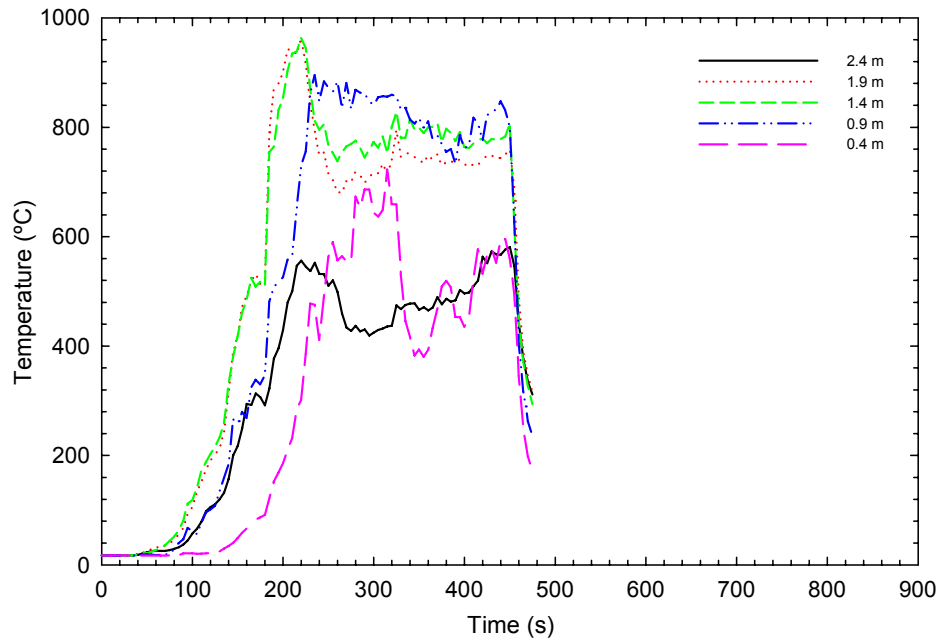
Figure 29. Temperatures on the first storey at the top of the stairs from the basement for Test UF-07
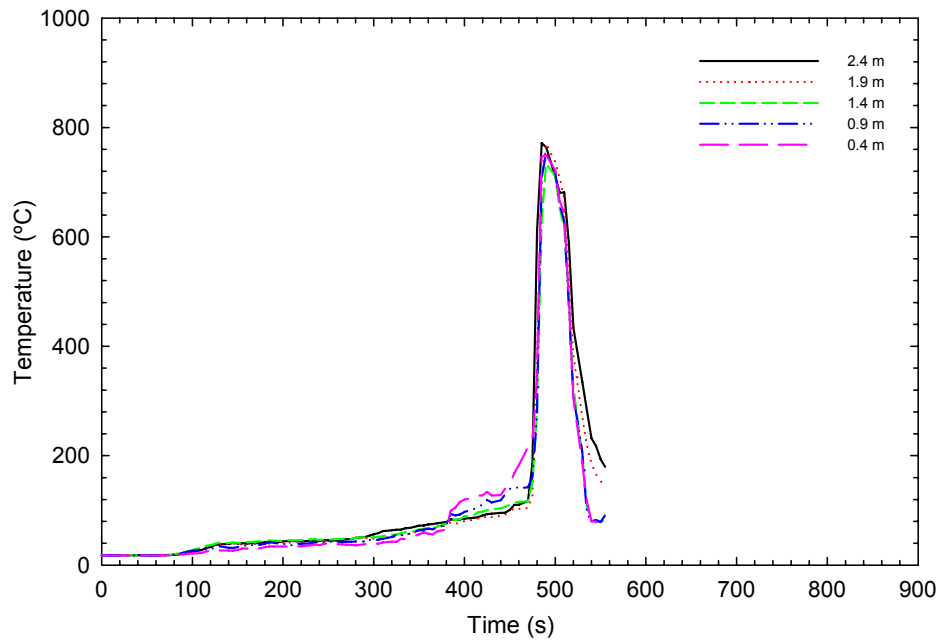
Figure 30. Temperatures on the first storey at the top of the stairs from the basement [unexposed side of basement door] for Test UF-08

NRC·CNRC

3.3.5   Temperatures on the Second Storey at the Top of the Stairs

Figure 31 shows the temperatures at the top of the stairs on the second storey at different heights for Test UF-07. The conditions remained at ambient temperature for about the first 110 s. After this, temperatures, at different heights, started increasing due to the migration of hot gases and smoke from the basement to the upper storeys. A maximum temperature of about 260ºC was reached at the 2.4 m height.

Figure 32 shows the temperatures at the top of the stairs on the second storey at different heights for Test UF-08. The conditions remained at ambient temperature for about the first 300 s.   After this time, the temperatures, at different heights, started increasing very gradually due to some migration of hot gases and smoke mainly through gaps around the floor assembly. The temperatures showed a sudden increase at about 480 s, which was related to flame penetrating into the first storey through the burning floor.   The temperatures started decaying after the extinguishment of the fire was initiated.
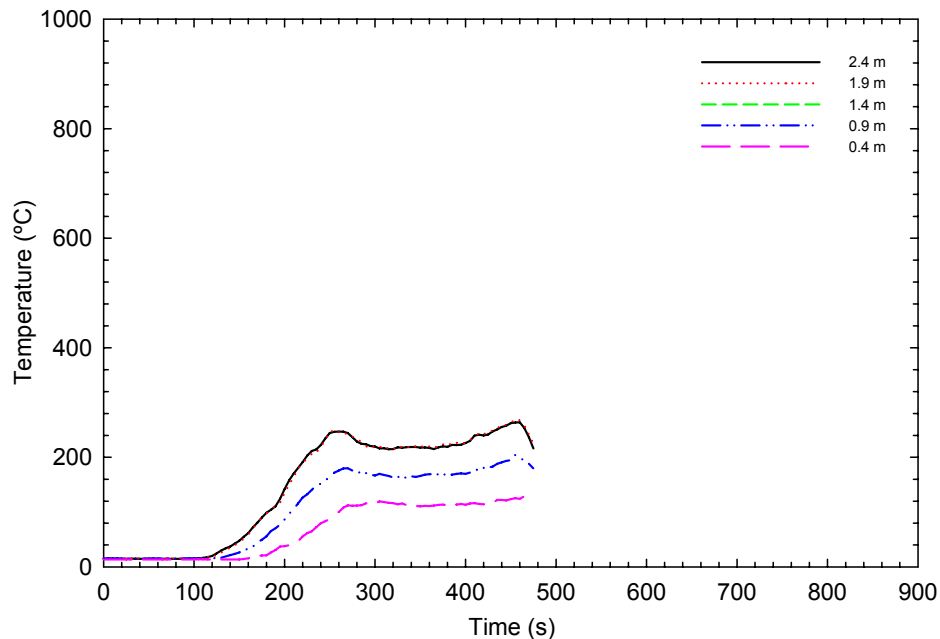
Figure 31. Temperatures on the second storey at the stairs for Test UF-07
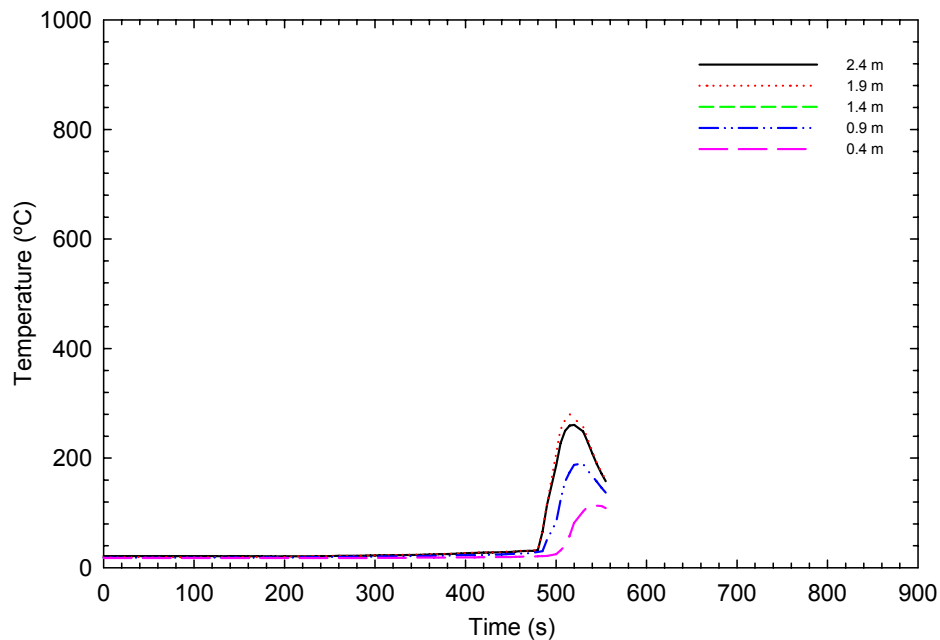
Figure 32. Temperatures on the second storey at the stairs for Test UF-08

3.3.6   Temperatures at the Outside Doorway on the First Storey

Figure 33 and Figure 34 show the temperatures at the exterior doorway on the first storey for Tests UF-07 and UF-08, respectively. The temperatures were remained at ambient for about the first 100 s and 200 s in Test UF-07 and Test UF-08, respectively. After these times, the temperatures increased reaching 350ºC at 220 s in Test UF-07 and 40ºC at 470 s in Test UF-08 due to smoke and hot fire gases exiting through the open exterior door (smaller increase in temperature in Test UF-08 with the closed basement doorway). The temperature in Test UF-07 decreased after the first peak due to the opening of the exterior door on the first storey. There was a sharp increase in temperatures near the end of both tests (due to flame penetration through the floor producing more radiation and hot gases in the vicinity of the exterior door). The temperatures started decaying after the extinguishment of the fire was initiated.

NRC·CNRC
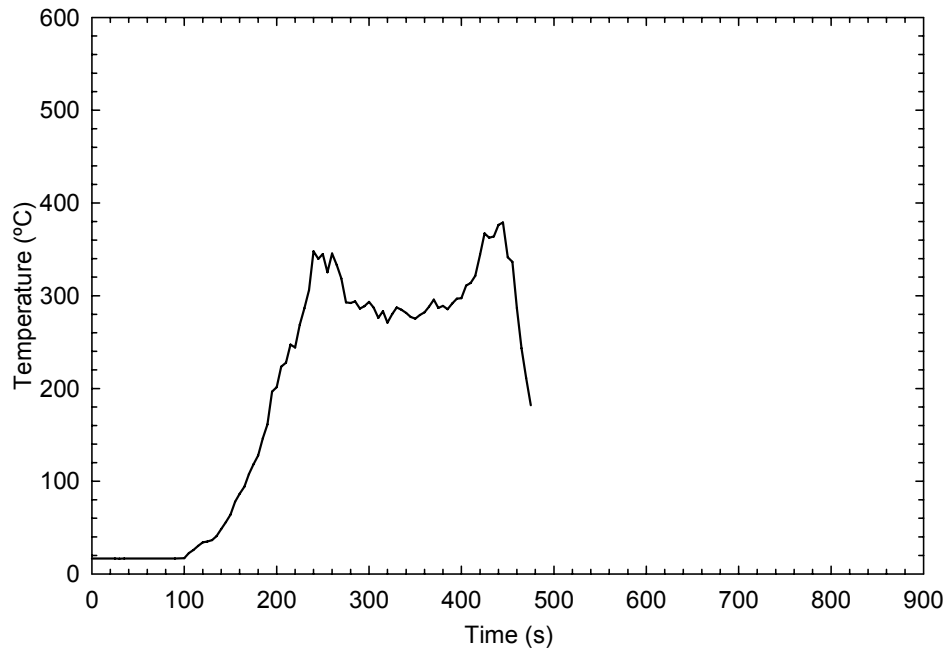
Figure 33. Temperatures at the outside doorway on the first storey for Test UF-07
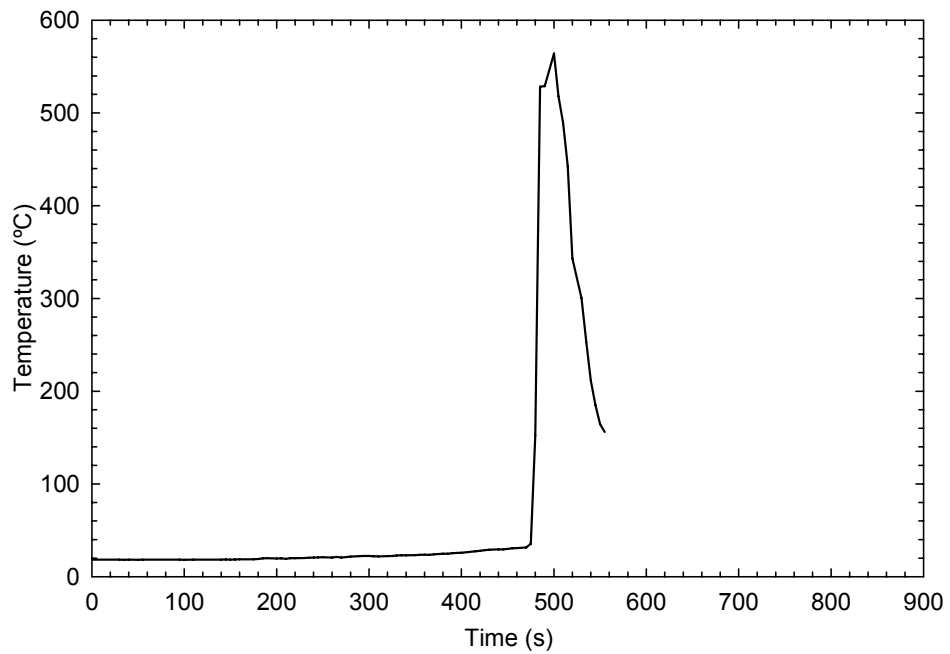
Figure 34. Temperatures at the outside doorway on the first storey for Test UF-08

43

3.3.7   Temperatures First Storey on the Unexposed Side of the Floor Assembly

3.3.7.1   Test UF-07

Figure 35 (a and b) show the temperatures measured by thermocouples (TCs) No. 1 to 9 and No. 89 through 94 located on the unexposed side (top) of the OSB subfloor in the floor assembly (see Figure 15 and Figure 16).   For TCs 1 to 9, the temperatures remained at ambient temperature for the first 200 s.   After this, the temperatures increased gradually until the test was terminated. The maximum temperature reached was about 80°C before the end of the test.   Temperatures at locations 89 to 94 had a similar trend with different values except for TC 91 which had a sudden increase in temperature at 325 s, indicating flame penetration through the floor.

It is worth mentioning that failure under standard fire test conditions [14], on the basis of temperature, is defined as a temperature rise of 140°C above ambient temperature for the average of the nine padded thermocouples or a temperature rise of 180°C above ambient temperature at any single point on the unexposed side.

3.3.7.2   Test UF-08

Figure 36 (a and b) show the temperatures measured by thermocouples No. 1 to 9 and No. 89 through 94 located on the unexposed side (top) of the OSB subfloor in the floor assembly (see Figure 15 and Figure 16). For TCs 1 to 9, the temperatures remained at ambient temperature for the first 160 s. After this, the temperatures increased gradually until 470 s; thereafter, the temperatures had a faster rate of increase.   This faster temperature rise was due to the critical positioning of the thermocouples and it is an indication that flames were penetrating through the floor as the floor was breached.   The temperatures increased to reach a maximum temperature of 560ºC at the end of the test.   The time corresponding to flames penetrating the floor was comparable to those recorded using the flame-sensing devices.   Subsequently, the temperatures decreased during the extinguishment of the fire.   Temperatures at locations 89 to 94 had a similar trend with a maximum temperature of 600ºC.
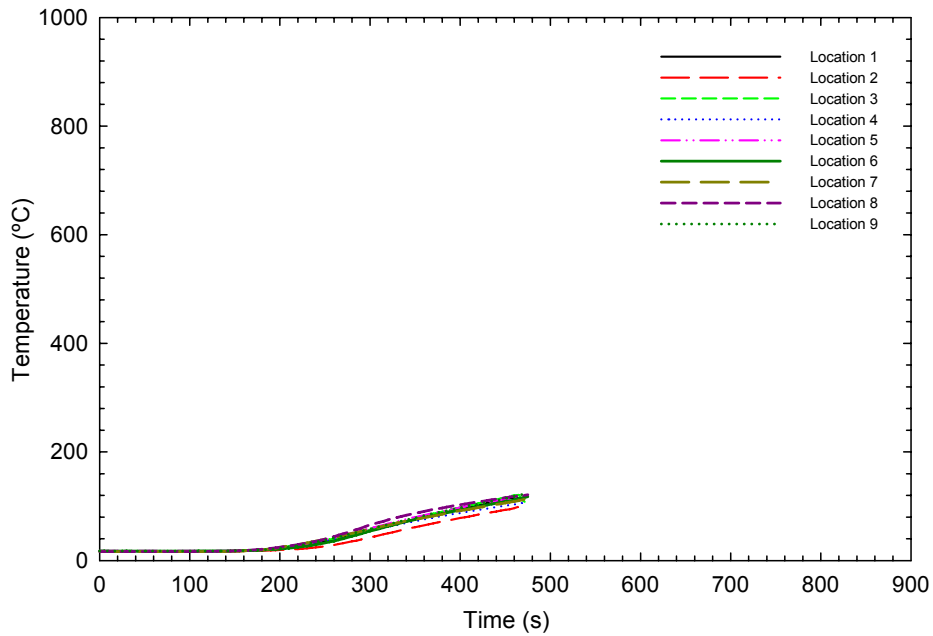
NRC·CNRC

a) Unexposed TCs under insulated pad on top of subfloor
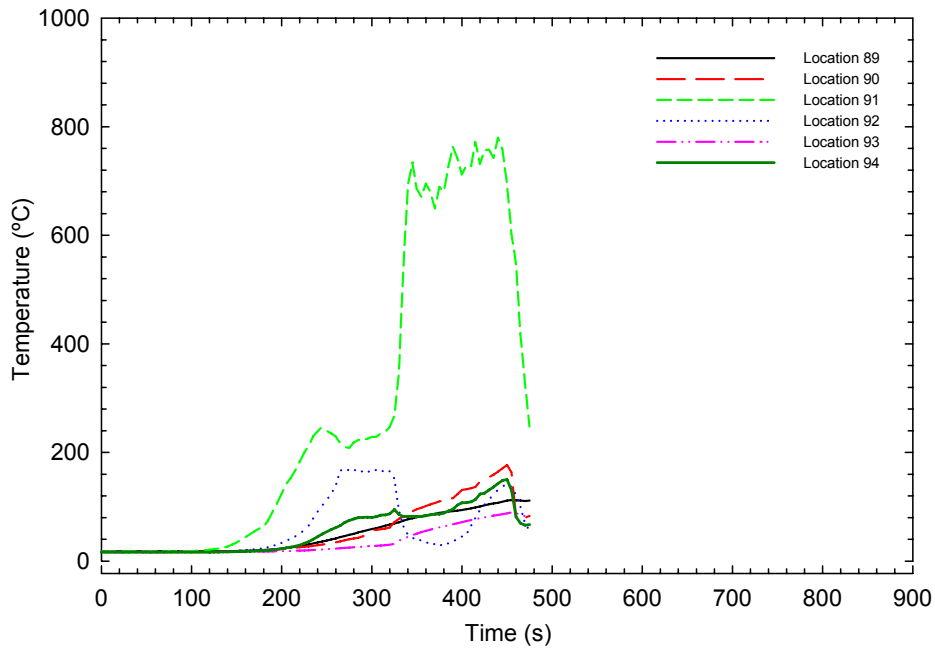
b) Bare TCs on the unexposed (top) side of subfloor

Figure 35. Temperatures at the unexposed side of subfloor for Test UF-07
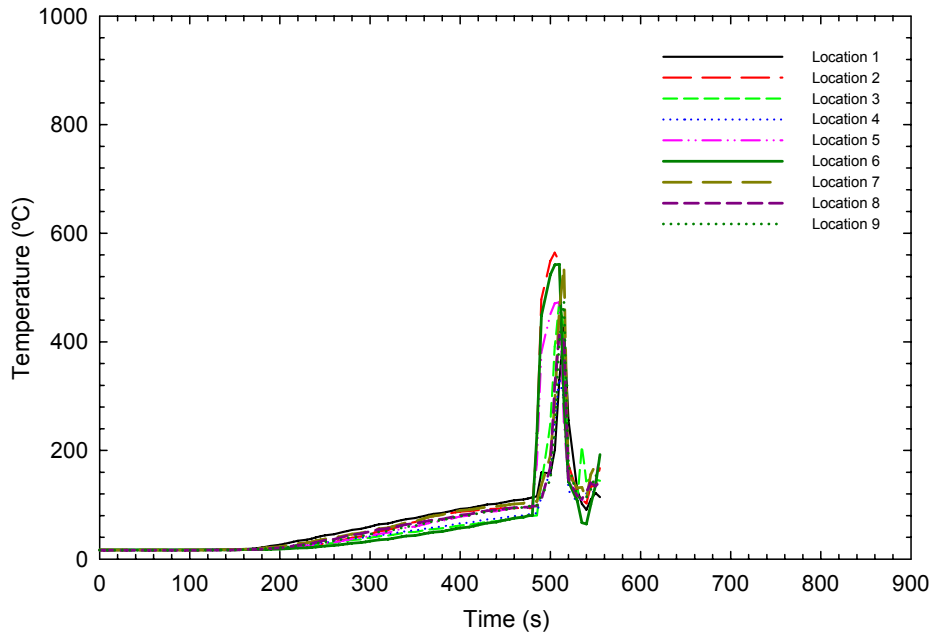
NRC·CNRC

a) Unexposed TCs under insulated pad on top of subfloor
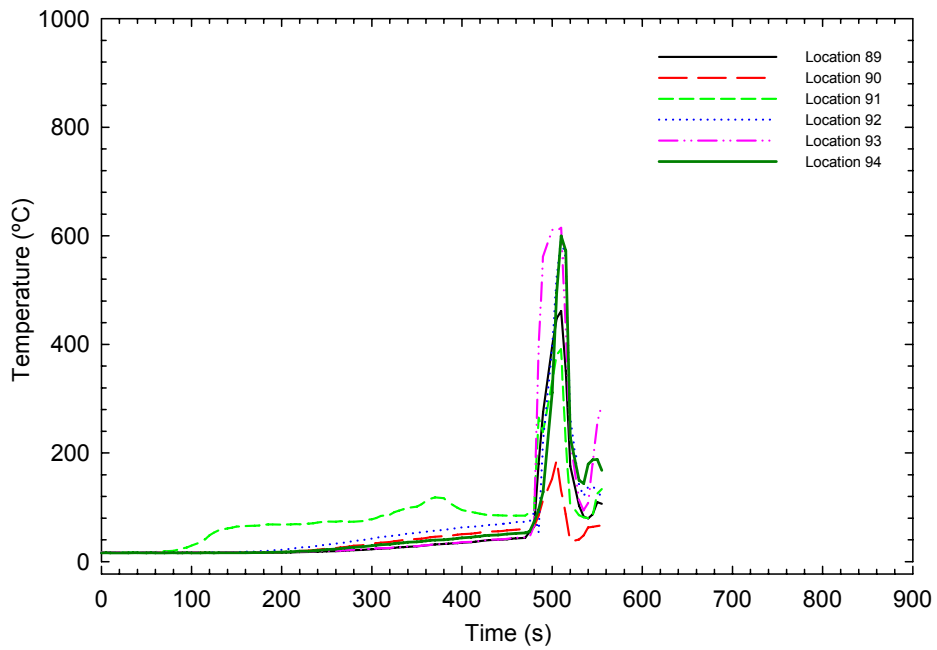
b) Bare TCs on the unexposed (top) side of subfloor

Figure 36. Temperatures at the unexposed side of subfloor for Test UF-08

NRC·CNRC

3.3.8 Temperatures on the Exposed Side of the Floor Assembly

The location of each grouping of thermocouples is identified by the Section label (A, B, C, D, E and CD) and the truss space shown on Figure 15 and Figure 16. For example, C-1 is the group of thermocouples located along Section C in Truss Cavity 1.

For the thermocouple groupings within the truss cavities with seven thermocouples at each section, the individual thermocouples are identified as follows: bottom of north truss (Bot MWT North (1)), mid-height of north truss (Mid MWT North (2)), between the north truss and the subfloor (SF/MWT North (3), on the subfloor mid-distance between the two trusses (SF/Cav (4)), between the south truss and the subfloor (SF/MWT South (5), mid-height of south truss (Mid MWT South (6)) and bottom of south truss (Bot MWT south (7)).

The temperatures on the exposed side of the floor assembly were measured at a number of locations distributed in such a way as to learn, as much as possible, the effect of the fire on the floor assemblies. As shown in Figure 15 and Figure 16 (Location of Thermocouples), in the locations at Sections A, B, C, E and CD, seven thermocouples were installed: 2 at the bottom of two adjacent trusses, 2 in the cavity at mid-height of the two trusses, 2 between the subfloor and the two trusses, and 1 in the cavity at the subfloor at mid-distance between the 2 trusses. Section D had only 1 thermocouple in the cavity at the subfloor at mid-distance between the 2 trusses.

3.3.8.1 Test UF-07

Figure 37 (a) to Figure 37 (n) show the temperatures measured by the thermocouples located on the exposed side of the floor. For all the locations with 7 thermocouples (A-2, A-7, A-12, B-7, C-1, C-5, C-7, C-9, C-11, C-13, E-1, CD-7 and CD-11), in almost every case the trend was similar with a sharp increase in temperatures for all the exposed thermocouples in the first 100 s to 120 s. For the thermocouples located at the interface between the top of a truss and the subfloor (SF/MWT), the temperature rise in most cases was relatively slow and gradual due to the shielding of the thermocouples by the trusses. When the temperatures for SF/MWT North (3) and SF/MWT South (5) showed a temperature increase, which was sudden in some cases, it was an indication that gaps were forming between the top of the trusses and the subfloor at these points and that the thermocouples were being exposed to the hot gases from the fire.

The increase in temperature happened at different times for the different locations. The difference in time between the two SF/MWT (North and South) thermocouples is partly due to the view factor relative to the burning fuel package. In some cases, the bulk of the fuel package was 'positioned' South of the thermocouple grouping. Consequently, the thermocouple at top of the North truss experienced a greater heat insult from both the convective and radiative effects from the burning fuel. For the thermocouple groupings with the bulk of the fuel package located to the North, the reverse effect occurred.

Of particular mention is Sections C-9, C-7, C11, CD-7 and CD-11 where the temperatures at SF/MWT North (3) and SF/MWT South (5) reached almost the same peak values as the temperatures at the exposed thermocouples in the first 100 s. This is an indication that gaps due to structural movement and charring of the wood at the

interface of the trusses and subfloor occurred much earlier at this location than other locations as it was directly above the mock-up sofa and very close to the wood cribs.

For the exposed thermocouples, the highest peak temperature (a value of about 830ºC) was recorded at sections C-7, C-9, C11 and C13 (located very close or directly over the burning mock-up sofa and wood cribs). In most cases, there was a drop in temperature measured by the exposed thermocouples just after 120 s, which may be attributed to the fresh air coming from the open basement window; the temperature dropped further after the exterior door on the first storey was opened at 180 s. However, the decrease in temperature lasted only about 80 s and then the temperatures started increasing again.

There were cases where there was no obvious drop in the temperature at 120 s (A-2, C-1 and E-1). This was because these locations were not in the proximity of the fuel package and thus had limited radiative impact from the fuel.

For Section D, points D-2 and D-12 have the same trend as the exposed thermocouples in sections A-2, A-12 and E1.

NRC·CNRC
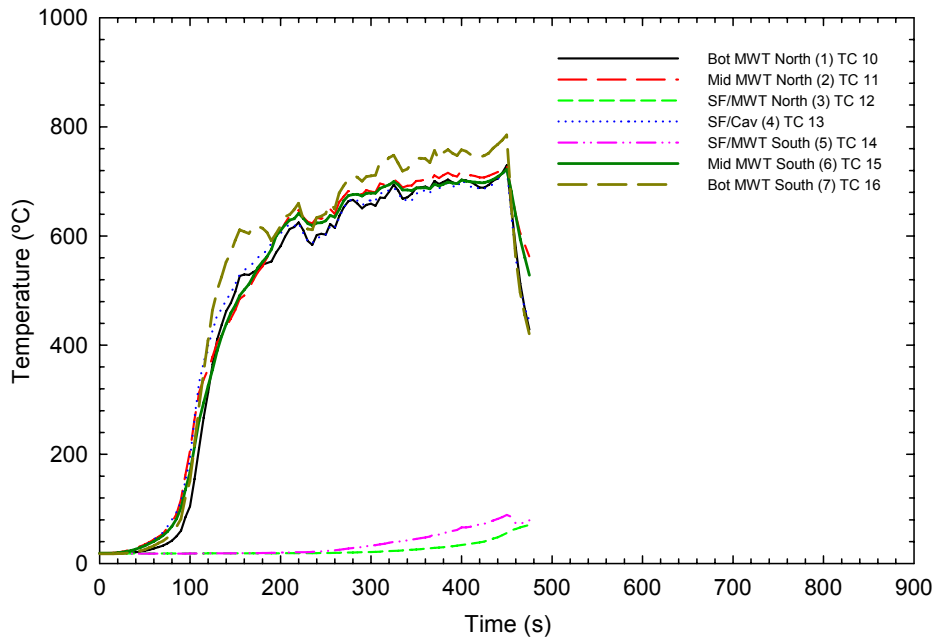
a) Thermocouples in cavity A-2
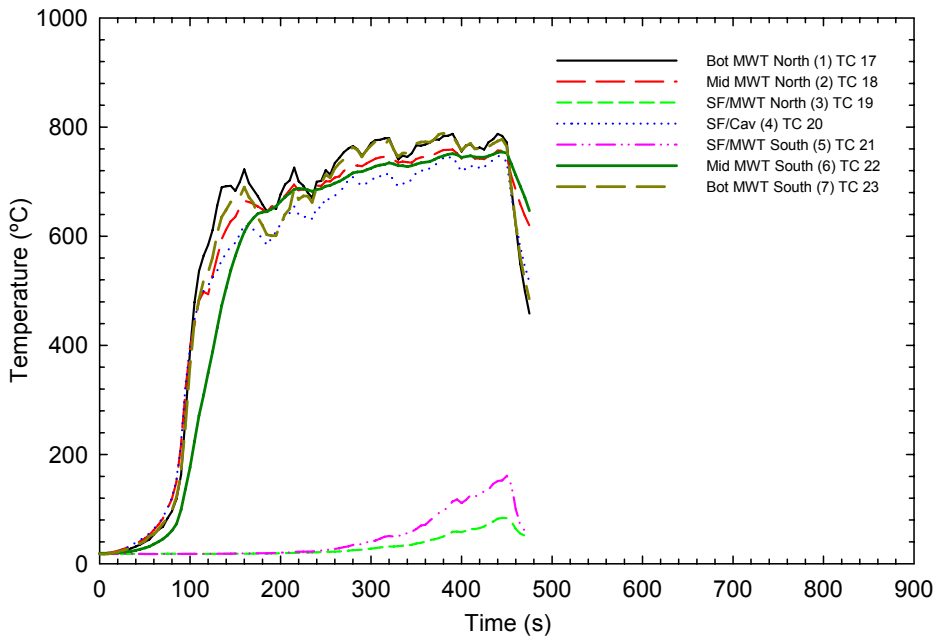
b) Thermocouples in cavity A-7

Figure 37 (a and b). Temperatures at the exposed side for Test UF-07

NRC·CNRC

c) Thermocouples in cavity A-12

d) Thermocouples in cavity B-7

Figure 37 (c and d). Temperatures at the exposed side for Test UF-07

NRC·CNRC

e) Thermocouples in cavity C-1
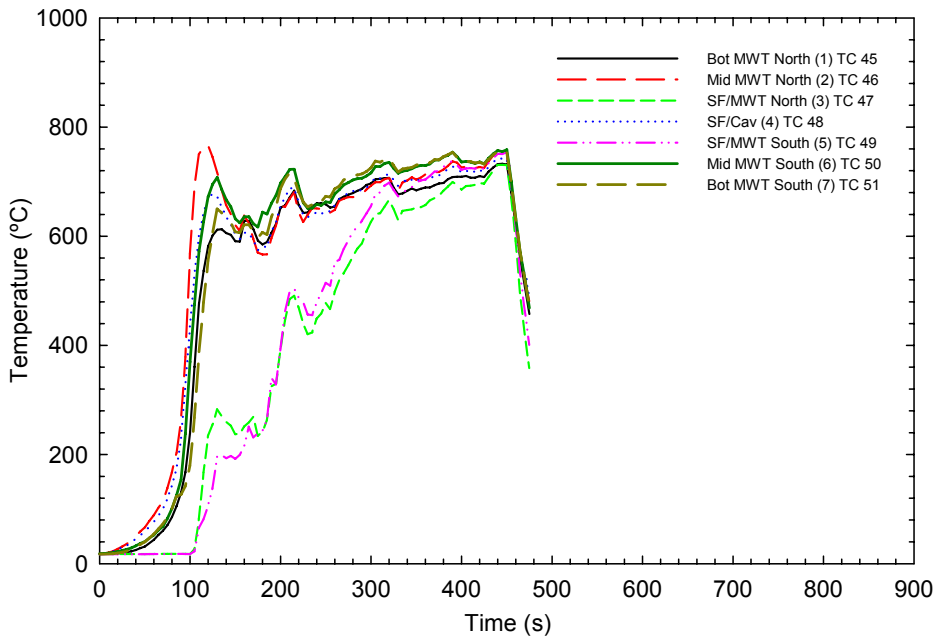
f) Thermocouples in cavity C-5

Figure 37 (e and f). Temperatures at the exposed side for Test UF-07

g) Thermocouples in cavity C-7
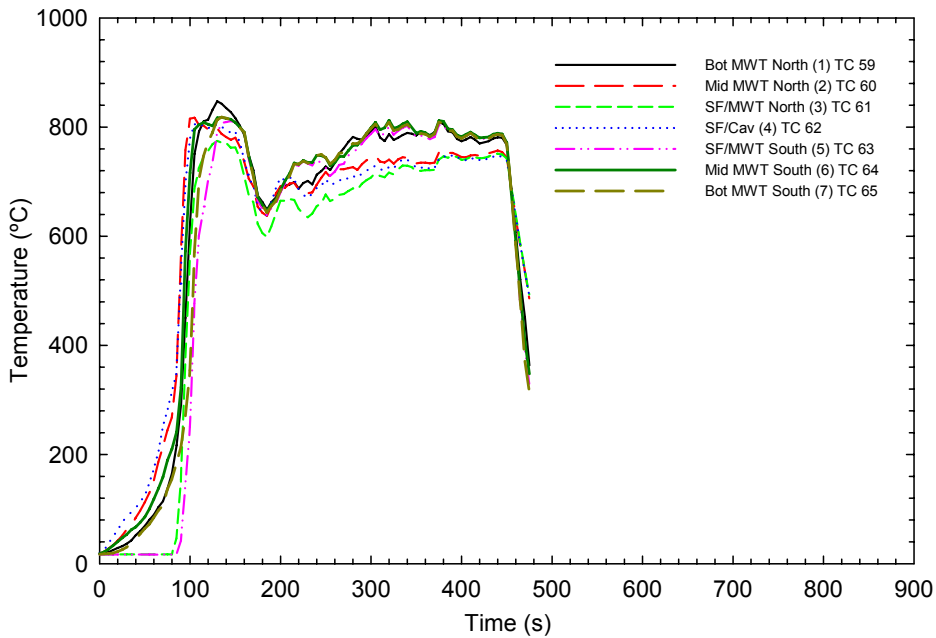
h) Thermocouples in cavity C-9

Figure 37 (g and h). Temperatures at the exposed side for Test UF-07

NRC·CNRC

i) Thermocouples in cavity C-11
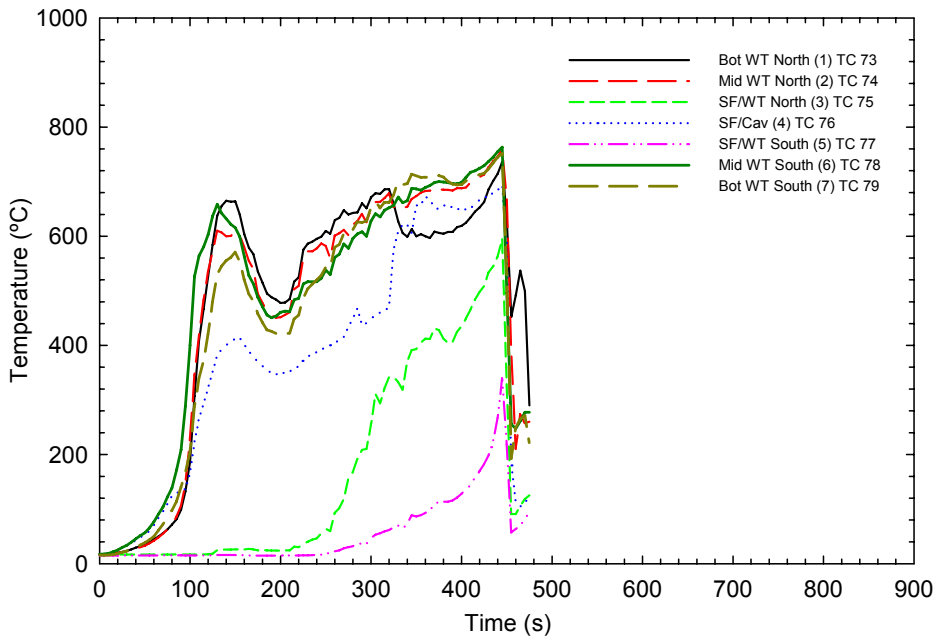
j) Thermocouples in cavity C-13

Figure 37 (i and j). Temperatures at the exposed side for Test UF-07

53
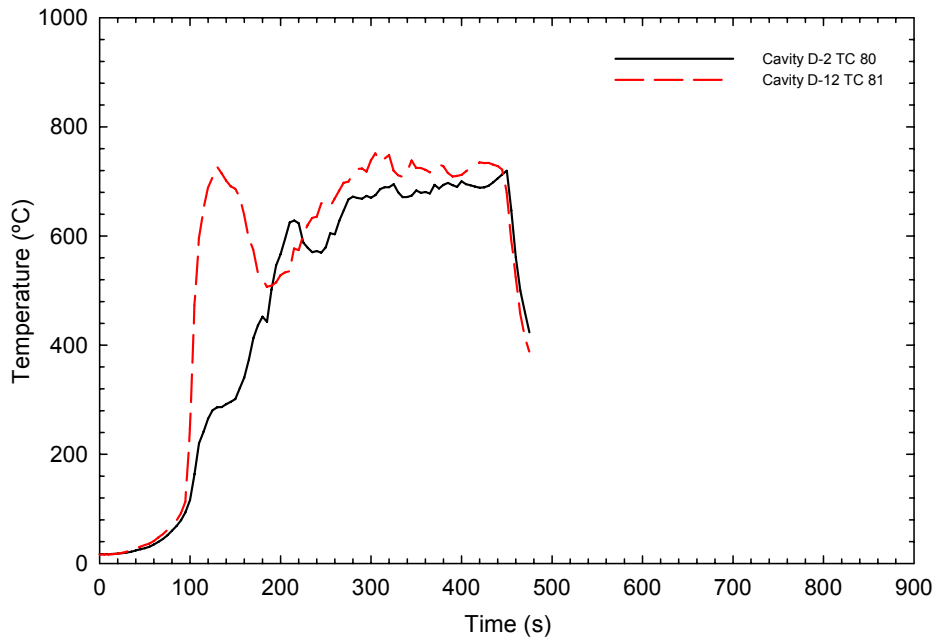
k) Thermocouples in cavity D-2 and D-12
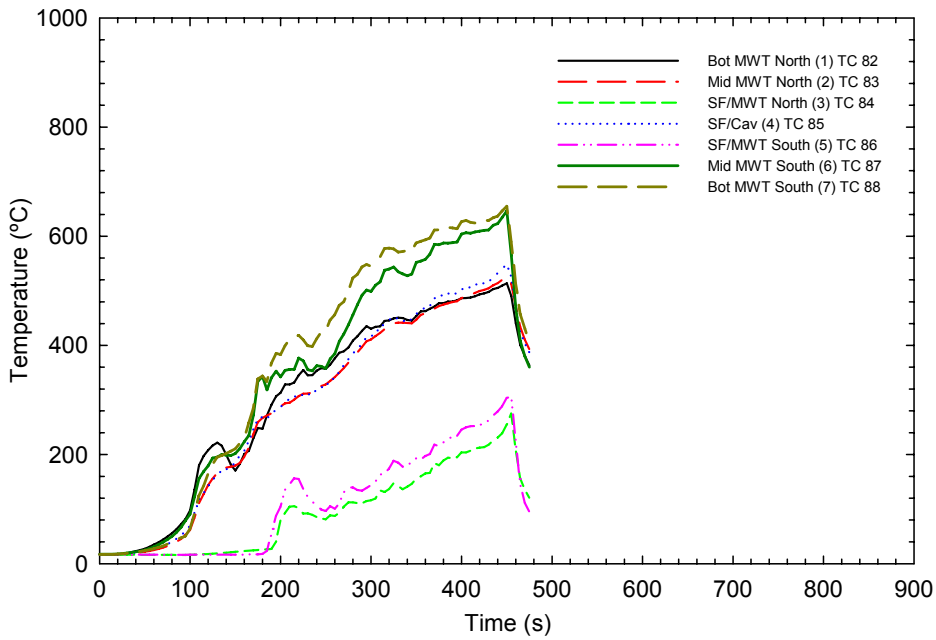
l) Thermocouples in cavity E-1

Figure 37 (k and l). Temperatures at the exposed side for Test UF-07

NRC·CNRC
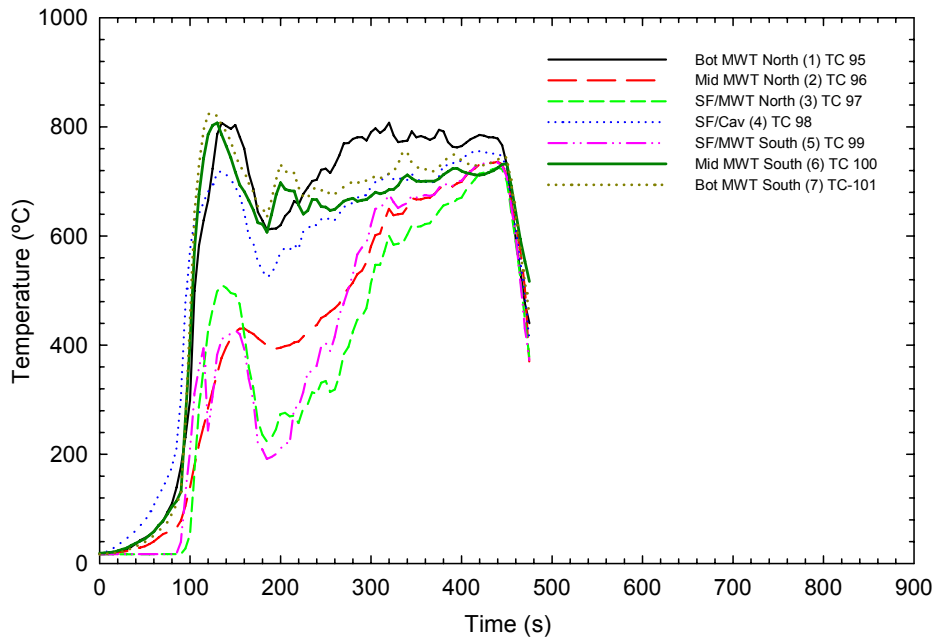
m) Thermocouples in cavity CD7
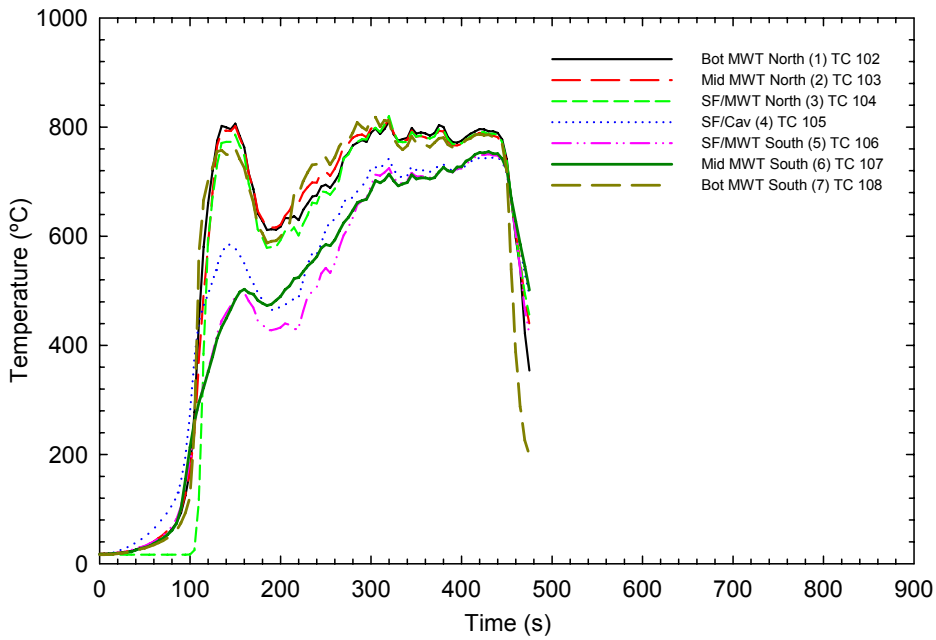
n) Thermocouples in cavity CD11

Figure 37 (m and n). Temperatures at the exposed side for Test UF-07

NRC·CNRC

3.3.8.2 Test UF-08

Figure 38 (a) to Figure 38 (n) show the temperatures measured by the thermocouples located on the exposed side of the floor. For all the locations with 7 thermocouples (A-2, A-7, A-12, B-7, C-1, C-5, C-7, C-9, C-11, C-13, E-1, CD-7 and CD-11), in almost every case the trend was similar with a sharp increase in temperatures for all the exposed thermocouples in the first 100 s to 120 s. For the thermocouples located at the interface between the top of a truss and the subfloor (SF/MWT), the temperature rise in most cases was relatively slow and gradual due to the shielding of the thermocouples by the trusses. When the temperatures at the SF/MWT North (3) and SF/MWT South (5) showed a temperature increase, which was sudden in some cases, it is an indication that gaps were forming between the top of the trusses and the subfloor at these locations allowing flames and hot gases into the gap. The increase in temperature happened at different times for the different locations.

Of particular mention are Sections C7 and C-9 where the temperatures at SF/MWT North (3) and SF/MWT South (5) reached the maximum values in the first 100-110 s. This is an indication that gaps due to structural movement and charring of the wood at the interface of the trusses and subfloor occurred much earlier at this location than other locations as it was directly above the mock-up sofa and very close to the wood cribs.

For the exposed thermocouples, the highest initial peak temperature (820ºC) was recorded at Sections C7 and C-9 (located directly over the burning mock-up sofa and the wood cribs).

In most cases, there was a drop in temperature just after 100 s to 120 s, which may be attributed to the fresh air coming through the open basement window. The decrease in temperature lasted only about 150 s and then the temperatures either stayed constant or started increasing again.

There were cases where there was no obvious decrease in temperature (A-2, C-1 and E-1). These locations were not close to the fuel package and thus had limited radiative impact from the fuel.

For section D, points D-1 and D-12 have the same trend as the exposed thermocouples in section A2 and E1 (away from the fire).

At 460-470 s, the temperatures at the different locations had a sharp increase probably because the flames penetrated the floor and allowed more fresh air to enter into the basement. The section on "flame penetration" indicates that flames started to penetrate into the first storey around 470 s. The temperatures started to decrease after the extinguishment of the fire was initiated.
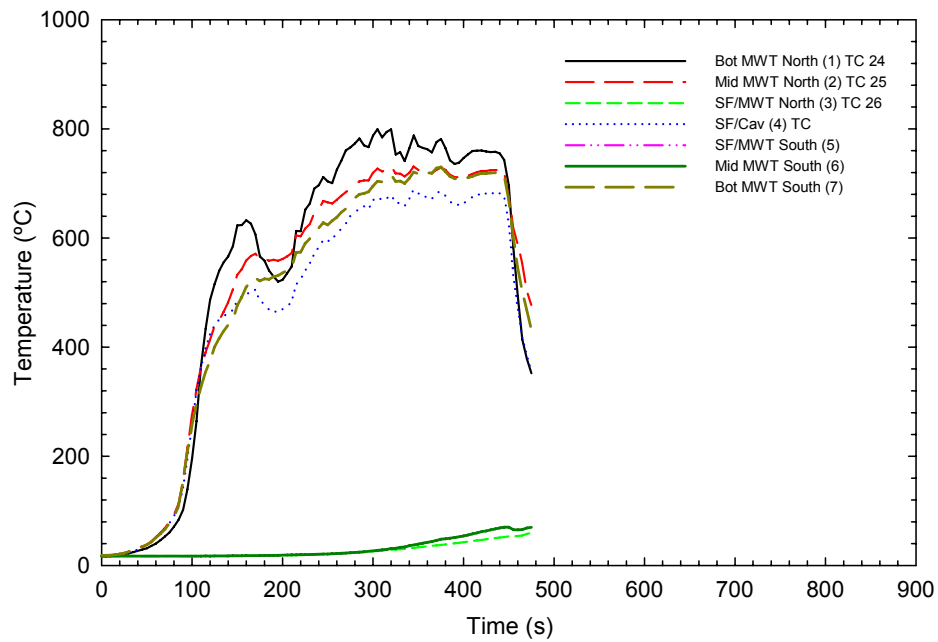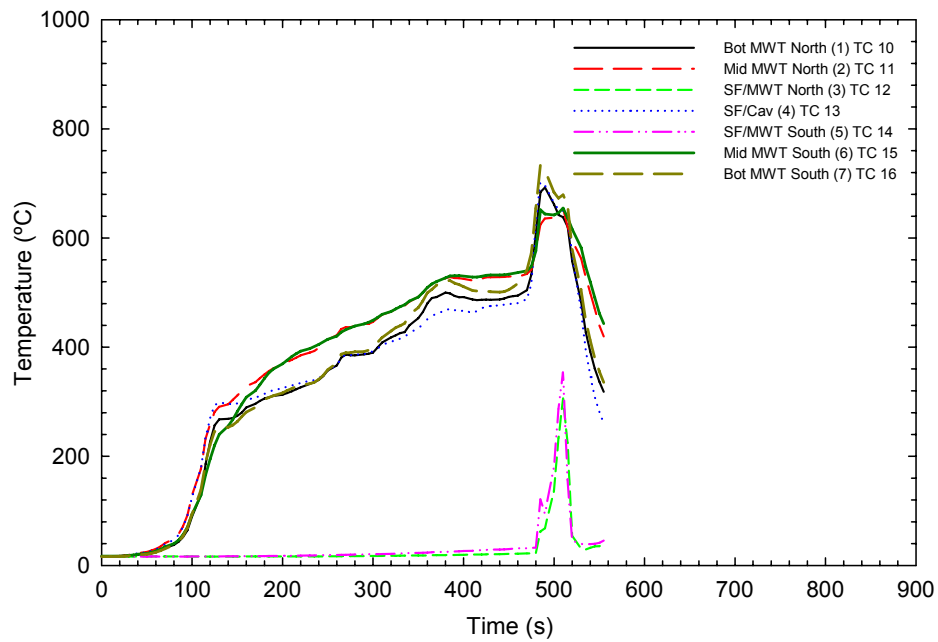
a) Thermocouples in cavity A-2
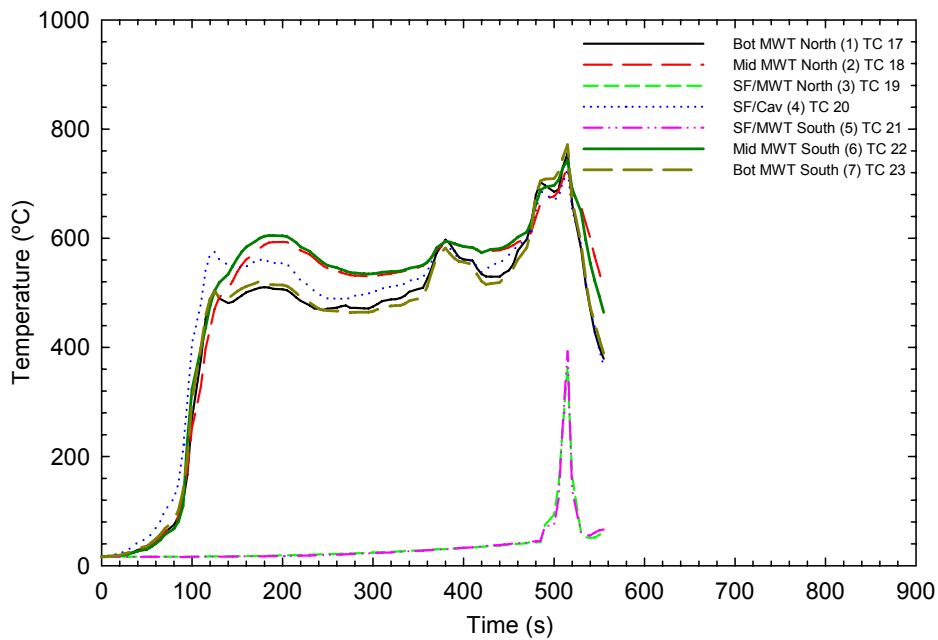
b) Thermocouples in cavity A-7

Figure 38 (a and b). Temperatures at the exposed side for Test UF-08

NRC·CNRC
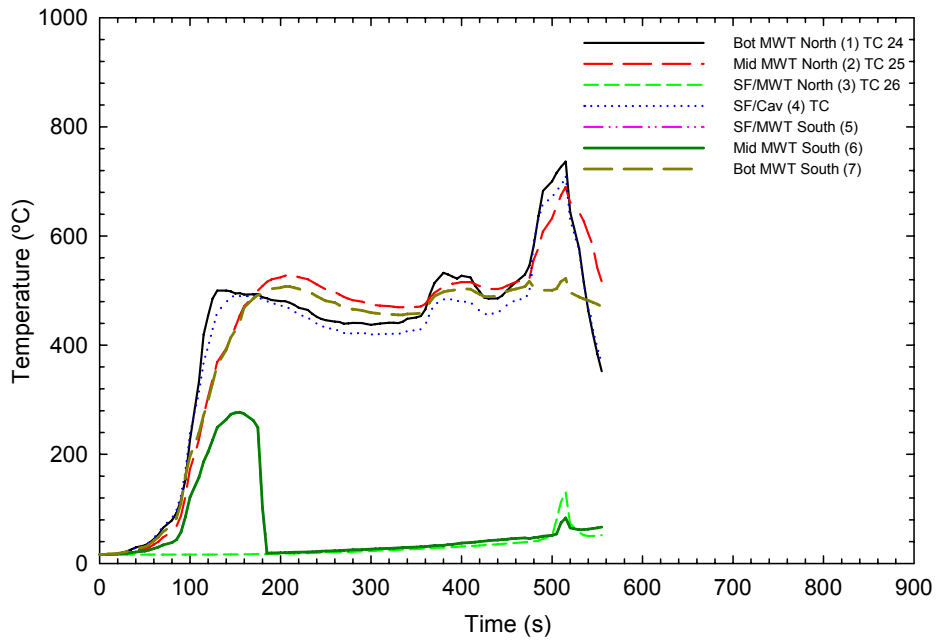
c) Thermocouples in cavity A-12
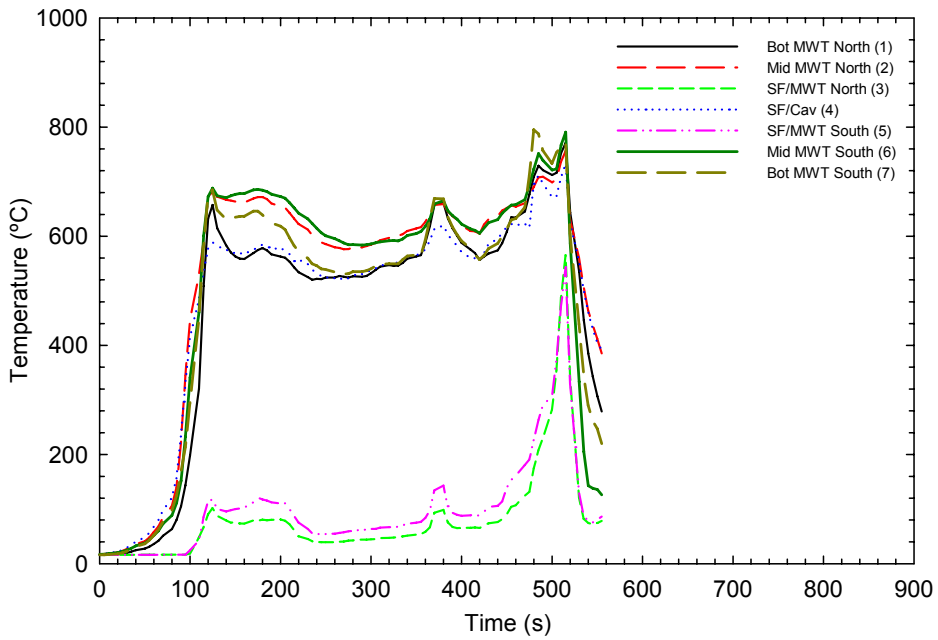
d) Thermocouples in cavity B-7

Figure 38 (c and d). Temperatures at the exposed side for Test UF-08

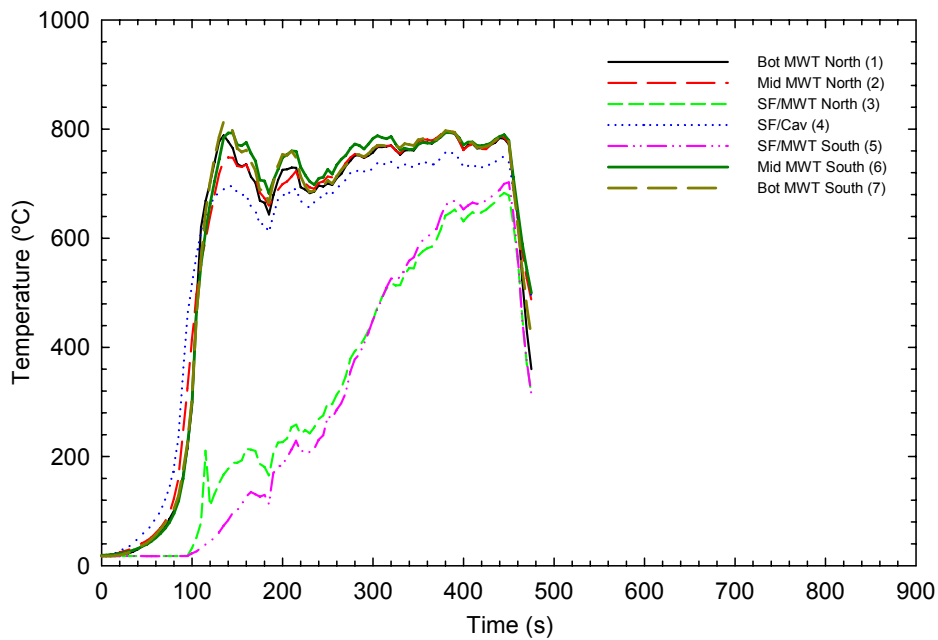NRC·CNRC
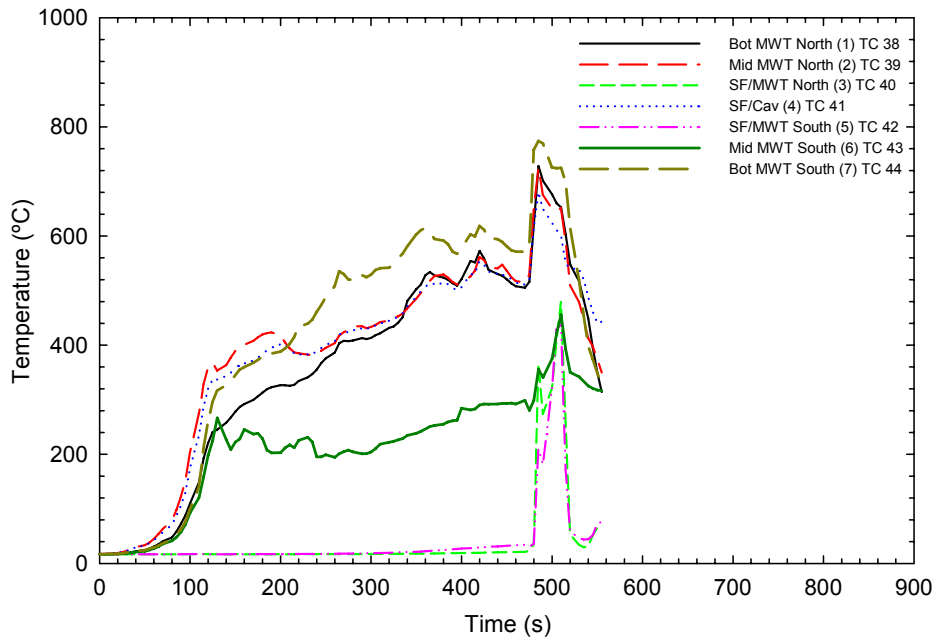
e) Thermocouples in cavity C-1
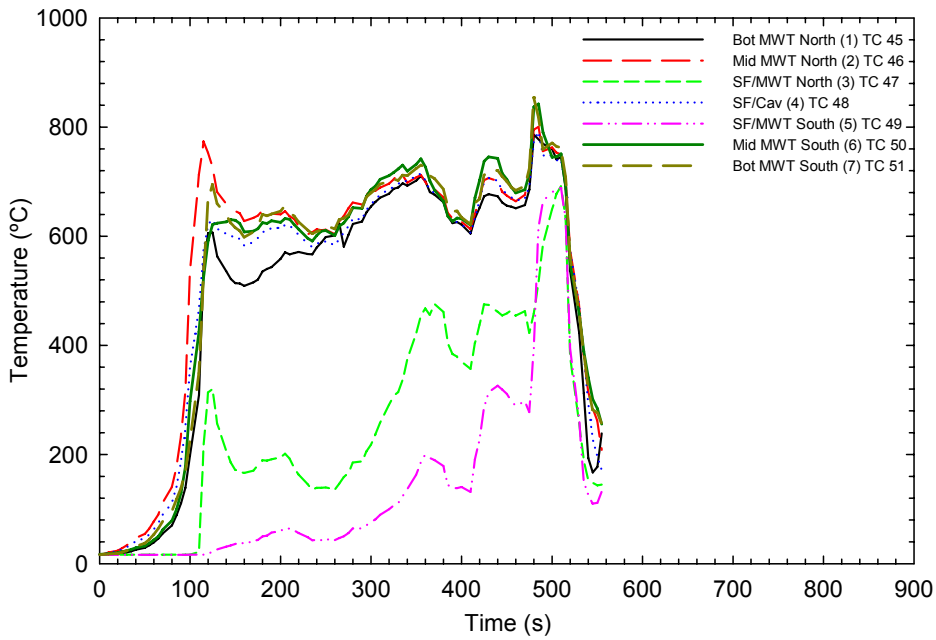
f) Thermocouples in cavity C-5

Figure 38 (e and f). Temperatures at the exposed side for Test UF-08

NRC·CNRC
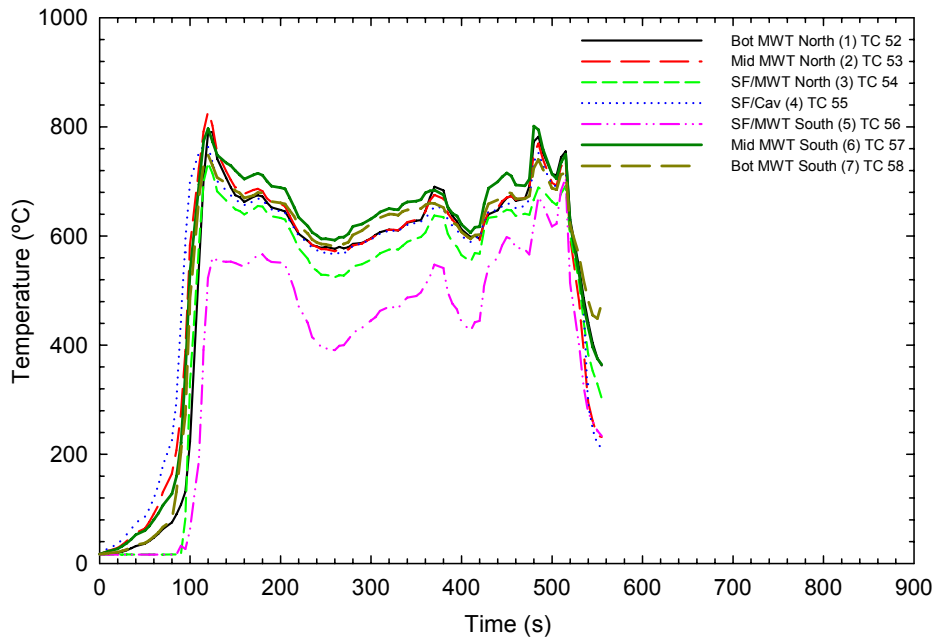
g) Thermocouples in cavity C-7
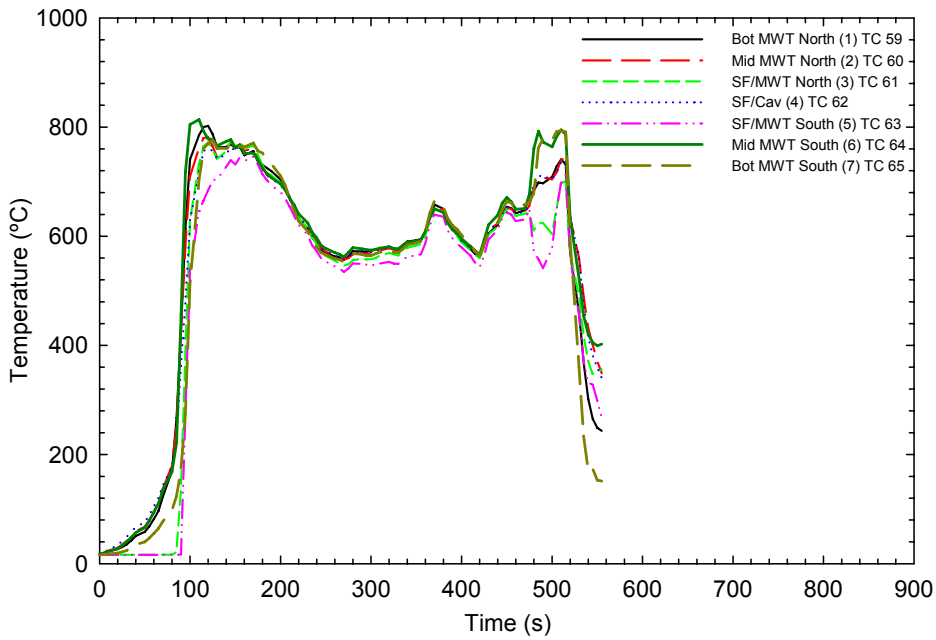
h) Thermocouples in cavity C-9

Figure 38 (g and h). Temperatures at the exposed side for Test UF-08

NRC·CNRC
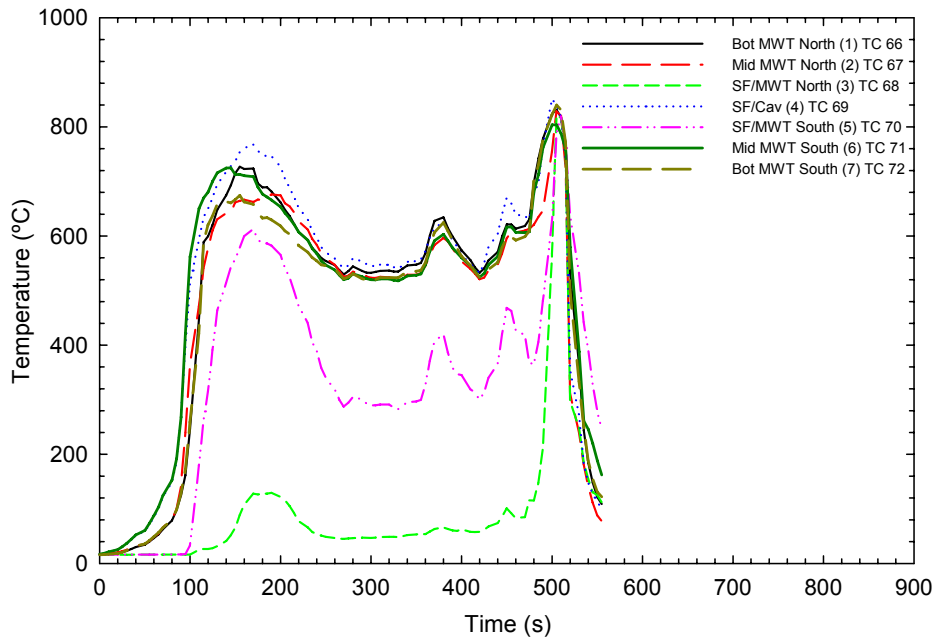
i) Thermocouples in cavity C-11
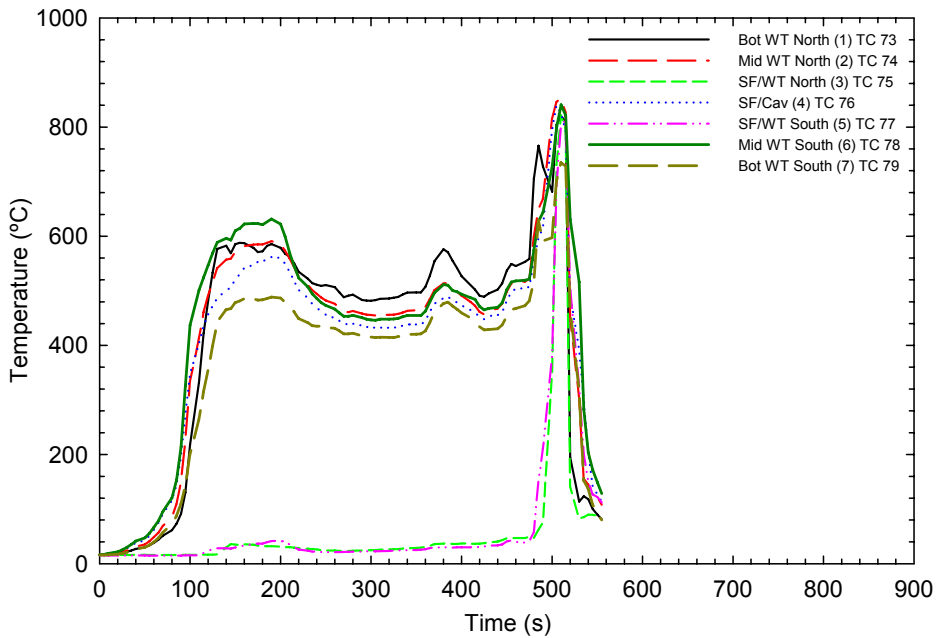
j) Thermocouples in cavity C-13

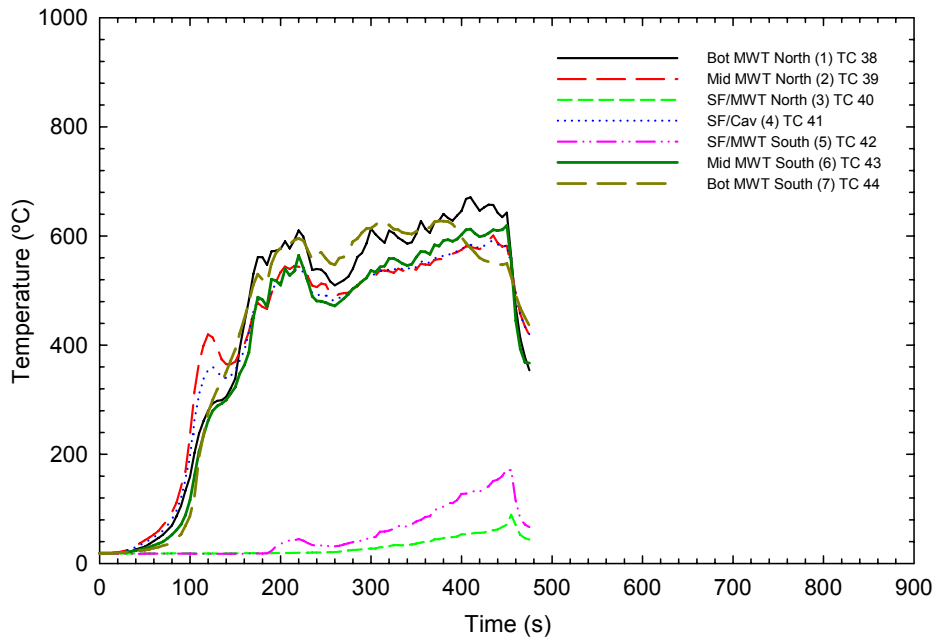**Figure 38 (i and j). Temperatures at the exposed side for Test UF-08**

NRC·CNRC
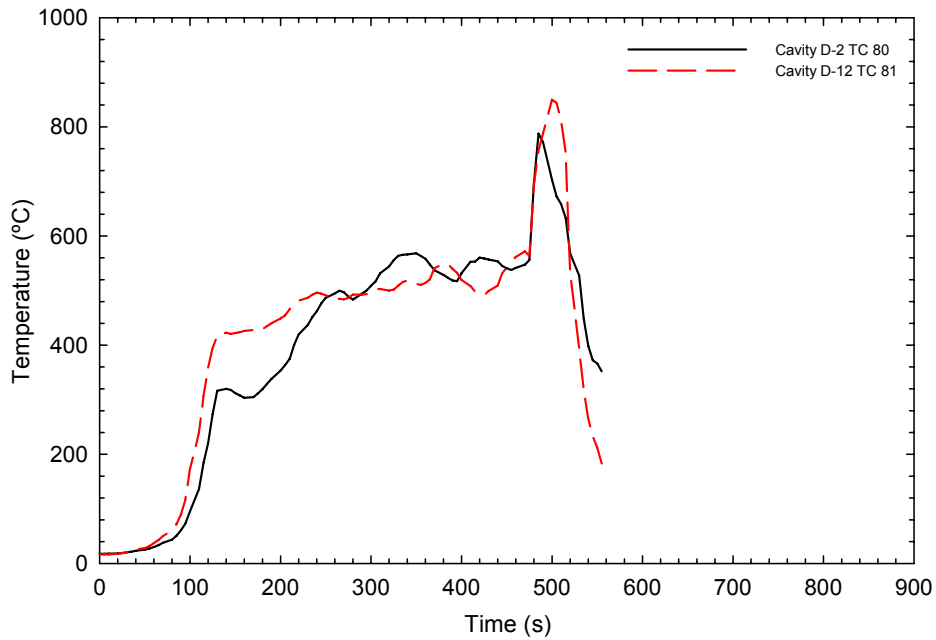
k) Thermocouples in cavity D-2 and D-12
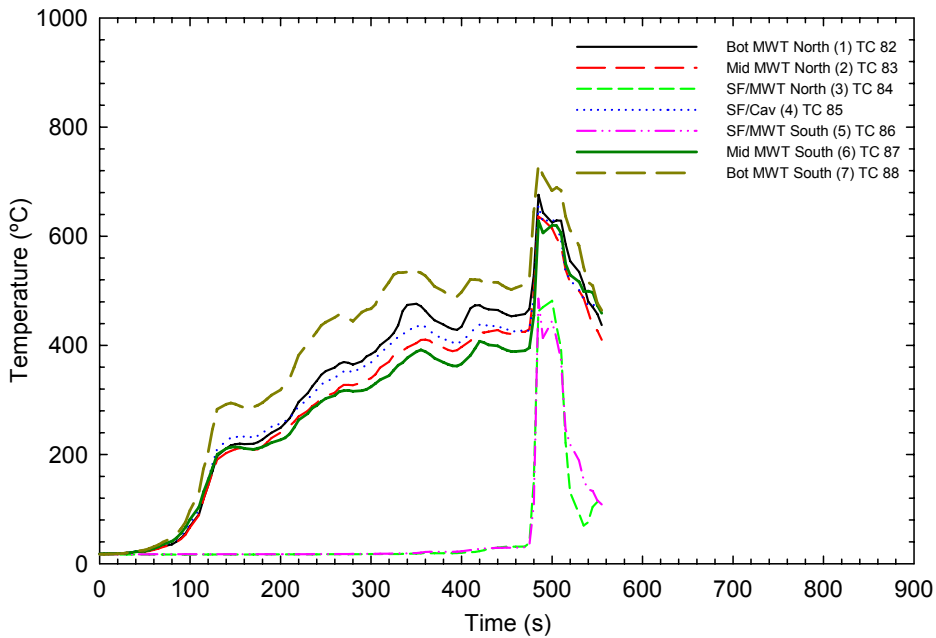
l) Thermocouples in cavity E-1

Figure 38 (k and l). Temperatures at the exposed side for Test UF-08

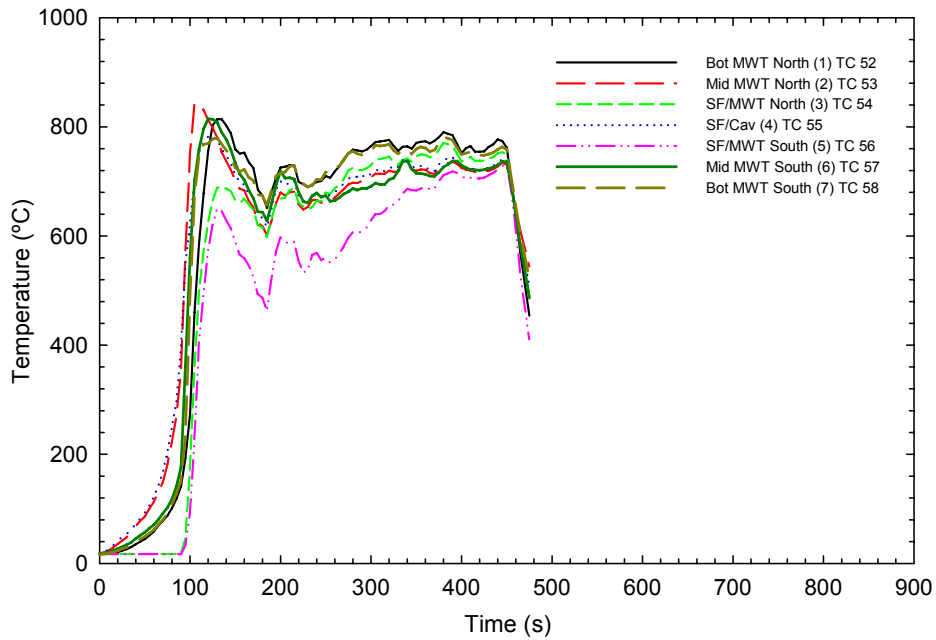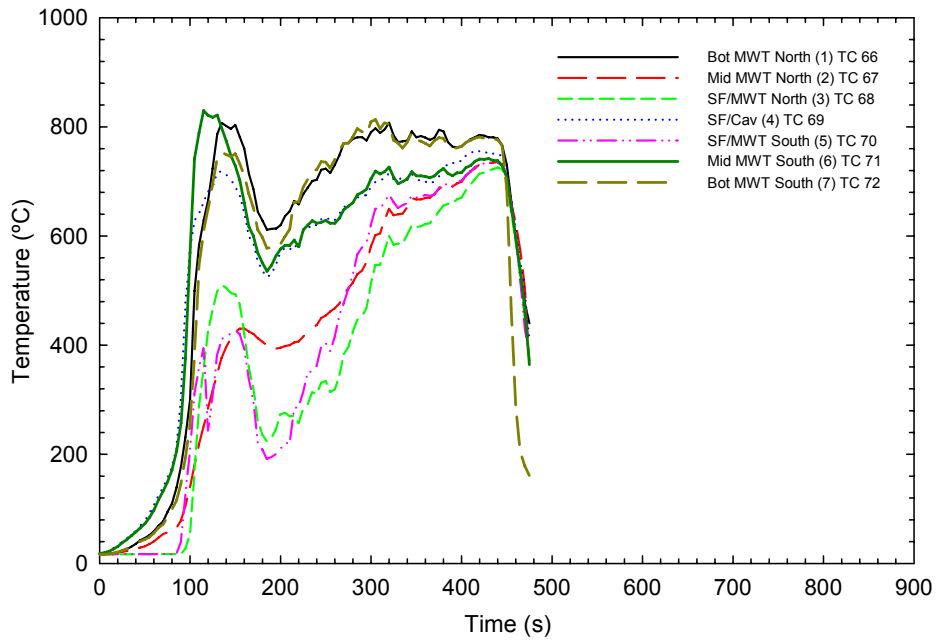**NRC·CNRC**
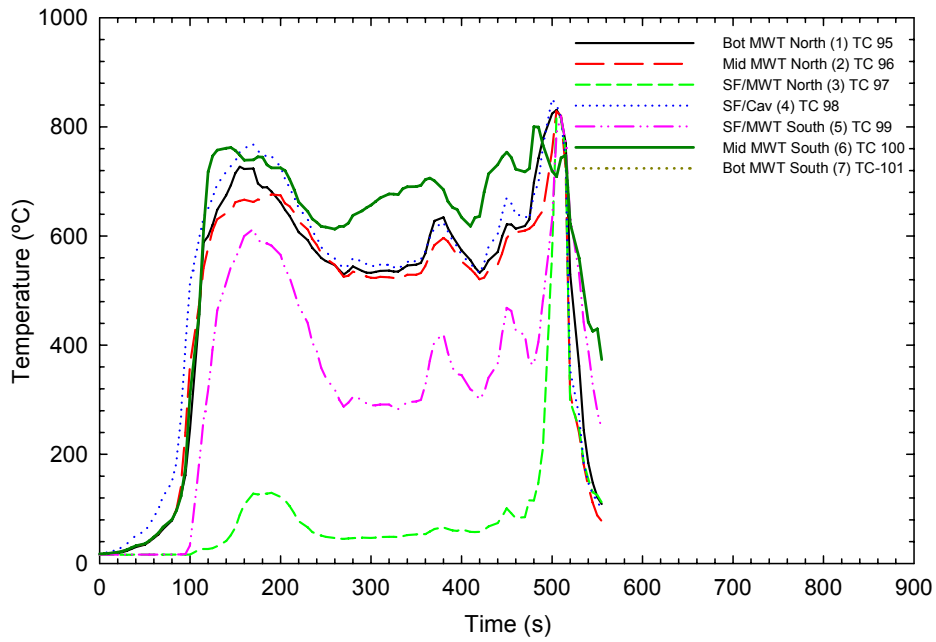
m) Thermocouples in cavity CD7
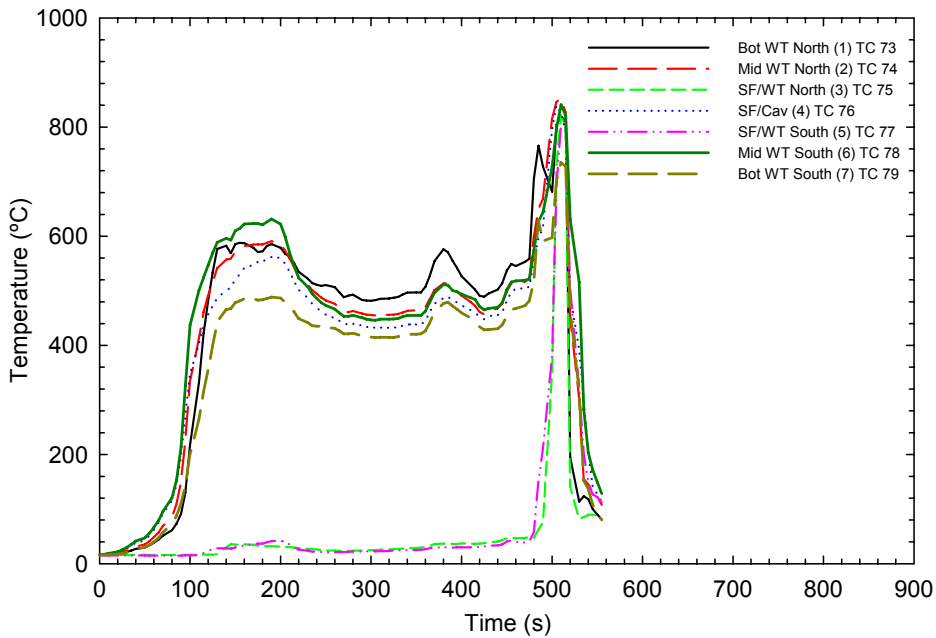
n)Thermocouples in cavity CD11

Figure 38 (m and n). Temperatures at the exposed side for Test UF-08

NRC·CNRC

3.4 Deflection Measurements Results and Structural Performance

Figure 39 shows the 9 deflection measurement points (see also Figure 11 for the truss closest to the deflection points). The points of measurement were chosen as they were located in the middle of the fire compartment just above the fire load where the impact of the fire on the structural integrity of the floor assembly was anticipated to be the greatest. Some measurement points were aligned with one of the trusses, while the other row was positioned between trusses. Figure 40 and Figure 41 show the deflections at the 9 measurement points for Tests UF-07 and UF-08.
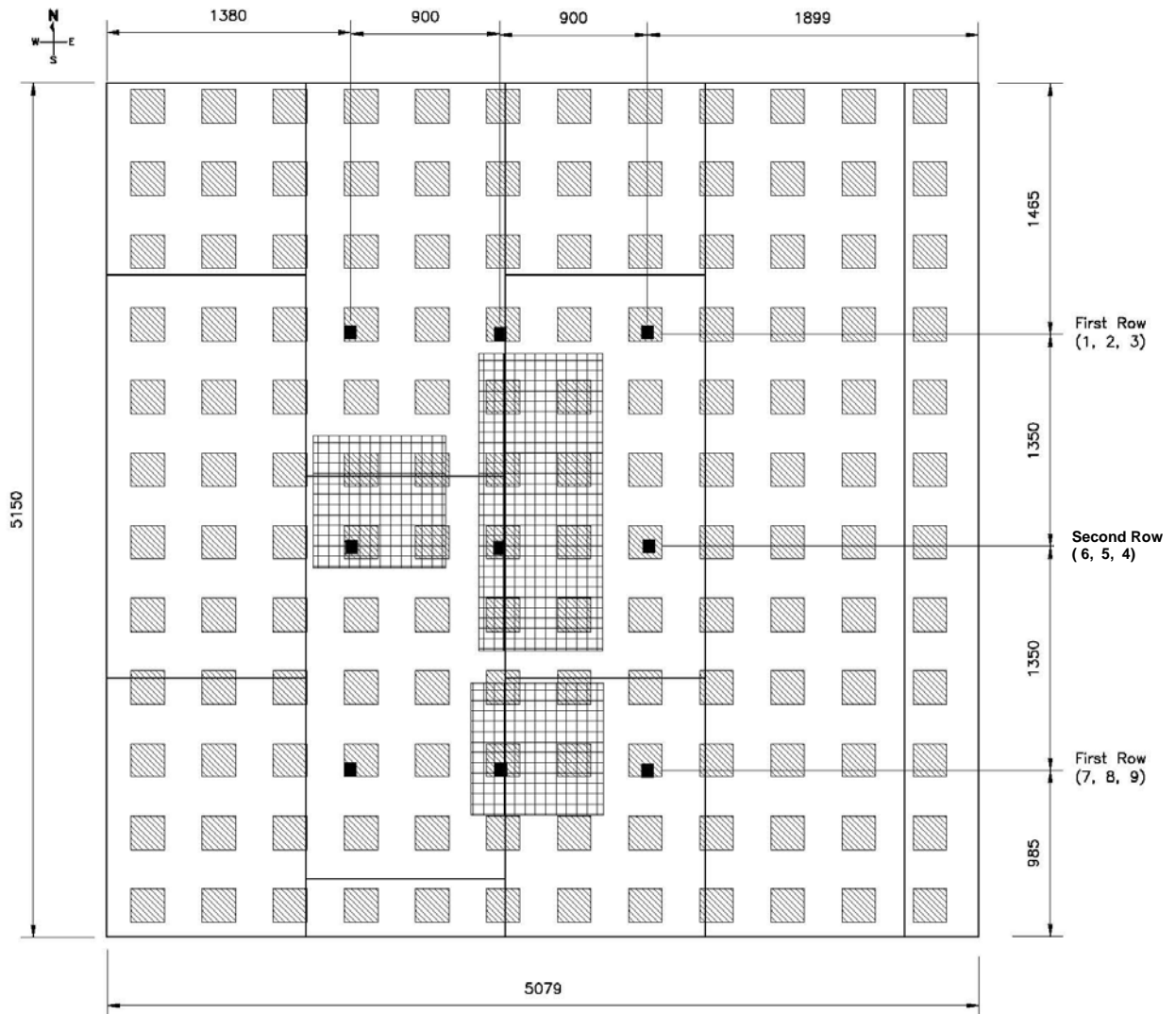
Figure 39. Deflection points measured (all dimensions in mm)

3.4.1 For Test UF-07

Figure 40 (a) shows the deflections measured in the first row (1, 2, and 3). Up to 200 s, the deflections were very small. After this time, the deflections increased at a relatively moderate rate, reaching about 120 mm at 320 s for point No. 1, 160 mm at 320 s for point No. 2, and 140 mm after 320 s for point No. 3. The sharp increase (vertical line) in deflection at 320 s indicates that the concrete blocks were falling and the floor was collapsing.

Figure 40 (b) shows the deflections measured in the second row (4, 5, and 6). Up to 200 s, the deflections were very small. After this time, the deflections increased at a relatively moderate rate, reaching about 170, 150 and 150 mm at 320 s for points 4, 5 and 6, respectively. The sharp increase (vertical line) in deflection at 320 s indicates that the concrete blocks were falling and the floor was collapsing.

Figure 40 (c) shows the deflections measured in the third row (7, 8, and 9). Up to 200 s, the deflections were very small. After this time, the deflections increased at a relatively moderate rate, reaching about 140 mm at point No. 7, 180 mm at point No. 8, and 140 mm at point No. 9. The sharp increase (vertical line) in deflection at 320 s indicates that the concrete blocks were falling and the floor was collapsing. The time of floor collapse was 325 s (visually observed through the basement window opening).
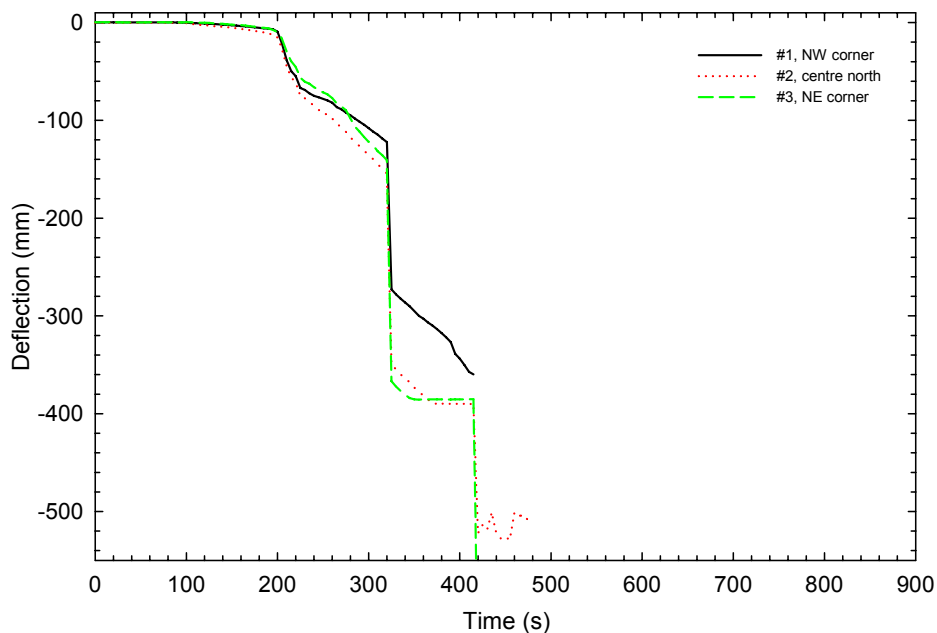
a) Floor Deflection, Row 1

Figure 40 (a). Deflection measurements for rows 1, 2 and 3 for Test UF-07

NRC·CNRC
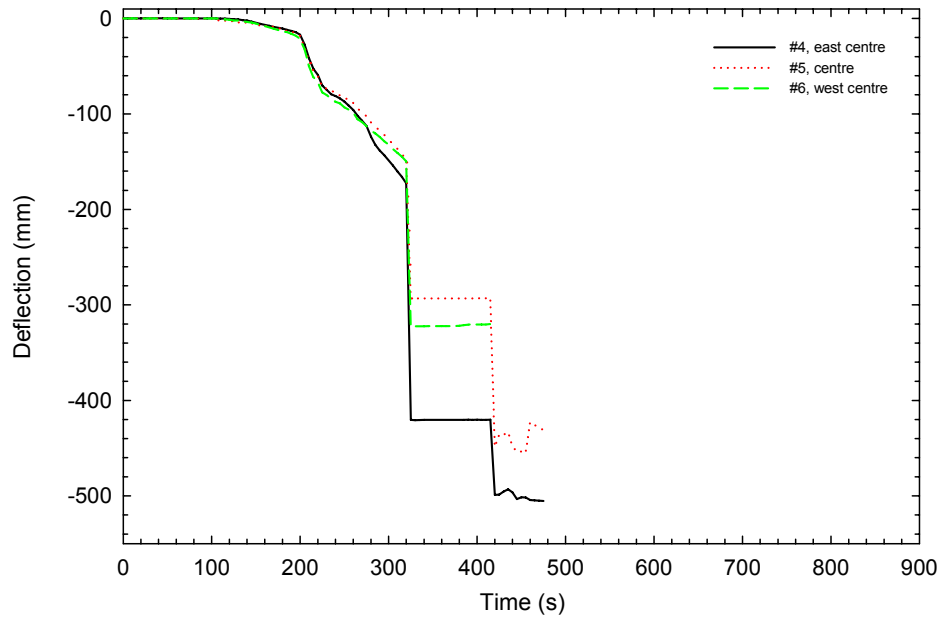
b) Floor Deflection, Row 2

Figure 40 (b). Deflection measurements for rows 1, 2 and 3 for Test UF-07
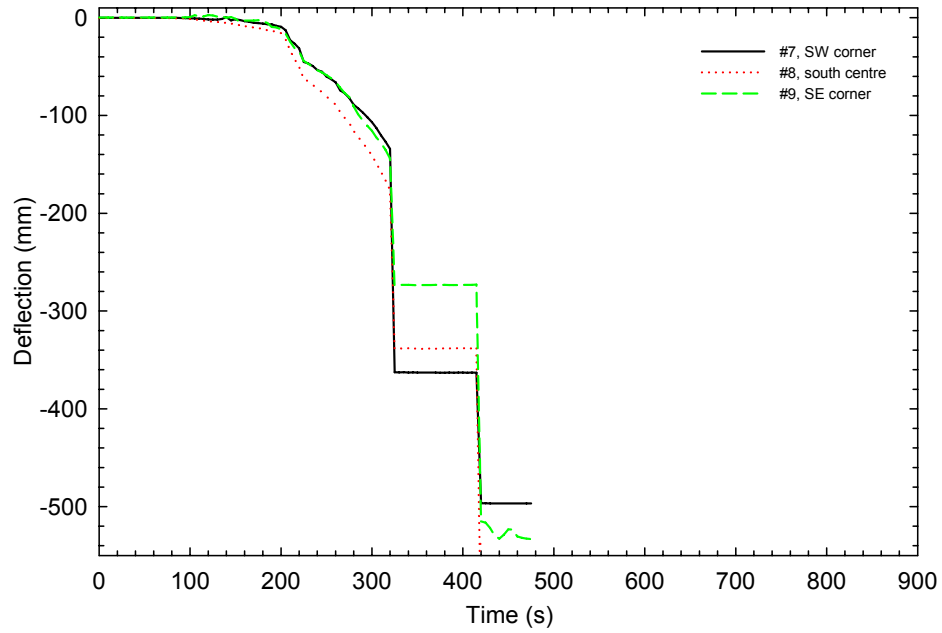
c) Floor Deflection, Row 3

Figure 40 (c). Deflection measurements for rows 1, 2 and 3 for Test UF-07

NRC·CNRC

3.4.2 For Test UF-08

Figure 41 (a) shows the deflections measured in the first row (1, 2, and 3). Up to 260 s, the deflections were very small. After this time, the deflections increased at a relatively moderate rate, reaching about 140 mm at point No. 1, 170 mm at point No. 2, and 180 mm at point No. 3 at 470 s. The sharp increase (vertical line) in deflection after 470 s indicates that the concrete blocks were falling and the floor was collapsing.

Figure 41 (b) shows the deflections measured in the second row (4, 5, and 6). Up to 200 s, the deflections were very small. After this time, the deflections increased at a relatively moderate rate, reaching about 250, 200 and 160 mm at 470 s at points 4, 5 and 6, respectively. The sharp increase (vertical line) in deflection after 470 s indicates that the concrete blocks were falling and the floor was collapsing.

Figure 41 (c) shows the deflections measured in the third row (7, 8, and 9). Up to 260 s, the deflections were very small. After this time, the deflections increased at a relatively moderate rate, reaching 120 mm at point No. 7, 150 mm at point No. 8, and 160 mm at point No. 9 at 470 s. The sharp increase (vertical line) in deflection after 470 s indicates that the concrete blocks were falling and the floor was collapsing. The time of floor collapse was 474 s (visually observed through the basement window opening).
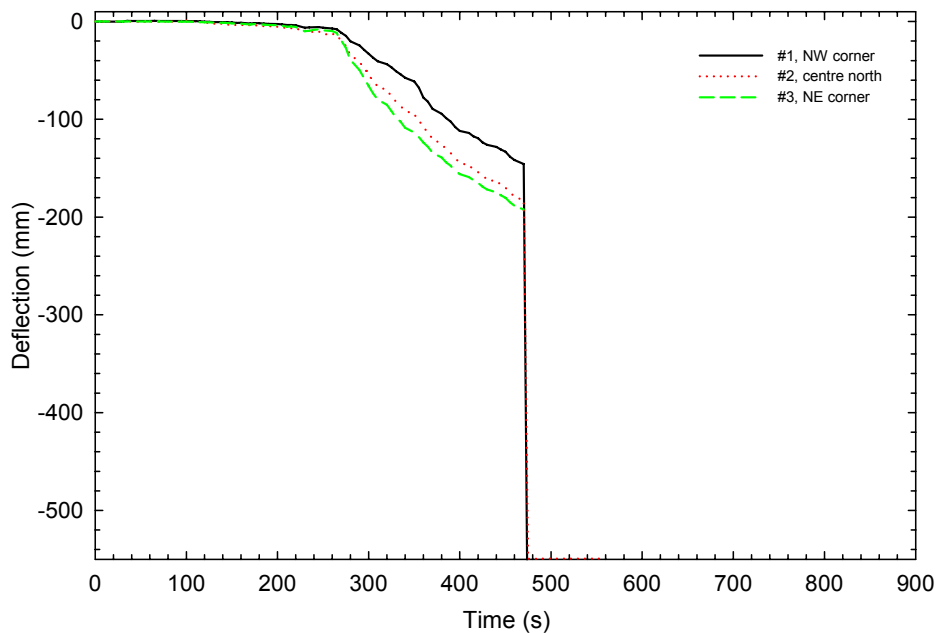
a) Floor Deflection, Row 1

Figure 41 (a). Deflection measurements for rows 1, 2 and 3 for Test UF-08

NRC·CNRC
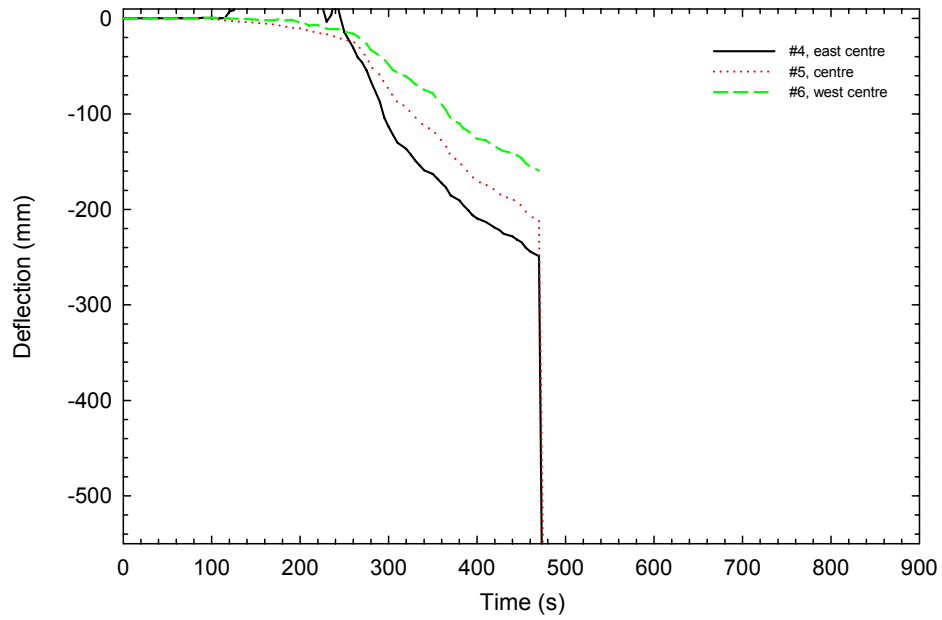
b) Floor Deflection, Row 2

Figure 41 (b). Deflection measurements for rows 1, 2 and 3 for Test UF-08
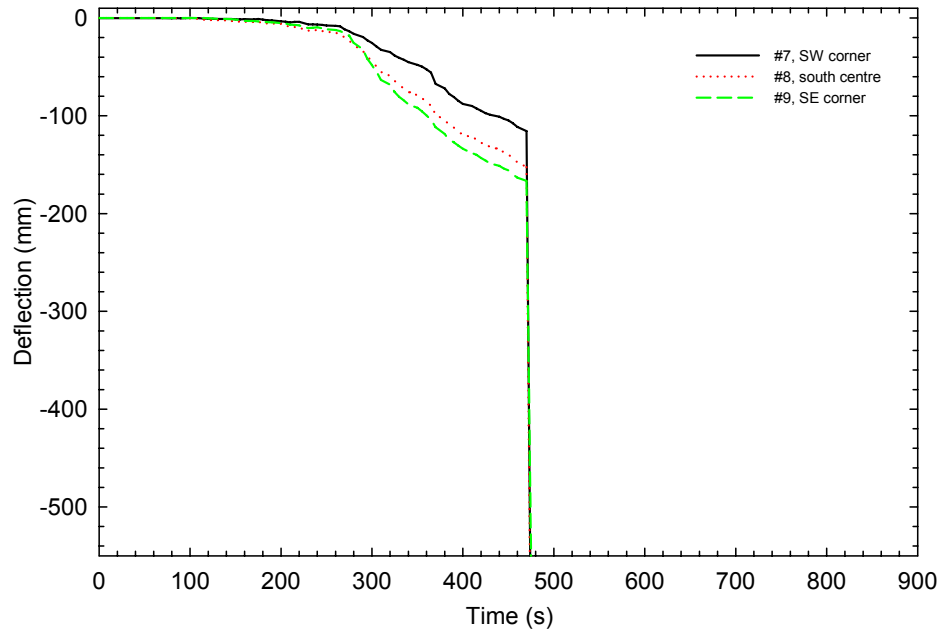
c) Floor Deflection, Row 3

Figure 41 (c). Deflection measurements for rows 1, 2 and 3 for Test UF-08

68

A comparison of the two tests (UF-07 and UF-08) shows that the fire scenario with the closed basement doorway resulted in a less severe fire impact, consequently the loadbearing capacity of the trusses and subfloor was extended, which, in turn, delayed the deflection of the floor and therefore the structural failure of the floor assembly. The time, after which the floor structure would be no longer usable for egress, was taken as the observed time of collapse of the floor (325 s for Test UF-07 and 474 s for Test UF-08), which was consistent with the time to reach the maximum deflection.

3.5 Flame Penetration Results

Flame penetration through the floor assembly is one of the important aspects of fire performance that is of interest in this project since this is also a failure criterion in standard fire resistance testing. Flames and combustion products penetrating through the floor can impact on the time available for evacuation. Any opening(s) created by the flames penetrating the subfloor or excessive deflection would also provide a means for hot fire gases to migrate from the basement fire room to the upper storey(s). As well, the holes would add to the overall weakening of the subfloor. To determine whether there was flame penetration through the floors, both a flame-sensing device and the time-temperature curves on the unexposed side of the floors were used.

3.5.1 For Test UF-07

Figure 42 shows the results of the flame-sensing devices. Three wire meshes were installed on the top of three joints (East, Centre and West) on the unexposed side of the floor as shown in Figure 17 (instrumentation figure). There was a sudden increase in the voltage output of the flame-sensing device when flames penetrated through the floor and struck the wire meshes. As indicated by Figure 42, flame penetration occurred at the Centre Joint at 320 s, which was very close to the failure of the floor assembly.

3.5.2 For Test UF-08

Figure 43 shows the results from the three flame-sensing devices, which were installed on the top of three joints (East, Centre and West) on the unexposed side of the floor as shown in Figure 17 (instrumentation figure). There was an increase in the voltage output of the device when flames penetrating through the floor struck the device. As indicated by Figure 43, the flames penetrated at all joints at 470 s, which was very close to the failure of the floor assembly.

Figure 36 (thermocouples 1 to 9 and 89 to 94 on the unexposed side) shows an increase in temperatures at about 470-480 s. This also indicates that flames breached the floor at this time. This time was also close to the time recorded by the flame-sensing device towards the end of the test. In addition, Figure 23 shows time-temperature curves at different heights at the middle of different quadrants on the first storey. As illustrated in the figure, there was an increase in temperatures at about 470-480 s indicating the possibility of flames penetrating to the unexposed side of the floor and hot smoke migrating to the upper storeys.

NRC·CNRC
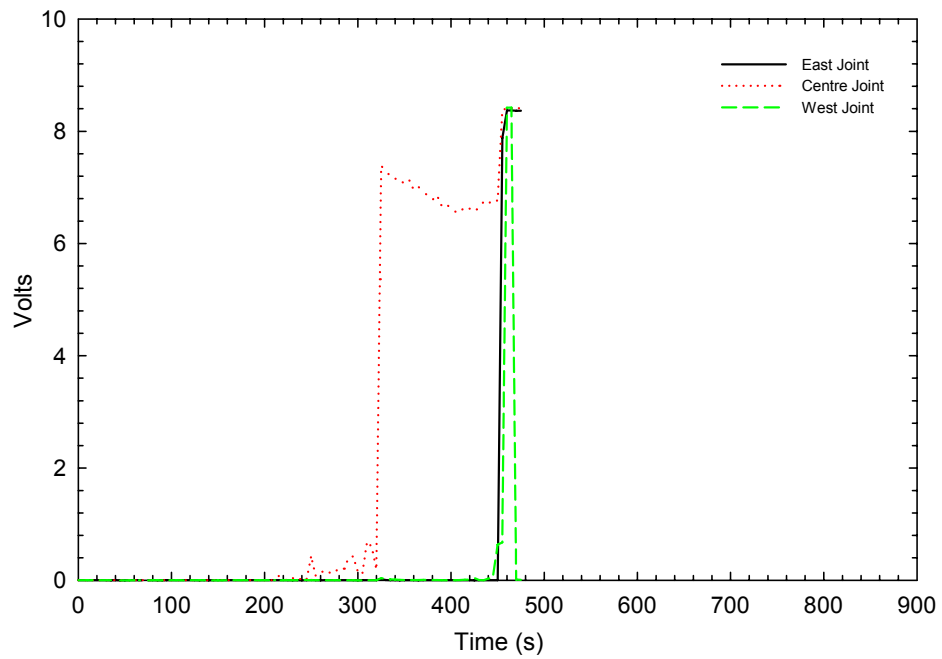
Figure 42. Results of flame sensors at different joints for Test UF-07
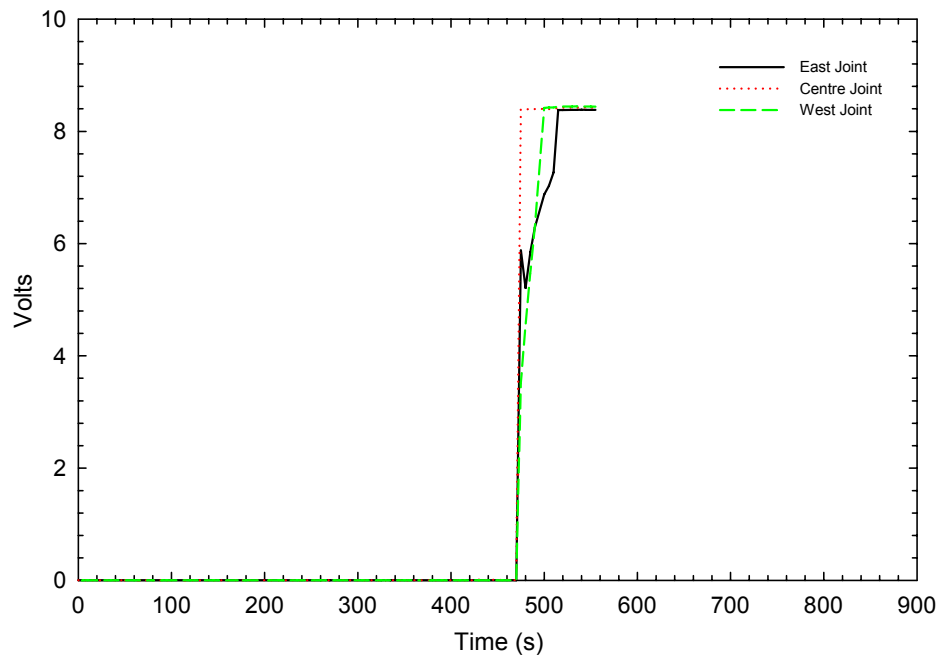
Figure 43. Results of flame sensors at different joints for Test UF-08

NRC·CNRC

3.6 Detection Times

Residential photoelectric and ionization smoke alarms were installed on the ceiling in each bedroom, second storey corridor, first storey and the basement fire compartment. These smoke alarms were powered by batteries and were not interconnected. The ionization smoke alarm was not installed in the basement fire room in order to avoid dealing with radioactive materials in the cleanup of debris after the fire tests. Since photoelectric smoke alarms are generally slower in detecting flaming fires than ionization smoke alarms, using the photoelectric smoke alarms in the basement resulted in more conservative estimates for activation times for the fire scenarios used in the experiments. New smoke alarms were used in each experiment.

Table 2 shows the activation times of the smoke alarms installed in the test facility. The photoelectric smoke alarms in the basement fire compartment took 50 s to activate. With the open basement doorway, it took up to 80 s longer for the smoke alarms in the second storey corridor to activate and up to 160 s longer for the smoke alarms in the closed bedroom to activate. With the closed basement doorway, the smoke alarms installed on the upper storeys took even longer to activate – 155 s longer for the smoke alarms in the second storey corridor and 465 s longer for the smoke alarms in the closed bedroom. This highlights the importance of having the smoke alarms interconnected to activate simultaneously when one of them detects a fire. Note that in Test UF-07 (open basement doorway), the ionization smoke alarm located on the first stoery detected the basement fire first at 40 s (10 s earlier than the photoelectric smoke alarm located in the basement fire room).

Table 2. Smoke Alarm Activation Times after Ignition (in seconds)

Location	Basement Fire room	First storey		Second storey corridor		SE bedroom (door closed)		SW bedroom (door open)	
Alarm Type	P	I	P	I	P	I	P	I	P
UF-07	50	40	55	110	130	190	210	130	145
UF-08	50	85	95	205	205	515	515	220	210

Notes:
1. See section on instrumentation in compartment (Figure 8 to Figure 10)
2. I: ionization, P: photoelectric, SE: South East, SW: South West

The results show that the activation time for the basement smoke alarm was very similar for the two tests, while the times to activation for the smoke alarms on upper storeys took longer in the case of UF-08, primarily due to the doorway from the basement being closed.

NRC·CNRC

3.7　Results of Smoke and Gas Measurements and Tenability Analysis

Fires produce heat, narcotic and irritant gases, and smoke that obscures vision. The temperature and the production of combustion products depend upon the fire characteristics, enclosure geometry and ventilation. The increased temperature and combustion products can, either individually or collectively, create conditions that are potentially untenable for occupants.

Tenability analysis involves examination of the production of heat and toxic products of combustion during the fire tests. It also involves estimation of the potential exposure of occupants, who would have been in the test house, to heat and toxic smoke and of the potential effects as a result of the exposure. The purpose of tenability analysis is to provide an estimation of the time available for escape — the calculated time interval between the time of ignition and the time after which conditions become untenable for an individual occupant.

There are various endpoints for tenability analysis, such as incapacitation, lethality/fatality, etc. For this project, *incapacitation* – a state when people lose the physical ability to take effective action to escape from a fire – was chosen as the endpoint for the tenability analysis related to heat and toxic products of combustion. The time available for escape thus calculated is the interval between the time of ignition and the time after which conditions become incapacitating for an individual occupant.

ISO 13571 and the SFPE Handbook of Fire Protection Engineering provide guidance and methodologies for evaluating the time available for occupants to escape from a fire [15, 16]. These methodologies are used in this report to calculate the time available for escape as an input to the hazard analysis for each fire scenario used in the project. The methodologies include a fractional effective dose (FED) approach to quantify the time at which the accumulated exposure to each fire effluent exceeds a specified threshold criterion for incapacitation. This time then is taken to represent the time available for escape relative to the specified threshold.

The calculated time available for escape depends not only on the time-dependent temperatures, concentrations of combustion gas products and density of smoke in the test house, but also on the characteristics of occupants. The age and health of the occupants (such as body weight and height, lung and respiratory system function, blood volume and hemoglobin concentration, skin, vision, etc.) as well as the degree of activity at the time of exposure have an effect on the consequences of exposure to fire effluents and heat. Since the general population has a wide range of susceptibility to fire effluents and heat, the exposure thresholds for incapacitation can change from subpopulation to subpopulation. Thus, each occupant is likely to have a different time available for escape.

This section of the report does not try to debate what FED criterion should be used as the incapacitation threshold but rather to present the results of the analysis for 2 typical FED values (e.g. FED = 1 and FED = 0.3). The methodology can be used to estimate the time available for escape associated with other FED values, if required.

The time available for escape calculated based on FED =1 represents the time available for a healthy adult of average susceptibility. The distribution of human responses to the

NRC·CNRC

fire effluents is unknown but is assumed to be a logarithmic normal distribution [15]. Under this distribution, the time available for escape calculated at FED =1 also represents statistically the time by which 50% of the general population would have been incapacitated but the conditions would still be tenable for the other 50% of the population.

For a more susceptible person, the threshold can be lower and the time available for escape would be shorter than for an average healthy adult. If FED = 0.3 is used as a criterion to determine the time available for escape, it would statistically represent the time by which 11% of the population would have been incapacitated but the conditions would still be tenable for the other 89% of the population [15].

The location of the occupant who would have been in the test house has an effect on the time available for escape. The analysis focused on the fire conditions affecting tenability, as measured on the first and second storeys of the test facility, and the impact on any occupant assumed to be present on the upper storeys of the test house at the time of ignition. In real fire situations, the occupant would move through different locations during egress. Therefore, the time to incapacitation would be in-between the times calculated for different locations. The conditions in the basement fire room would not be survivable once flashover occurred.

The methodology used does not address quantitatively any interaction (combined effects) between heat, combustion gas products and smoke obscuration. Each component is treated as acting independently on the occupants to create incapacitating conditions and the time available for escape is the shortest of the times estimated from consideration of exposure to combustion gas products, heat and visual obscuration.

It is necessary to recognize that 2 types of uncertainty exist in the tenability analysis: the uncertainties associated with the experimental data and the uncertainties associated with the equations used for FED calculations. Fortunately, with the fast-growing fire used in the project, the resulting uncertainty in the estimated time available for escape is much smaller than the uncertainty in the calculated FED due to their non-linear relationship. More details are provided in the following sections.

3.7.1   Exposure to Toxic Gases

Exposure to toxic products of combustion from fires has been a major cause of death and injury in many fire incidents. Understanding the toxic effect of the smoke products and predicting the exposure time necessary to cause incapacitation are complex problems.

In regards to the fuel package used in this study, with the combined flaming combustion of polyurethane foam and wood cribs, the primary gas products were toxic carbon monoxide (CO) and asphyxiant carbon dioxide (CO_2) in a vitiated oxygen (O_2) environment. Given the amount of polyurethane foam in the fuel package and the volume of the test house, hydrogen cyanide (HCN) produced from the combustion of polyurethane foam would not reach a concentration of concern for occupant life safety. A literature review by Beyler concluded that exposure to products of flaming combustion of flexible polyurethane foam would result in CO levels in the blood of test animals generally consistent with simple CO exposure, despite the toxicological role of HCN [17].

NRC·CNRC

The fuel package contained no chemical components that would produce acid halides in the combustion gases. In this report, the analysis involved CO and CO_2 and oxygen vitiation only.

Table 3 shows the maximum CO and CO_2 concentrations and the minimum O_2 concentrations for Tests UF-07 and UF-08. Figure 44 to Figure 46 and Figure 48 to Figure 50 (figures commence on page 85) show the CO, CO_2 and O_2 concentration-time profiles measured during Tests UF-07 and UF-08. The gases were well mixed in the test house.

The SFPE Handbook of Fire Protection Engineering contains information on the tenability limits for incapacitation or death after a 5-min exposure [16], shown in Table 4, which indicate the test results that need to be analyzed. In the following sections, tenability due to each gas is first analyzed independently; the interaction between the gases is then considered.

Table 3. Maximum CO and CO_2 Concentrations and Minimum O_2 Concentration (%)

		Test UF-07	Test UF-08
2nd storey	CO	2.4	0.6
	CO_2	13.5	1.5
1.5 m high	O_2	5.9	19.0
2nd storey	CO	2.0	0.5
	CO_2	13.2	1.4
0.9 m high	O_2	7.3	19.5
1st storey	CO	2.6	0.6
	CO_2	13.9	1.5
1.5 m high	O_2	5.5	19.0
1st storey	CO	>1.0	0.4
	CO_2	>10.0	1.1
0.9 m high	O_2	7.1	19.6

Notes:
1. ">" indicating the concentration beyond the measurement range of the gas analyzer;
2. All concentrations before the structural failure.

Table 4. Tenability Limits for Incapacitation or Death after 5-min Exposure [16]

Gas	Incapacitation	Death
CO	6000 – 8000 ppm (0.6 – 0.8%)	12,000 – 16,000 ppm (1.2 – 1.6%)
Low O_2	10 – 13%	< 5%
CO_2	7 – 8%	> 10%

NRC·CNRC

3.7.1.1 Exposure to O_2 vitiation

Fires consume oxygen and create a low oxygen atmosphere. Past human experiments in an oxygen-depleted atmosphere indicated that most people could tolerate a 15% O_2 atmosphere [16]. Healthy individuals could also tolerate a 12% O_2 level for a short period (<5 min) [18]. When oxygen diminished to below 10%, unconsciousness could occur rapidly. For healthy adults, the following equation was derived from the experiments with human subjects [16] and can be used to predict the time, t_{in,O_2} (minute), to loss of consciousness due to lack of oxygen alone.

$$t_{in,O_2} = \exp[8.13 - 0.54(20.9 - \%O_2)]$$

With the changing O_2 concentration, the fractional effective dose approach has to be used in the analysis. The incapacitation dose for oxygen vitiation can be expressed by $(20.9 - \%O_2) \times t_{in,O_2}$. The fractional effective dose is the accumulation of the ratio of the actual exposure dose $(20.9 - \%O_2) \times \Delta t$ and the incapacitation dose at each discrete increment of time:

$$F_{in,O_2} = \sum_{t1}^{t2} \frac{(20.9 - \%O_2) \cdot \Delta t}{(20.9 - \%O_2) \cdot t_{in,CO_2}} = \sum_{t1}^{t2} \frac{\Delta t}{\exp[8.13 - 0.54(20.9 - \%O_2)]}$$

where Δt (minute) is the discrete increment of time, i.e. the time interval for data sampling. Table 5 shows the calculated times for the fractional effective dose reaching 0.3 and 1.0 for exposure to O_2 vitiation alone.

In Test UF-07 (see Figure 45), the O_2 concentration on both the first and second storeys dropped to below 10% in 240 s and to 5% at 325 after ignition. The O_2 vitiation alone would cause incapacitation after 330-335 s (1st storey-2nd storey) using $F_{in,O_2} = 1$ as a criterion, or after 285-290 s (1st storey-2nd storey) using $F_{in,O_2} = 0.3$.

In Test UF-08 (see Figure 49), the O_2 concentrations in both storeys were above 19% for the first 480 s, after which the O_2 concentrations fell to below 5%. The O_2 vitiation alone would not result in incapacitation until after structural failure.

3.7.1.2 Exposure to CO_2

CO_2 is not toxic at concentrations of up to 5%. Above 7%, CO_2 becomes an asphyxiant gas; the danger of loss of consciousness of an exposed person increases. Loss of consciousness could occur in approximately 2 minutes at 10% CO_2, for example. The following equation can be used to predict the time, t_{in,CO_2} (minute), to loss of consciousness due to the CO_2 asphyxiant effect [16]:

$$t_{in,CO_2} = \exp(6.1623 - 0.5189 \cdot \%CO_2)$$

With the changing CO_2 concentration, the fractional effective dose approach has to be used. The incapacitation dose for CO_2 exposure can be expressed by $\%CO_2 \times$

NRC·CNRC

t_{in,CO_2} above which loss of consciousness would occur for people of average susceptibility. At each discrete increment of time, the increment of the fractional effective dose was calculated as the actual exposure dose (CO_2 concentration $\times$ time increment) divided by the incapacitation dose. The fractional effective dose values expressed in Table 5 are the accumulation of this ratio of each time increment:

$$F_{in,CO_2} = \sum_{t1}^{t2} \frac{\%CO_2 \cdot \Delta t}{\%CO_2 \cdot t_{in,CO_2}} = \sum_{t1}^{t2} \frac{\Delta t}{\exp(6.1623 - 0.5189 \cdot \%CO_2)}$$

In Test UF-07 (see Figure 46), the CO_2 concentration exceeded 10% in 240 s. The increased concentration of CO_2 alone would cause incapacitation after 290-295 s (1st storey-2nd storey) using F_{in,CO_2} = 1 as a criterion, and after 260-265 s (1st storey-2nd storey) using F_{in,CO_2} = 0.3.

In Test UF-08 (see Figure 50), the CO_2 concentrations in both storeys were below 2% for the first 480 s, after which the CO_2 concentrations increased sharply up to 16%. CO_2 alone would only cause incapacitation on the first storey 500 s after ignition.

3.7.1.3 Exposure to CO

CO is known to be the most important toxicant of the fire gases. The lowest CO concentration in air that has been reported to cause human death is 5,000 ppm for a 5 min exposure [19]. The toxic effect of CO is due to its affinity with the hemoglobin in human blood to form carboxyhemoglobin (COHb), which reduces the transport of oxygen in the blood to various parts of the body. When COHb in the blood increases to a threshold concentration, loss of consciousness or death may occur. The time for the toxic effect to occur depends on the uptake rate of CO into the blood of a victim and the threshold COHb concentration for that victim.

The CO uptake rate is determined by the difference between the CO concentration inhaled and that already in the body, and varies with the breathing rate, the degree of activity, the lung function, the body size, the blood volume and hemoglobin concentration of the victim and the exposure duration. The complexity of the CO uptake is described by the theoretical Coburn-Forster-Kane (CFK) equation, which takes account of a wide range of variables to predict the COHb concentration [20]. For high-concentration and short-duration exposures such as the fire scenarios used in the FPH tests, one can use a simpler equation that was derived from human exposure experiments with healthy adults [16, 21]:

$$\%COHb = 3.317 \times 10^{-5} [CO]^{1.036} RMV \cdot t$$

where [CO] is the inhaled carbon monoxide concentration in *parts per million*, RMV (respiratory minute volume) is the volume of air breathed in *litres per minute*, and *t* is the exposure duration in *minutes*. This equation gives equally good predictions as the CFK equation for average healthy adults. Since the CO concentration in the experiments varied with time, %COHb was calculated as a summation of the CO uptake at each discrete time step:

NRC·CNRC

$$\% COHb = \sum_{t_0}^{t} 3.317 \times 10^{-5} [CO]^{1.036} RMV \cdot \Delta t$$

For an average adult, the normal breathing rate is 20 L/min with light activity. The breathing rate is affected by the presence of CO_2 in a fire situation. In the concentration range of 2 to 6%, CO_2 can stimulate breathing. A CO_2-induced hyperventilation factor, VCO_2, for breathing can be estimated using [16]:

$$VCO_2 = \exp(\frac{\% CO_2}{5})$$

The hyperventilation increases the uptake rate of other toxic gases, such as CO, from the fire. This effect should be considered when CO_2 concentration is above 2%. The presence of 5% CO_2 could triple the normal breathing rate, for example. Considering the CO_2-induced hyperventilation in a fire situation, the breathing rate would be

$$RMV = 20 \cdot \exp(\frac{\% CO_2}{5})$$

For the same individual, the CO uptake rate changes if the breathing rate changes, which also depends on the degree of activity of that individual. The CO uptake rate varies from person to person for a given smoke atmosphere.

The COHb incapacitating concentration at which loss of consciousness may occur is in the range of 25-40% depending on the degree of activity of the occupant among other variables [16, 22]. The threshold of 40% is more appropriate for those at rest and 30% for those engaged in light activity [16]. Certain susceptible populations may be incapacitated at lower COHb concentrations.

With the rate of CO uptake and the likely incapacitating concentration of COHb, time to incapacitation due to CO exposure can be predicted. For those engaged in light activity, the fractional effective dose for incapacitation due to the CO uptake can be expressed as the COHb concentration in the blood divided by the incapacitating COHb concentration

$$F_{in,CO} = \frac{\% COHb}{30} = 2.2113 \times 10^{-5} \sum_{t_0}^{t} [CO]^{1.036} \Delta t \cdot \exp(\frac{\% CO_2}{5})$$

Alternatively, the fractional effective dose for incapacitation due to CO can also be calculated using the approach given in ISO TS 13571 for short exposure to CO at high concentrations [15]:

$$F_{in,CO} = \sum_{t1}^{t2} \frac{[CO] \cdot \Delta t}{35000} \exp(\frac{\% CO_2}{5})$$

where the incapacitation dose is 35000 ppm·min, which is consistent with the tenability limits of 6000 to 8000 ppm for incapacitation for 5-min exposure given in the SFPE Handbook of Fire Protection Engineering [16]. For the FPH tests, the difference between the incapacitation times predicted using these two equations is relatively small.

NRC·CNRC

The time to incapacitation determined using $F_{in,CO}$ = 1 as a criterion represents the time available for escape for healthy adults of average susceptibility. For more susceptible people, the exposure thresholds could be lower. The CO uptake and the COHb increase are known to be faster in small children than in adults [23]. Therefore, the incapacitation time for small children or a more susceptible subpopulation would be shorter than for average healthy adults. These can be addressed, to a certain degree, by using $F_{in,CO}$=0.3 as a criterion to determine the incapacitation time. Table 5 shows the calculated times for the fractional effective dose reaching 0.3 and 1.0. Calculation for the CO fractional effective dose was done with and without the CO_2 hyperventilation factor $exp(\%CO_2/5)$.

In Test UF-07 (see Figure 44), the maximum CO concentration prior to failure of the floor assembly was 28000 ppm at 320 s. The increased concentration of CO alone would cause incapacitation after 275-285 s (1st storey-2nd storey) using $F_{in,CO}$ = 0.3 as a criterion, and after 340-350 s (1st storey-2nd storey) using $F_{in,CO}$ = 1.0. With CO_2-induced hyperventilation, these times were reduced to 225-230 s (1st storey-2nd storey) for $F_{in,CO}$ = 0.3 and 265-275 s (1st storey-2nd storey) for $F_{in,CO}$ = 1.0.

In Test UF-08 (see Figure 48), closing the door to the basement prolonged the time available for escape, compared to Test UF-07. In Test UF-08, the second storey became untenable earlier than did the first storey. Using $F_{in,CO}$ = 0.3 as a criterion, the increased concentration of CO alone would cause incapacitation after 390 s on the second storey and 420 s on the first storey; with CO_2-induced hyperventilation, these times were reduced to 375 s on the second storey and 400 s on the first storey. Using $F_{in,CO}$ = 1.0 as a criterion, CO alone would not cause incapacitation ($F_{in,CO}$ did not reach 1); with CO_2-induced hyperventilation, the incapacitation times were 510 s on both storeys.

Table 5. Time (seconds) to the Specified FED for Exposure to O_2 Vitiation, CO_2 and CO

	Test UF-07		Test UF-08	
Fractional Effective Dose	**FED = 0.3**	**FED = 1.0**	**FED = 0.3**	**FED = 1.0**
CO alone – 1st storey	275	340	420	(FED ≤ 0.5)
CO with CO_2 hyperventilation – 1st storey	225	265	400	510
Low O_2 hypoxia – 1st storey	285	330	508	(FED ≤ 0.5)
CO alone – 2nd storey corridor	285	350	390	(FED ≤ 0.7)
CO with CO_2 hyperventilation – 2nd storey corridor	230	275	375	510
Low O_2 hypoxia – 2nd storey corridor	290	335	(FED ≤ 0.04)	(FED ≤ 0.04)
High CO_2 hypercapnia – 1st storey	260	290	501	507
High CO_2 hypercapnia – 2nd storey corridor	265	295	(FED ≤ 0.2)	(FED ≤ 0.2)

Note:
1. Based on concentrations at 1.5 m height

NRC·CNRC

3.7.1.4 Interaction of CO, CO_2 and O_2 vitiation

Interactions between these gases and their combined effect are not well understood. The asphyxiant effect of CO_2 is generally treated as being independent of other gases; the effect of O_2 vitiation (low oxygen hypoxia) is generally treated as being additive with the toxic effect of CO [16]. The effect of the smoke gases is determined by F_{in,CO_2} or $(F_{in,CO} + F_{in,O_2})$, whichever is larger (with $F_{in,CO}$ including the effect of CO_2-induced hyperventilation).

Table 6 shows examples of this treatment. The calculation shows that the O_2 vitiation did not add much to the effect at the time when CO was capable of producing incapacitation. CO was the most important toxicant of the smoke gases; increased CO uptake by CO_2-induced hyperventilation was the most important interaction. Therefore, the exposure to CO with CO_2-induced hyperventilation determined the incapacitation time for the gases analyzed. Assuming the rate of CO uptake remains unchanged, the time required from the incapacitation dose to the lethal dose for an average adult is estimated to be within 1 minute under the conditions of Test UF-07 (note that Test UF-08 did not last long enough to enable such an estimate)**.**

A recent paper by Gann includes an analysis of incapacitation by exposure to CO alone for a susceptible subpopulation such as people with coronary artery disease or small children; incapacitation could occur at an FED range of 0.14-0.21 (CO alone) [24]. As shown in Table 6, when the FED due to CO exposure with CO_2 hyperventilation reached 0.3, the FED due to CO exposure alone already reached this range. This shows consistency in the estimation of time to incapacitation.

Table 6. FED due to CO, CO_2, O_2 Vitiation at Specified Time

	Test UF-07 1st storey SW quadrant 1.5 m height		Test UF-08 2nd storey corridor 1.5 m height	
Time	**225 s**	**265 s**	**375 s**	**510 s***
CO alone	0.15	0.24	0.26	0.60
CO × CO_2 hyperventilation	0.32	1.2	0.32	1.2
Low O_2 hypoxia	0.008	0.12	0.003	0.04
CO × CO_2 hyperventilation + low O_2 hypoxia	0.33	1.3	0.32	1.2
High CO_2 hypercapnia	0.03	0.4	0.02	0.19

Note:
1. *Occurred after structural failure.

For exposure to the gases, each calculation for estimating incapacitation in this section was associated with a particular position where the concentrations were measured – each calculated time applies to an occupant who would stay at that particular location. In real fire situations, the occupant would move through different locations during egress. Therefore, the time to incapacitation would be in-between the times calculated for different locations.

NRC·CNRC

3.7.2 Exposure to Heat

Convected heat is the most important source of heat exposure for occupants in the first and second storeys. Figure 22 to Figure 25 and Figure 29 to Figure 32 show the temperature-time profiles measured on the two upper storeys during the tests. The temperatures at the 1.4 m height above the floor were used for the analysis of convected heat exposure.

The rate of convective heat transfer from hot gases to the skin depends on temperature, ventilation, humidity of the enclosure and clothing over the skin [16]. The tolerable time of exposure to convected heat is 15 min for dry air of 100°C or saturated air of 80°C. For hot air at temperatures above 120°C and with water vapour of less than 10%, pain and skin burns would be likely to occur in minutes; assuming unclothed or lightly clothed subjects, the time to incapacitation due to exposure to convected heat, $t_{in,conv}$ *(minutes)*, can be estimated for a constant temperature T *(°C)* using [15, 16]:

$$t_{in,conv} = 5 \times 10^7 T^{-3.4}$$

Since the temperatures in the FPH experiments were changing, the exposure was estimated using the fractional effective dose analogy at each discrete increment of time, Δt *(minutes)*:

$$\frac{\Delta t}{t_{in,conv}} = \frac{T^{3.4}}{5 \times 10^7} \Delta t$$

When the temperature is increasing or stable, the fractional effective dose for incapacitation due to the convected heat exposure can be calculated using the following equation:

$$F_{in,heat} = \sum_{t1}^{t2} \frac{\Delta t}{t_{in,conv}} = \sum_{t1}^{t2} \frac{T^{3.4}}{5 \times 10^7} \Delta t$$

The calculated time to incapacitation due to the convected heat exposure is given in Table 7. Radiant heat is important when the hot smoke layer is over 200°C, which corresponds to the threshold radiant heat flux of 2.5 kW·m^{-2} required to produce the second degree burning of skin [25]. The calculation indicated that the convected heat exposure would result in incapacitation before the radiant heat began to play a major role on the first and second storeys.

Each calculation was associated with a particular position where the temperature was measured; in other words, each calculated time applies to an occupant who would stay at the location of a particular thermocouple tree. In real fire situations, the occupant would move through different locations during egress. Therefore, the time to incapacitation would be in-between the times calculated for different locations.

For Test UF-07, the convective heat exposure alone would produce incapacitation, but the time depended on the location in the test house. In the corridor on the second storey, the incapacitation time would be after 225 s and 255 s for $F_{in,heat}= 0.3$ and $F_{in,\ heat}= 1$, respectively. In the open bedroom, the incapacitation time would be after 305 s for $F_{in,heat}= 0.3$ but $F_{in,\ heat}$ did not reach 1. Heat exposure would not contribute to

NRC·CNRC

incapacitation in the closed bedroom. On the first storey, the incapacitation time would be after 192-198 s using $F_{in,heat}$= 0.3 as a criterion, and 207-217 s using $F_{in,heat}$= 1.

In Test UF-08, the closed door in the doorway to the basement fire room impeded the transport of hot gases to the upper storeys, as indicated by the temperature profiles (Figure 22 to Figure 32). Incapacitation conditions due to heat exposure were reached in open areas on upper storeys after the structural failure of the test floor assembly. Heat exposure would not contribute to incapacitation in the bedrooms for the duration of the test.

Table 7. Time (in seconds) to the Specified FED for Exposure to Convected Heat

	Test UF-07		Test UF-08	
Fractional Effective Dose	**FED = 0.3**	**FED = 1.0**	**FED = 0.3**	**FED = 1.0**
1st storey SE quadrant	192	207	476	479
1st storey SW quadrant	192	207	482	486
1st storey NE quadrant	195	215	481	485
1st storey NW quadrant	198	217	486	489
2nd storey corridor	225	255	507	n.r. (FED < 0.5)
2nd storey open bedroom	305	n.r. (FED < 0.9)	n.r. (FED < 0.1)	n.r. (FED <0.1)
2nd storey closed bedroom	n.r. (FED < 0.003)	n.r. (FED < 0.003)	n.r. (FED < 0.003)	n.r. (FED < 0.003)

Notes:
1. Based on temperatures at 1.4 m height;
2. n.r. – not reached.

3.7.3 Visual Obscuration by Smoke

Visual obscuration by the optically dense smoke tended to be the first hazard to arise that could impede evacuation by the occupants. Although visual obscuration would not directly cause incapacitation, it would cause delays in movement by the occupants and thus prolong exposure of occupants to other hazards. In this report, the smoke obscuration is expressed as the optical density per meter (OD in m^{-1}):

$$OD = \frac{1}{L} \log_{10} \left(\frac{I_0}{I} \right)$$

where I_0 is the intensity of the incident light, I is the intensity of the light transmitted through the path length, L (m), of the smoke. The optical density is related to the extinction coefficient (k in m^{-1}) by $OD = k/2.303$.

Studies by Jin indicated that the optical density of smoke and visibility through smoke are related (the visibility is proportional to the reciprocal of the OD for non-irritating smoke, for example) [26]. Various threshold OD values related to the loss of visibility have been suggested for small buildings with occupants familiar with the egress route. The limiting OD value was suggested to be 0.5 m^{-1} for non-irritating smoke and 0.2 m^{-1} for irritating smoke [16,26]. A limiting OD value of 0.5 m^{-1} was also set by Babrauskas using the results of full-scale burns of upholstered chairs and mattresses [22,27]. A recent home smoke alarm study used an OD of 0.25 m^{-1} as the tenability limit for smoke

NRC·CNRC

obscuration [28]. In ISO 13571[15], the minimum visible brightness difference between an object and a background is used to estimate the smoke obscuration limit at which occupants cannot see their hands in front of their faces (a distance of 0.5 m or less). These calculations indicate that occupants cannot see their hands in front of their faces and become disoriented at an optical density of 3.4 m^{-1}. For an occupant whose vision is impaired, this can happen at an optical density of 2 m^{-1} or less.

Video records were also analyzed for visual obscuration. The video images became completely obscure when the optical density was approaching 2 m^{-1}. Note that there were at least 2 halogen lamps (2 x 500 Watts) providing lighting in the view direction of each video camera on the first and second storey. This lighting condition was much better than that in a real house.

In this report, a tenability limit for optical density is set at OD_{Limit} = 2 m^{-1}, recognizing that this limit could be lower for people with impaired vision. The time to untenable smoke obscuration is the moment when the optical density reaches this limit. Times to reach other smoke levels are also provided for discussion.

Figure 47 and Figure 51 show the optical density-time profiles measured on the first and second storeys. The times to reach various optical density levels at different locations for this series of the tests are listed in Table 8. It must be pointed out that the smoke density meters used for the first storey had a narrower range of signal output (0.15 to 0 V) while the smoke density meters used for the second storey had a wider working range (1 to 0 V). The starting voltage (0.15 or 1 V when there was no smoke) decreased due to smoke residue left over from the preceding tests on the light source and the detector inside the meters. This reduced the working range particularly for the smoke density meters used for the first storey, which became saturated at a lower OD level than the meters used for the second storey. The smoke density meters used for the first storey were not able to measure the smoke obscuration of OD = 2 m^{-1} and beyond. The analysis of video records indicated that by the time when OD = 2 m^{-1} was reached in the corridor on the second storey, there was complete smoke obscuration in the test house.

In a separate study, fire scenario (FS) tests were conducted in the test facility with the ceiling of the basement fire room lined with two layers of non-combustible cement board (no structural floor was installed above the fire room). Ventilation and door openings in Test FS-1 were the identical to those in Test UF-07; Test FS-4 identical to those in Test UF-08. Information about Tests FS-1 and FS-4 can be found in data compilation and analysis reports [6, 29].

In Test UF-07, the increase in the optical density at each measurement location was quite fast. The times to reach various optical density levels of interest were very similar to the fire scenario Test FS-1. The combustion of the polyurethane foam produced sufficient smoke for conditions to reach the smoke obscuration limit. Both the optical density measurements and video records indicate that complete visual obscuration occurred around 170 s in the test house. (Due to the exterior door was opened at 180 s, the optical density on the first storey temporarily decreased after opening the exterior door then increased again.)

With the basement door closed in Test UF-08, the increase in OD was slower at various measurement points than in Test UF-07 (compare Figure 47 and Figure 51). The OD_{Limit} = 2 m^{-1} was reached at 360 s in the corridor on the second storey. Both the

NRC·CNRC

optical density measurements and video records indicate that complete visual obscuration occurred by this time in the test house.

Psychological effects of smoke on occupants may accelerate the loss of visibility [26]. Possible reduction of time to untenable smoke level due to psychological effect is not addressed in this report.

Table 8. Time (in seconds) to the Specified Smoke Optical Density

	Test UF-07				Test UF-08			
OD (m^{-1}) =	0.25	0.50	1.0	2.0	0.25	0.50	1.0	2.0
1st storey SW quadrant 1.5 m height	123	131	134	n.a.	180	210	220	n.a.
1st storey SW quadrant 0.9 m height	143	150	161	n.a.	275	320	340	455
2nd storey corridor 1.5 m height	135	145	155	170	200	210	265	360
2nd storey corridor 0.9 m height	145	155	165	295	230	260	290	385

Note:
1. n.a. – not available due to limited measurement range of the smoke meters used for the first storey.

3.7.4 Summary of Estimation of Time to Incapacitation

Tenability was analyzed independently for gas exposure, heat exposure and smoke obscuration to estimate the time available for escape, using incapacitation as the endpoint. The combined incapacitating effect as a result of simultaneous exposure to the combustion gases, heat and smoke obscuration is not well understood. Table 9 summarizes the estimated times to the onset of untenable conditions, where each value is the shortest time among each set of values from Table 5, Table 7 and Table 8.

Table 9. Summary of Estimation of Time to Specified FED and OD (in seconds)

	OD = 2 m^{-1}	FED = 0.3		FED = 1	
Test	2nd storey	1st storey	2nd storey	1st storey	2nd storey
Tests with open basement doorway					
FS-1	190±5	*245±15*	*260±15*	*290±20*	*325±30*
UF-07	170±5	**192±2**	*230±25*	**207±5**	**255±10**
Tests with closed basement doorway					
FS-4	not reached	*1550±410*	*1100±300*	not reached	not reached
UF-08	360±5	*400 (-55, +40)*	*375±35*	**486±1**	*510 (-50, +*)*

Notes:
1. Values determined using the measurements at 1.5 m height (for gas concentrations and OD) or 1.4 m height (for temperatures);
2. The number with the *Italic* font represents the calculated time for reaching the CO incapacitation dose, while the number with the bold Arial font represents the calculated time for reaching the heat incapacitation dose, whichever occurred first;
3. All values shown in the table are before fire suppression;
4. * Upper range of uncertainty in timing is unavailable due to commencement of fire suppression.

NRC·CNRC

The uncertainty in the calculation of the FED is estimated to be ±25% for the heat exposure and ±40% for the CO exposure (with CO_2 induced hyperventilation) [15]. With the fast-growing fire used in the FPH project, the resulting uncertainty in the estimated time is much smaller than the uncertainty in the calculated FED due to the non-linear relationship. The uncertainty in the timing of the optical density measurement is ±5 s. Table 9 lists the uncertainty in the estimated time.

Smoke obscuration was the first hazard to arise. Although smoke obscuration would not directly cause incapacitation, it could impede evacuation and prolong exposure of occupants to other hazards. In Test UF-07, the time to reach various optical density levels of interest was very similar to that of Test FS-1 and the combustion of polyurethane foam was mainly responsible for reaching the smoke obscuration limit. With the basement door closed in Test UF-08, the increase in *OD* was slower than in Test UF-07. It must be pointed out that people with impaired vision could become disoriented at a lower optical density.

Because of the variation in susceptibility to heat and/or gas exposure, the time to untenable conditions was not a single value. The times corresponding to FED = 0.3 and FED = 1 in Table 9 represent this variation to a certain extent. There was also a slight variation of the corresponding time on the 2 different storeys, which is reflected by the time range for each FED in Table 9.

Closing the door to the basement fire room prolonged the time available for escape for occupants on the upper storeys. For Test UF-08 with the door to the basement closed, the products of combustion were initially transported into the first storey through the undercut of the basement door. It was recognized that the air-tightness around the perimeter of the floor-ceiling test assembly could have an impact on the time to untenable conditions on the upper storeys. Efforts were made during the construction of the test assembly to minimize potential leakage by putting ceramic fibre blankets in the small gaps around the perimeter but actual leakage was not measured.

For the closed bedroom, only heat exposure could be estimated. Based on the temperature measurements and the heat exposure calculation, during both tests, the conditions in the closed bedroom on the second storey would not reach untenable conditions associated with FED = 0.3 or 1.

The analysis so far addressed a potential exposure that started at the time of ignition, which applies to occupants who would have been in the open spaces of the house.

Further analysis was also conducted for exposure starting at times later than ignition. This further analysis is important for occupants who would have been in the closed bedroom but tried to open the bedroom door to escape through the normal routes. Figure 52 and Figure 53 show the time remaining to incapacitation calculated from the convected heat and hyperventilated CO exposure for people of average susceptibility (FED=1) and for more susceptible occupants (FED=0.3) as a function of onset of exposure. Again, this calculation was associated with particular positions where the concentrations or temperatures were measured (each calculated time applies to an occupant who would have stayed at that particular location). The actual time to incapacitation would be in between the times calculated for different locations since an occupant would have moved through different locations during egress.
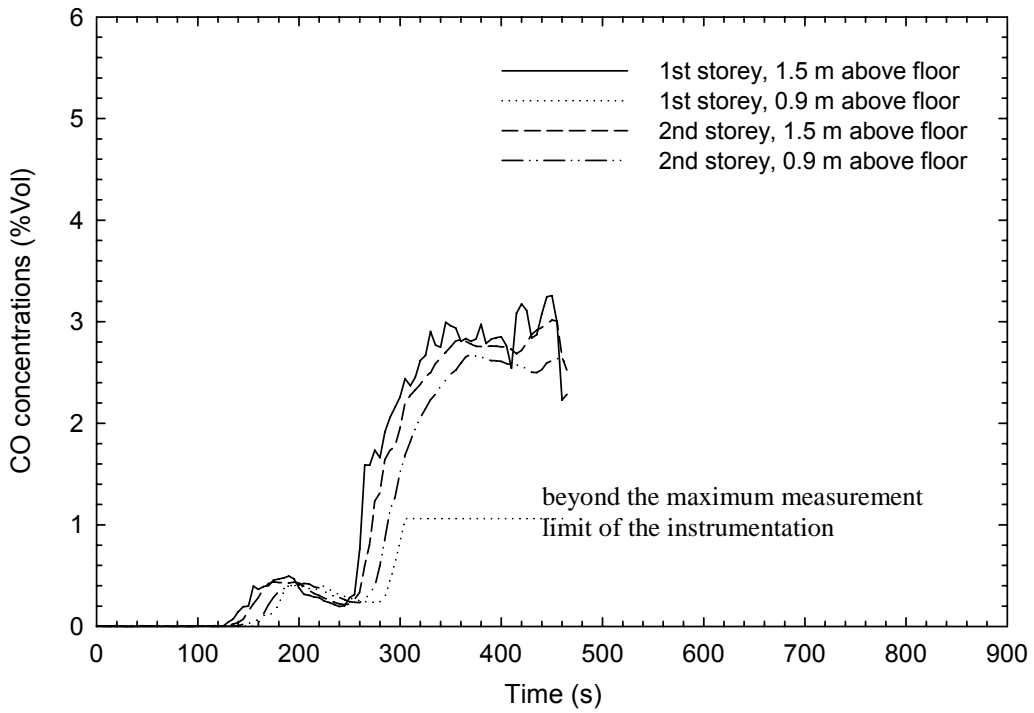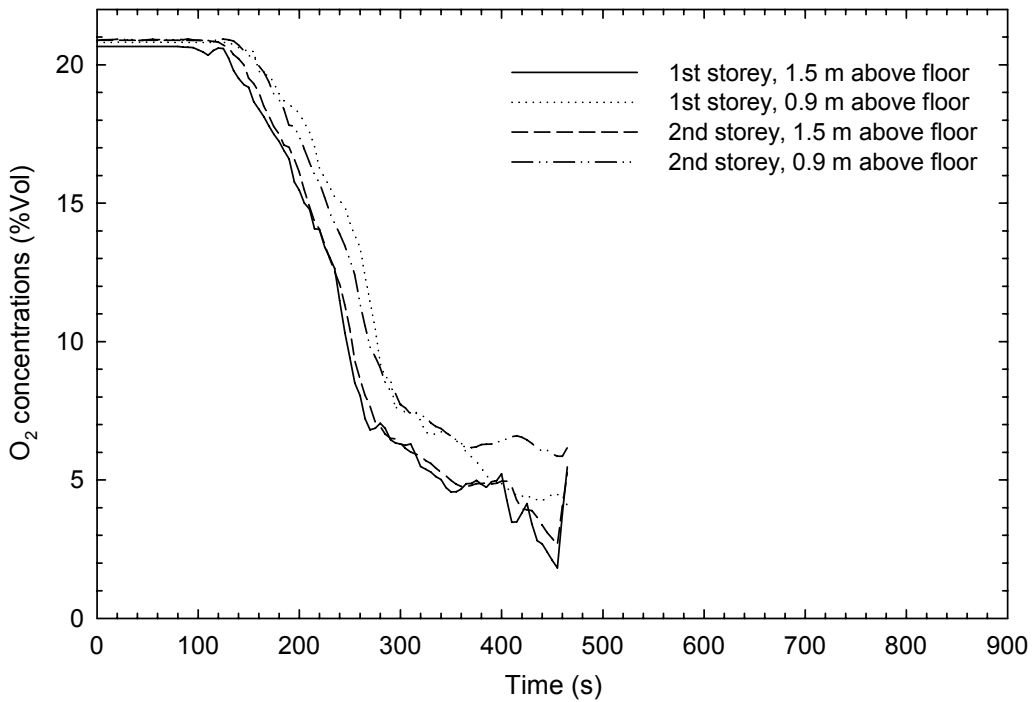
NRC·CNRC

Figure 44. CO measurements for Test UF-07

Figure 45. O₂ measurements for Test UF-07

NRC·CNRC

Figure 46. CO$_2$ measurements for Test UF-07

NRC·CNRC

a) Smokemeters - 1st storey SW quadrant.

b) Smokemeters - 2nd storey corridor

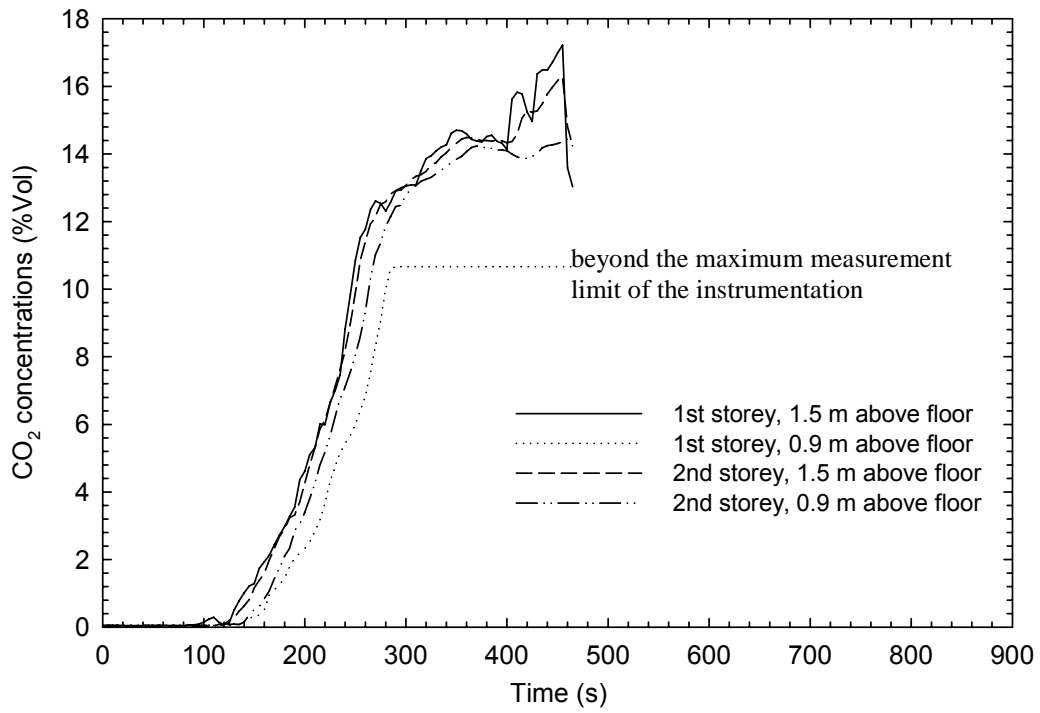**Figure 47. Optical density measurements for Test UF-07**

NRC·CNRC

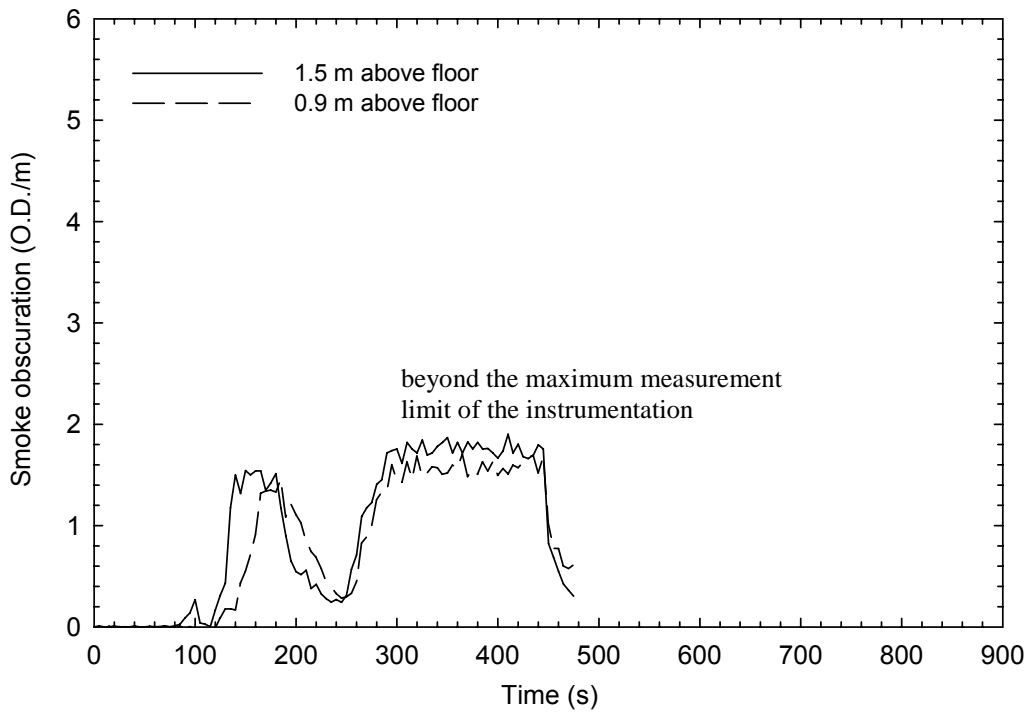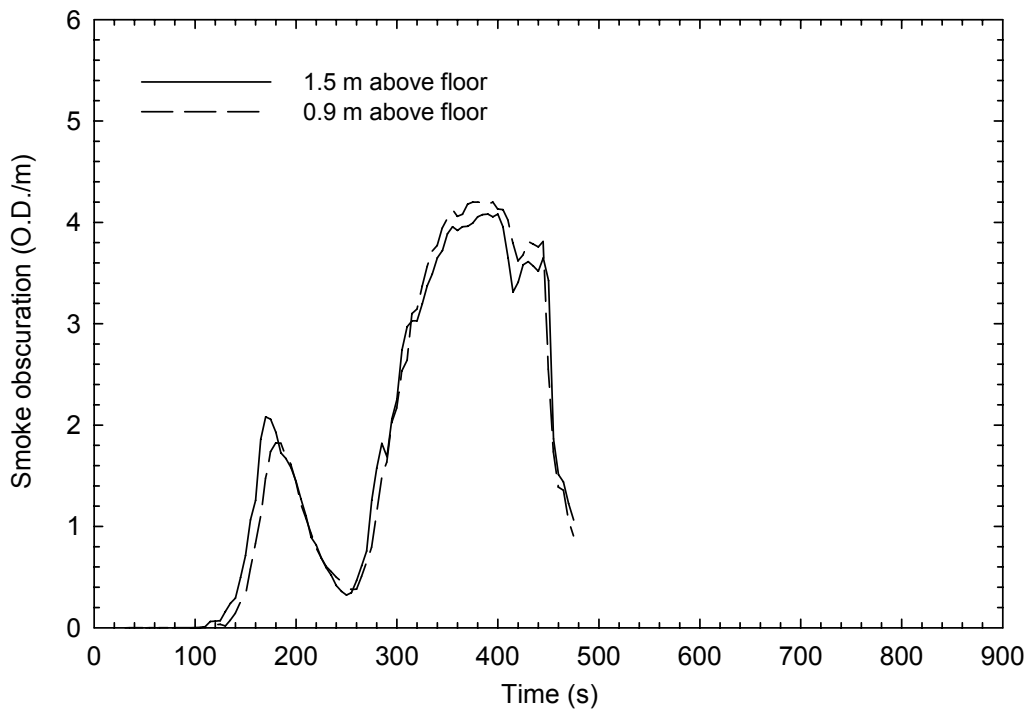**Figure 48. CO measurements for Test UF-08**
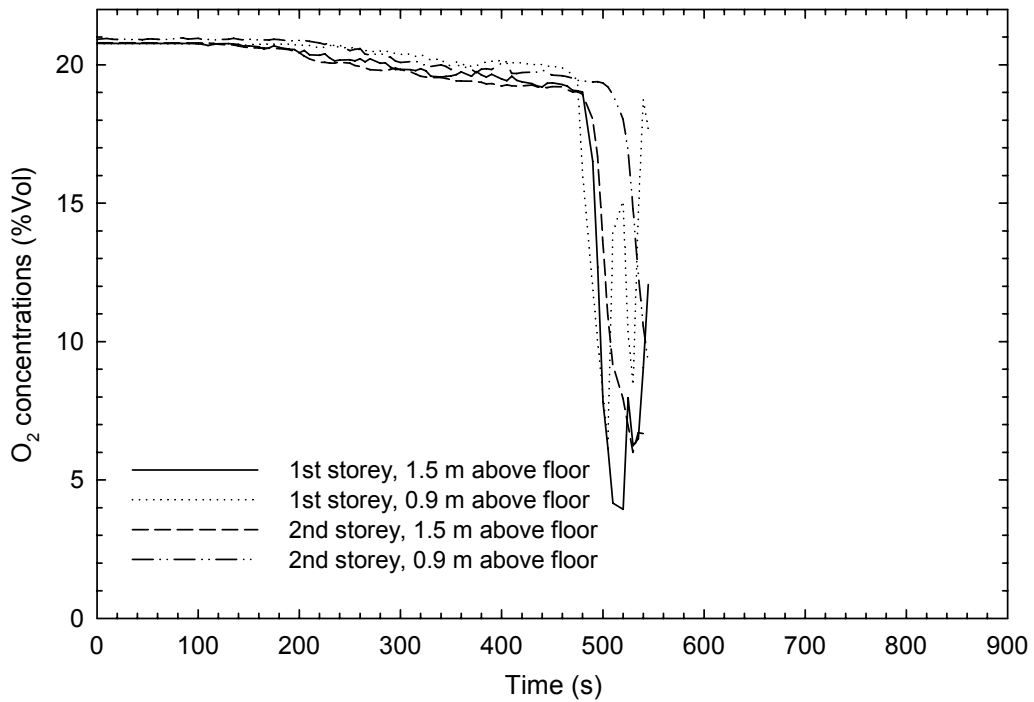
Figure 49. O₂ measurements for Test UF-08

NRC·CNRC
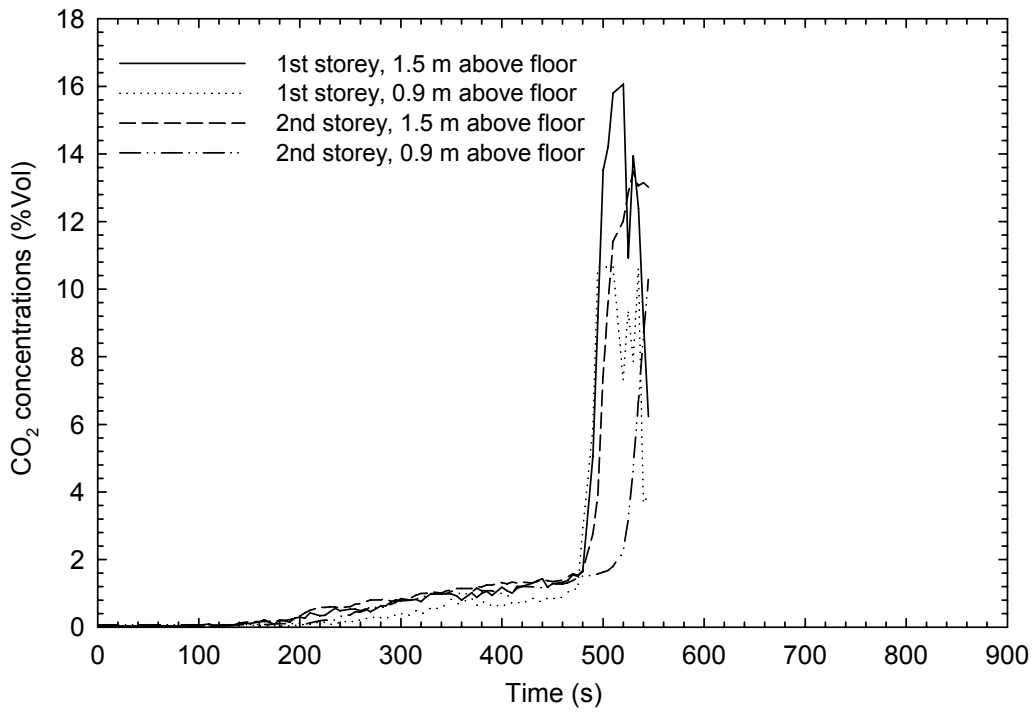
Figure 50. CO$_2$ measurements for Test UF-08
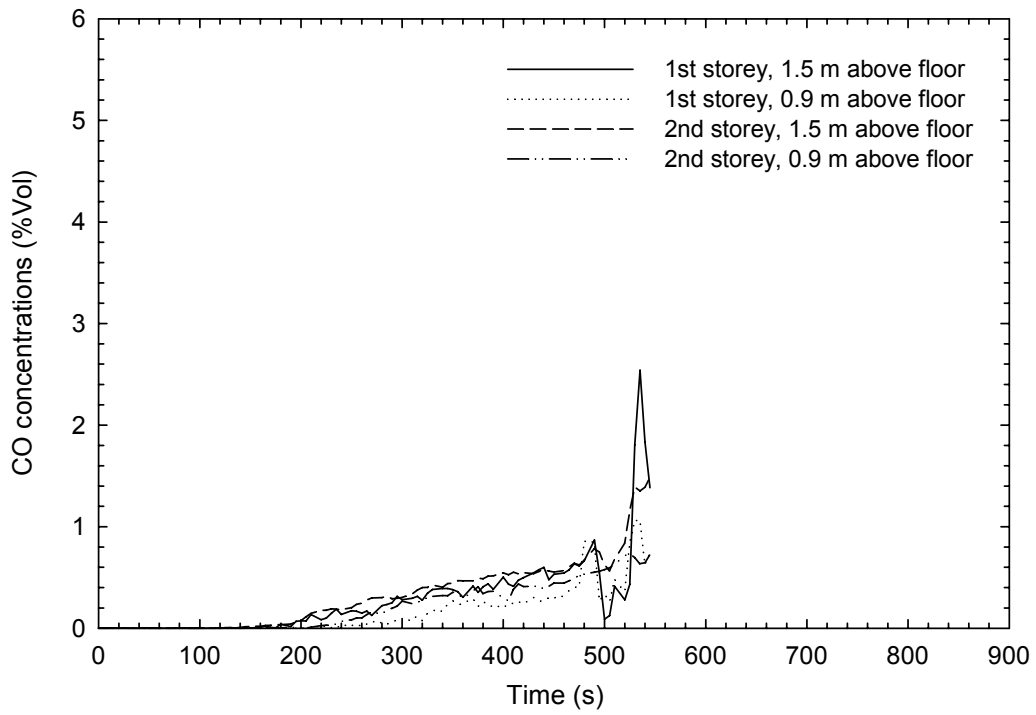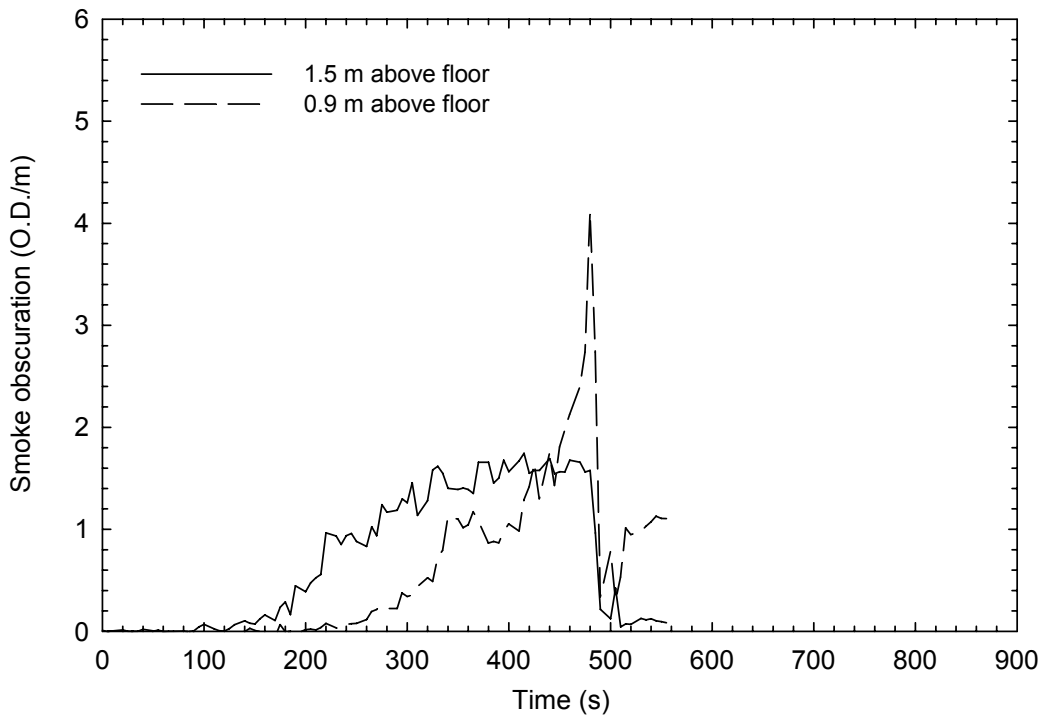
a) Smokemeters - 1st storey SW quadrant.
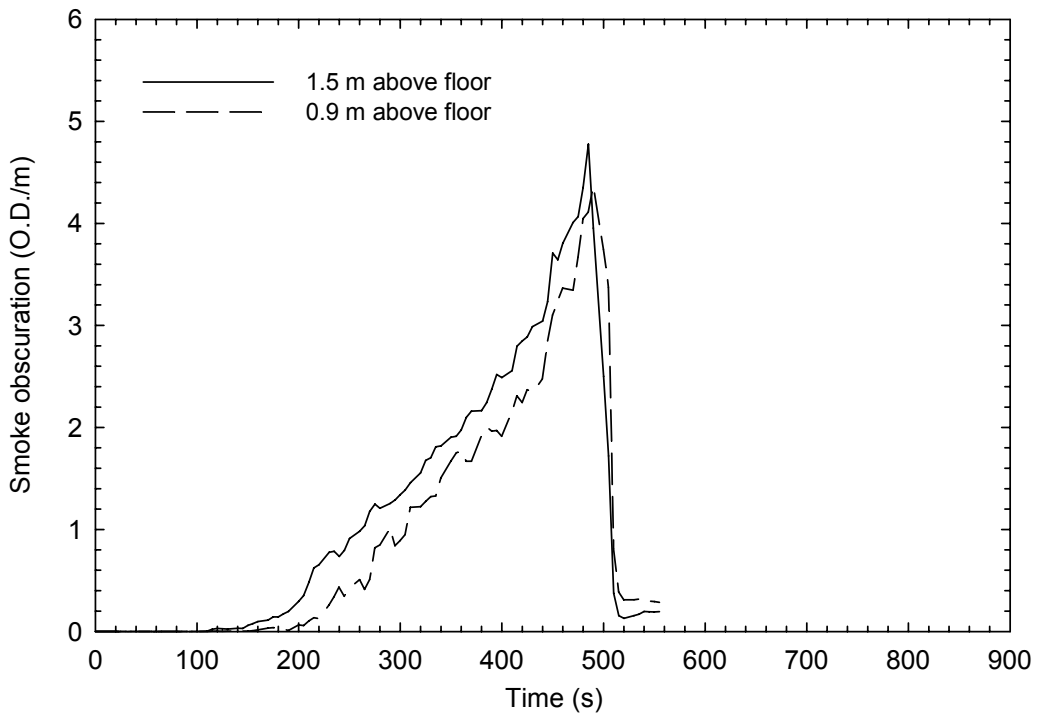
b) Smokemeters - 2nd storey corridor

Figure 51. Optical density measurements for Test UF-08

NRC·CNRC
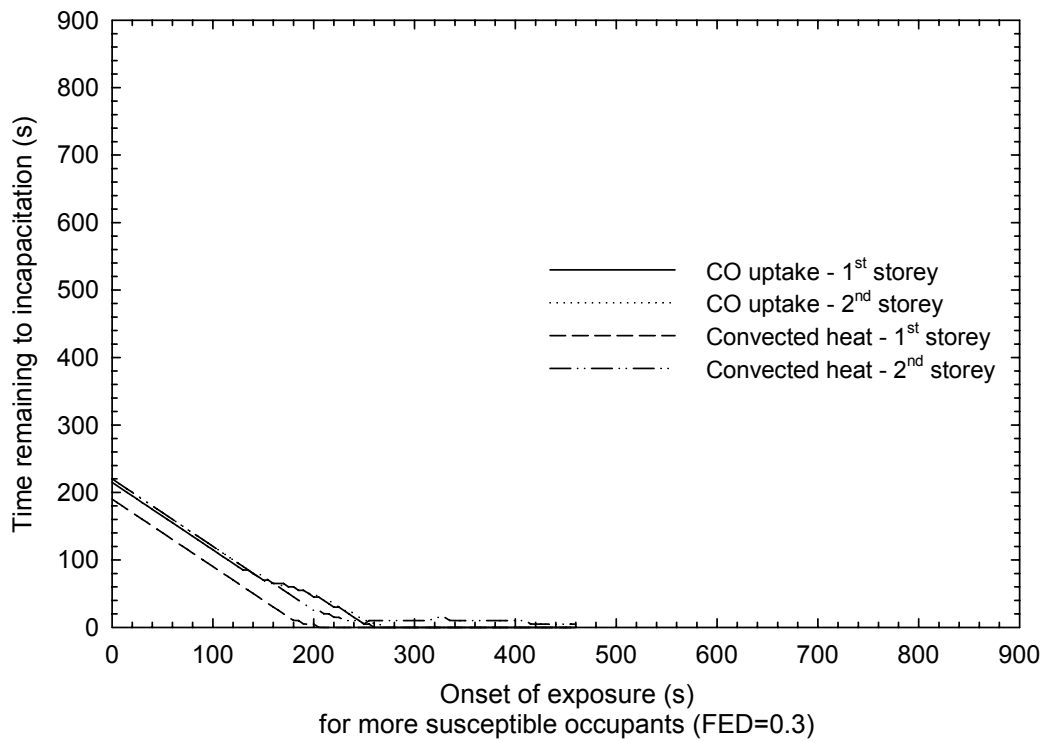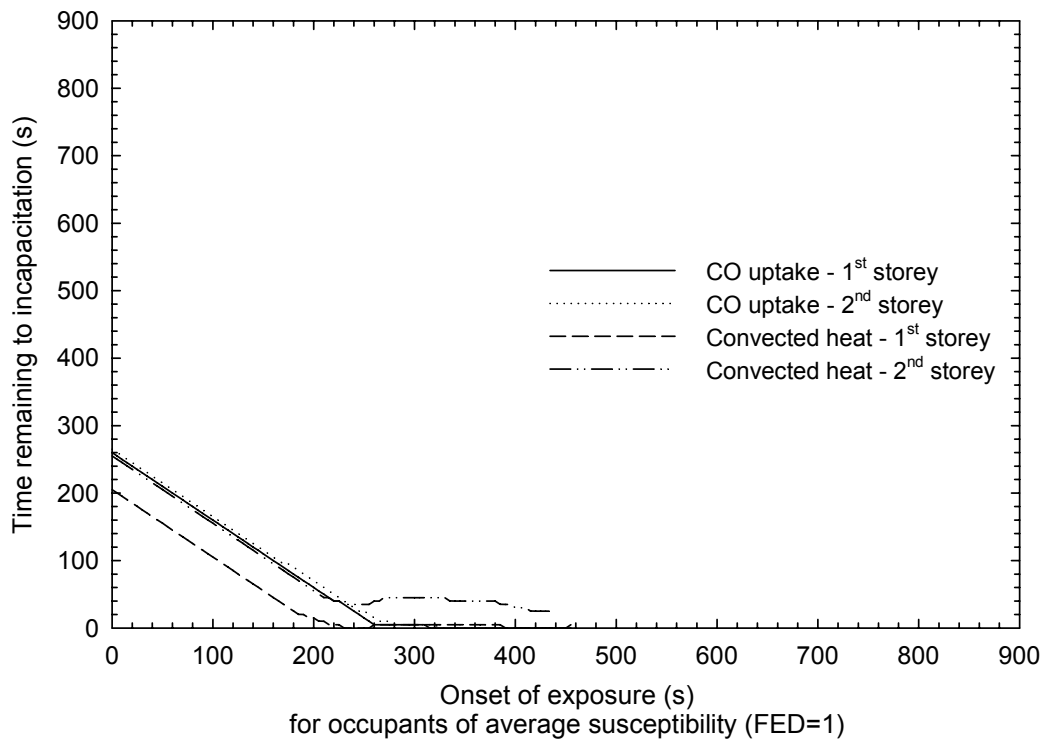
Figure 52. Time remaining to incapacitation versus onset of exposure for Test UF-07 (ignition at time zero)

NRC·CNRC
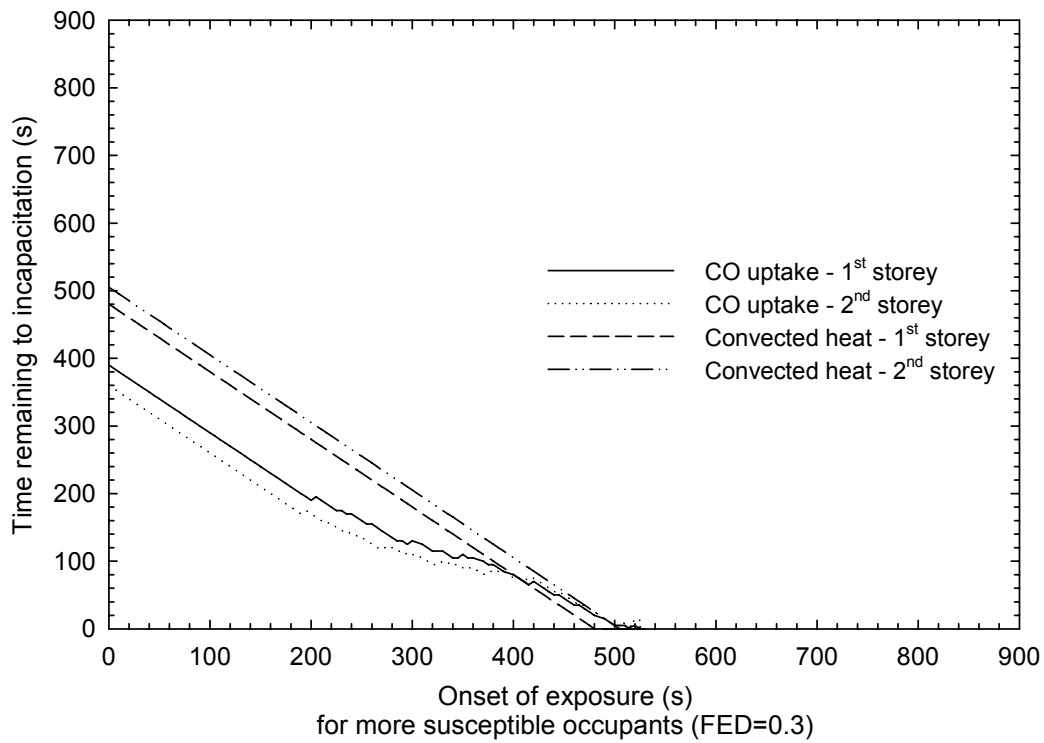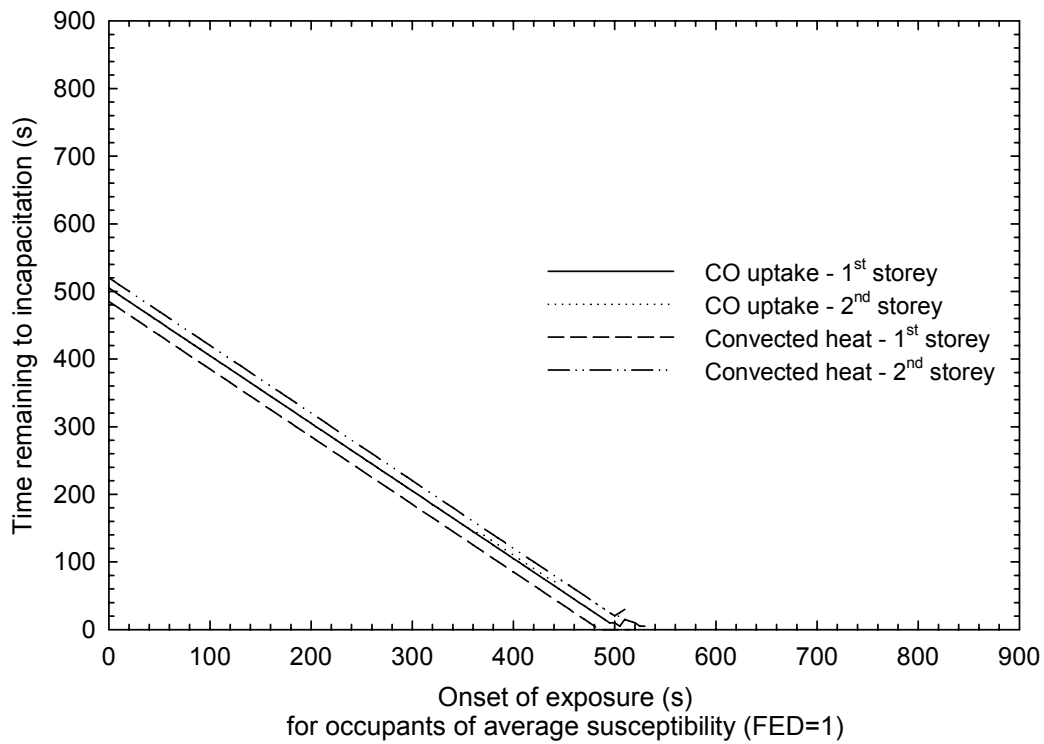
Figure 53. Time remaining to incapacitation versus onset of exposure for Test UF-08 (ignition at time zero)

3.8   The Sequence of Events

Figure 54 and Figure 55 show the chronological sequence of the fire events in Tests UF-07 and UF-08, respectively. The smoke alarms in the basement detected the fire quickly. In both Test UF-07 and Test UF-08, the smoke alarm (photoelectric) located in the basement activated at 50 s. Note that in Test UF-07 (open basement doorway), the ionization smoke alarm located on the first stoery detected the basement fire first at 40 s (10 s earlier than the photoelectric smoke alarm located in the basement fire room). Interconnecting all of the smoke alarms in the house would help ensure an early fire alert.

The basement window was opened after it reached 300°C at 95 s in Test UF-07 and at 90 s in Test UF-08. The exterior door on the first storey was opened at 180 s in both tests.
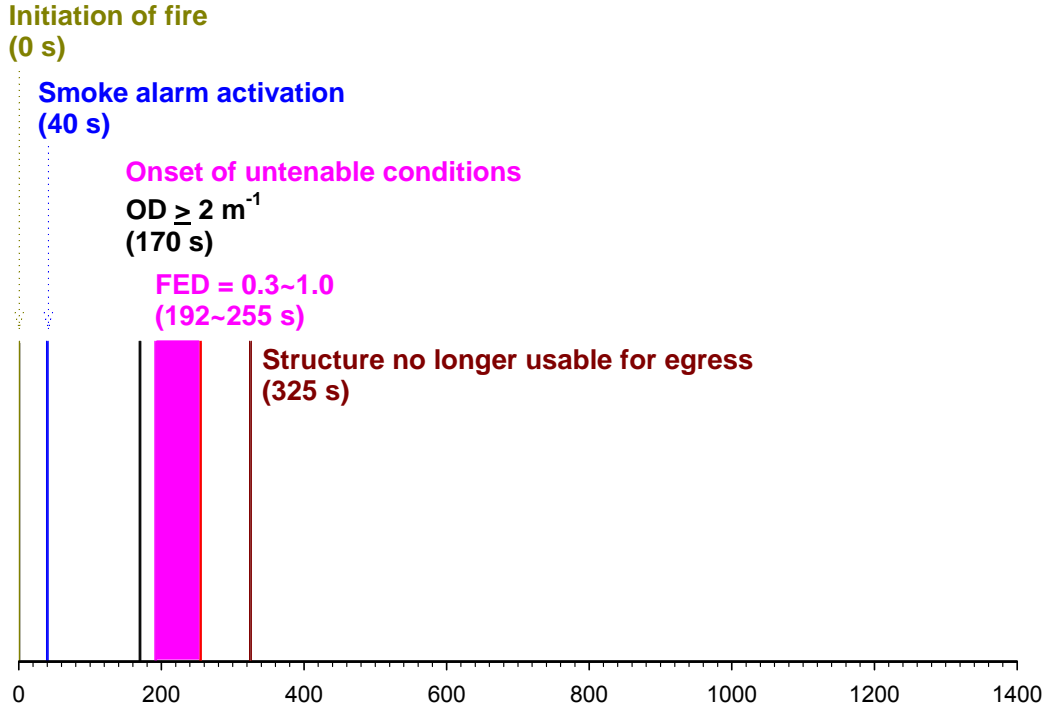
The timing for onset of potentially untenable conditions includes those for the complete smoke obscuration (OD $\geq$ 2 m^{-1}) and for exposure to heat and narcotic gases for susceptible (FED =0.3) and average (FED=1.0) occupants (see Section 3.7 for detailed discussions). The time after which the floor structure would be no longer usable for egress (325 s for UF-07 and 474 s for UF-08) was based on the shortest time to reach the maximum deflection. The tests were terminated after the floor failure.

In Test UF-07 (open basement doorway), the untenable conditions were reached before the structural failure of the floor assembly.

In Test UF-08, the presence of the closed door to the basement reduced the rate of fire growth in the basement, and slowed down the transport of combustion products from the basement to the upper storeys. This prolonged the time available for escape before the onset of untenable conditions, and also delayed the time for the test assembly above the basement to reach structural failure. In this closed basement doorway scenario, the floor assembly failed structurally before the tenability limits were reached for healthy adults of average susceptibility. Because the floor failed structurally before the tenability limits were reached, this would represent a risk factor for occupants.

NRC·CNRC

**Initiation of fire
(0 s)**

**Smoke alarm activation
(40 s)**

Onset of untenable conditions

OD $\geq$ 2 m^{-1}
(170 s)

**FED = 0.3~1.0
(192~255 s)**

**Structure no longer usable for egress
(325 s)**

0   200   400   600   800   1000   1200   1400

Figure 54. Sequence of fire events in Test UF-07 (s)

**Initiation of fire
(0 s)**

**Smoke alarm activation
(50 s)**

Onset of untenable conditions

OD $\geq$ 2 m^{-1}
(360 s)

**FED = 0.3~1.0
(375~510 s)**

**Structure no longer usable for egress
(474 s)**

0   200   400   600   800   1000   1200   1400
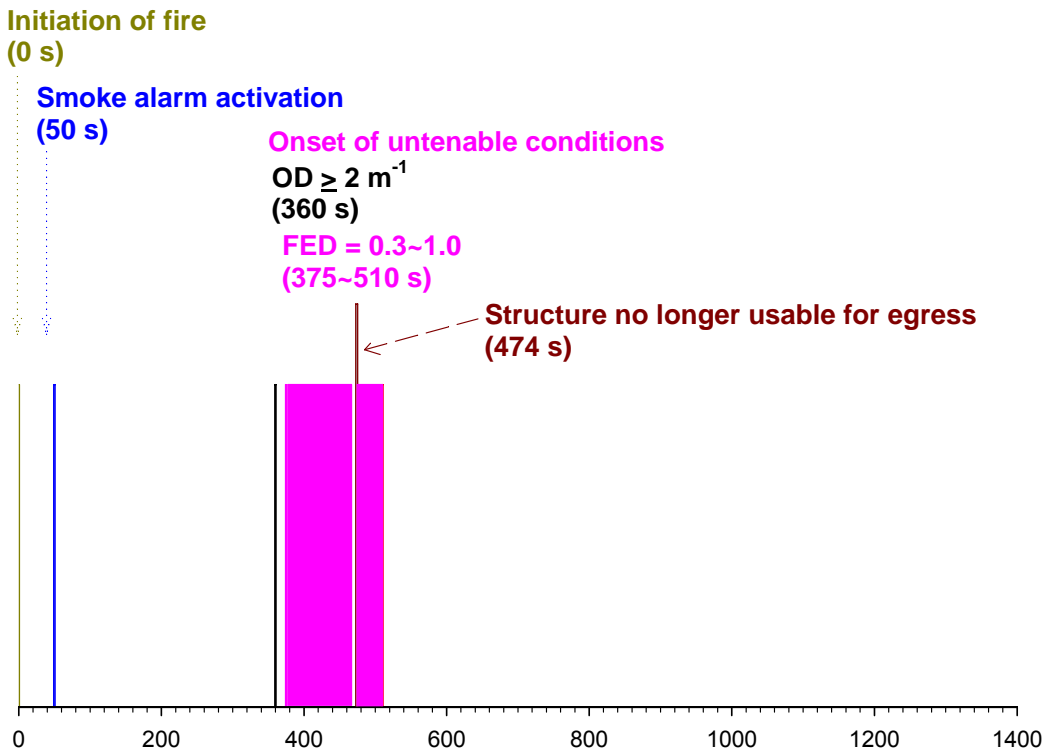
Figure 55. Sequence of fire events in Test UF-08 (s)

94

4   SUMMARY

This report presents the results and analysis of Tests UF-07 and UF-08 as part of the research project on fire performance of houses. The tests were conducted in the test facility that simulated a typical two-storey single-family house complying with the minimum code requirements in the NBCC. The two tests were identical except for the state of the door in the basement doorway. In Test UF-07, there was no door in this doorway (open basement doorway) while in Test UF-08 there was a door in this doorway in the closed position (closed basement doorway).

The tests were conducted on loaded unprotected metal-web-connected wood truss floor assemblies (also basement ceilings) using fire scenarios that were characterized in a study documented in reference [6]. A number of measurements were conducted during the tests including temperatures at various locations (in the compartments and on the floor assemblies), fire detection times at various locations, gas measurements, smoke density measurements, flame penetration and deflection measurements for the floor assemblies.

The activation times of the smoke alarms in the basement were the same for the two tests. For the open basement doorway scenario, structural failure occurred after the onset of untenable conditions (using incapacitation as an end point). The results showed that, in a basement fire test scenario, closing the door to the basement delayed the onset of untenable conditions for occupants on the first and second storeys and also delayed the structural failure of the unprotected floor assembly constructed over the basement.

Two relatively severe basement fire scenarios were used in the full-scale fire experiments to establish the sequence of the events that would affect the ability of occupants to escape the house in the event of a basement fire. The test results must be interpreted within the context of the fire scenarios used in the experiments.

5   ACKNOWLEDGMENTS

NRC·CNRC

6 REFERENCES

1. Canadian Commission on Building and Fire Codes; National Building Code of Canada; National Research Council of Canada, Ottawa, Canada, 2005.
2. Canadian Commission on Building and Fire Codes, User's Guide – NBC 2005, Application and Intent Statements, National Research Council of Canada, Ottawa, Canada, 2006.
3. Proulx, G., Cavan, N.R., Tonikian, R., Egress Times From Single Family Houses, Research Report 209, Institute for Research in Construction, National Research Council Canada, 2006.
4. Bwalya, A.C., An Extended Survey of Combustible Contents in Canadian Residential Living Rooms, Research Report 176, Institute for Research in Construction, National Research Council Canada, 2004
5. Leroux, P., Kanabus-Kaminska, J.M., Séguin, Y.P., Henrie, J.P., Lougheed, G.D., Bwalya, A.C., Su, J.Z., Bénichou, N., Thomas, J.R. Small-Scale and Intermediate-Scale Fire Tests of Flooring Materials and Floor Assemblies for the Fire Performance of Houses Project, Research Report 211, Institute for Research in Construction, National Research Council Canada, 2007.
6. Taber, B.C., Bwalya, A.C., McCartney, C., Bénichou, N., Bounagui, A., Carpenter, D.W., Crampton, G.P., Kanabus-Kaminska, J.M., Kashef, A., Leroux, P., Lougheed, G.D., Su, J.Z., Thomas, J.R., Fire Scenario Tests in Fire Performance of Houses Test Facility - Data Compilation, Research Report 208, Institute for Research in Construction, National Research Council Canada, 2006.
7. "ASTM E1537-02a: Standard Test Method for Fire Testing of Upholstered Furniture", American Society for Testing and Materials, PA, USA, 2002.
8. Crampton, G.P. The Design and Construction of a Flame Conductivity Device to Measure Flame Penetration through Floor Systems, Research Report 223, Institute for Research in Construction, National Research Council Canada, 2006.
9. Forte, N. and Crampton, P., The Design and Construction of Electronic Deflection Gauges to Measure the Movement of Floor Assemblies in a Fire, Research Report 202, Institute for Research in Construction, National Research Council Canada, 2005.
10. EC1, Eurocode 1, "Basis of design and design actions on structures", Part 2-2: Actions on Structures Exposed to Fire, ENV 1991-2-2, European Committee for Standardization, Brussels, Belgium, 1994.
11. SNZ, "Code of practice for the general structural design and design loadings for buildings", SNZ 4203, Standards New Zealand, Wellington, New Zealand. 1992.
12. AS/NZS, "Structural design actions, Part 0: General principles", AS/NZS 1170.0, Australia/New Zealand Standard, 2002.
13. ASCE 7-98, ASCE Standard, "Minimum design loads for buildings and other structures", American Society of Civil Engineering, Reston, Virginia, 2000.
14. CAN/ULC-S101-04; Standard Methods of Fire Endurance Tests of Building Construction and Materials; Underwriters' Laboratories of Canada, Scarborough, Canada, 2004.

NRC·CNRC

15. ISO Technical Specification 13571, "Life-threatening Components of Fire—Guidelines for the Estimation of Time Available for Escape Using Fire Data," International Organization for Standardization, Geneva, 2002.
16. Purser, D.A., "Toxicity Assessment of Combustion Products," in The SFPE Handbook of Fire Protection Engineering, ed. P.J. DiNenno, D. Drysdale, C.L. Beyler, W.D. Walton, R.L.P. Custer, J.R. Hall, Jr. and J.M. Watts, Jr., 3rd edition, Society of Fire Protection Engineers /National Fire Protection Association, Quincy, Massachusetts, 2002, Section 2, Chapter 6.
17. Beyler, C., "Toxicity Assessment of Products of Combustion of Flexible Polyurethane Foam," Fire Safety Science -- Proceedings of the Eighth International Symposium, International Association for Fire Safety Science, 2005, pp.1047-1058
18. Laursen, T., "Overview of Toxicity/Effectiveness Issues", Proceedings of Halon Alternatives Technical Working Conference, Albuquerque, NM, 1993, pp. 357-367.
19. Sax, N.I. and Lewis, R.J., "Dangerous Properties of Industrial Materials" (7th ed.), Van Nostrand Reinhold, New York, 1989.
20. Peterson, J.E. and Stewart, R.D., "Predicting the carboxyhemoglobin levels resulting from carbon monoxide exposures," Journal of Applied Physiology, Vol. 39, No. 4, pp. 633-638, 1975
21. Stewart, R.D., Peterson, J.E., Fisher, T.N., Hosko, M.J., Baretta, E.D., Dodd, H.C. and Herrmann, A.A., "Experimental Human Exposure to High Concentrations of Carbon Monoxide," Archives of Environmental Health, Vol. 26, pp. 1-7, 1973
22. Babrauskas, V., "Combustion of Mattresses Exposed to Flaming Ignition Sources, Part I. Full-Scale Tests and Hazard Analysis," NBSIR 77-1290, National Bureau of Standards, Washington, DC, September 1977.
23. Hauck, H. and Neuberger, M., "Carbon monoxide uptake and the resulting carboxyhemoglobin in man," European Journal of Applied Physiology, Vol. 53, pp.186-190, 1984.
24. Gann, R.G., "Estimating Data for Incapacitation of People by Fire Smoke," Fire Technology, Vol. 40, pp.201-207, 2004.
25. Christopher J. Wieczorek and Nicholas A. Dembsey, "Human Variability Correction Factors for Use with Simplified Engineering Tools for Predicting Pain and Second Degree Skin Burns", Journal of Fire Protection Engineering, Vol. 11, No. 2, 88-111, 2001
26. Jin, T., "Visibility and Human Behavior in Fire Smoke," in The SFPE Handbook of Fire Protection Engineering, ed. P.J. DiNenno, D. Drysdale, C.L. Beyler, W.D. Walton, R.L.P. Custer, J.R. Hall, Jr. and J.M. Watts, Jr., 3rd edition, Society of Fire Protection Engineers /National Fire Protection Association, Quincy, Massachusetts, 2002, Section 2, Chapter 4.
27. Babrauskas, V., "Full-Scale Burning Behavior of Upholstered Chairs," NBS Technical Note 1103, National Bureau of Standards, Washington, DC, August 1979.
28. Bukowski, R.W., Peacock, R.D., Averill, J.D., Cleary, T.G., Bryner, N.P., Walton, W.D., Reneke, P.A., Kuligowski, E.D., "Performance of Home Smoke Alarms - Analysis of the Response of Several Available Technologies in Residential Fire Settings," NIST Technical Note 1455, National Institute of Standards and Technology, December 2003.
29. Su, J., Bwalya, A., Lougheed, G., Bénichou, N., Taber, B., Kashef, A., Leroux, P. and Thomas, R., Fire Scenario Tests In Fire Performance Of Houses Test Facility – Data Analysis, Research Report 210, Institute for Research in Construction, National Research Council Canada, 2007.

NRC·CNRC

Table A 1. Test Summary for Test UF-07

- Test ID: UF-07
- Test Date: Feb. 8, 2007
- Atmospheric Conditions: Temp: -8°C   RH: 71%   Pres: 100.9 kPa$\uparrow$
- Structure Tested:
    Metal-web wood truss, 302 mm deep
    15.1 mm (5/8") OSB floor
    0.95 kPa load (144 concrete blocks, 2490 kg, 61 m pipe, 143 kg)

- Fire Load:
    Mock-up sofa at centre of basement (9.20 kg foam)
    Wood crib located 200 mm behind mock-up sofa (61.6 kg, 6 % MC)
    Wood crib located 200 mm from west side of mock-up sofa (61.1 kg, 6 % MC)
    Two wood cribs located under the mock-up sofa (32.5 kg, 31.0 kg, 6 % MC)
    80 s ignition with 19 kW burner (13 l/min)

- Ignition time after start of data: <u>1:00</u>

- Doors: SE bedroom door closed / SW bedroom door open
            Door at top of basement stairs open
            First floor exterior door opened at 3:00 after ignition

- Window: Window opened at <u>1:35</u> after ignition (300 ^{O}C)

- Floor collapse: <u>5:25</u> (325 s) after ignition

- Smoke Detector Activation Times:

	Activation _(time from ignition)_
Smoke Detector #2, Photoelectric, Basement, bottom of stairs	50 s
Smoke Detector #3, Ionization, 1st Floor, top of stairs	40 s
Smoke Detector #4, Photoelectric, 1st Floor, top of stairs	55 s
Smoke Detector #5, Ionization, 2nd Floor, top of stairs	110 s
Smoke Detector #6, Photoelectric, 2nd Floor, top of stairs	130 s
Smoke Detector #7, Ionization, SE bedroom, closed	190 s
Smoke Detector #8, Photoelectric, SE bedroom, closed	210 s
Smoke Detector #9, Ionization, SW bedroom, open	130 s
Smoke Detector #10, Photoelectric, SW bedroom, open	145 s

Table A 2. Test Summary for Test UF-08

- Test ID: UF-08
- Test Date: April 24, 2007
- Atmospheric Conditions: Temp: *10°C*   RH: *56%*   Pres: *101.8 kPa*↑
- Structure Tested:
     Metal-web wood truss, 302 mm deep
     15.1 mm (5/8") OSB floor
     0.95 kPa load (144 concrete blocks, 2490 kg, 61 m pipe, 143 kg)

- Fire Load:
     Mock-up sofa at centre of basement (9.32 kg foam)
     Wood crib located 200 mm behind mock-up sofa (61.3 kg, 6 % MC)
     Wood crib located 200 mm from west side of mock-up sofa (65.0 kg, 6 % MC)
     Two wood cribs located under the mock-up sofa (32.0 kg, 31.5 kg, 6 % MC)
     80 s ignition with 19 kW burner (13 l/min)

- Ignition time after start of data: <u>1:00</u>

- Doors: SE bedroom door closed / SW bedroom door open
                 Door at top of basement stairs closed
                 First floor exterior door opened at 3:00 after ignition

- Window: Window opened at <u>1:30</u> after ignition (300 ^{O}C)

- Floor collapse: <u>7:54</u> (474 s) after ignition

- Smoke Detector Activation Times:

	Activation *(time from ignition)*
Smoke Detector #2, Photoelectric, Basement, bottom of stairs	50 s
Smoke Detector #3, Ionization, 1st Floor, top of stairs	85 s
Smoke Detector #4, Photoelectric, 1st Floor, top of stairs	95 s
Smoke Detector #5, Ionization, 2nd Floor, top of stairs	205 s
Smoke Detector #6, Photoelectric, 2nd Floor, top of stairs	205 s
Smoke Detector #7, Ionization, SE bedroom, closed	515 s
Smoke Detector #8, Photoelectric, SE bedroom, closed	515 s
Smoke Detector #9, Ionization, SW bedroom, open	220 s
Smoke Detector #10, Photoelectric, SW bedroom, open	210 s

NRC·CNRC